Review

Magnetic Hyperthermia with Iron Oxide Nanoparticles: From Toxicity Challenges to Theranostic Cancer Applications

Ioana Baldea , Cristian Iacoviță * , Raul Andrei Gurgu , Alin-Stefan Vizitiu , Vlad Răzniceanu , Daniela Rodica Mitrea

Posted Date: 12 August 2025

doi: 10.20944/preprints202508.0830.v1

Keywords: magnetic hyperthermia; iron oxide nanoparticles; cancer therapy; nanotheranostics; targeted drug delivery; ferroptosis; immunotherapy; biocompatibility; multifunctional nanoplatforms; clinical translation

Review

Magnetic Hyperthermia with Iron Oxide Nanoparticles: From Toxicity Challenges to Theranostic Cancer Applications

Ioana Baldea [1], Cristian Iacoviță [2,*], Raul Andrei Gurgu [1], Alin-Stefan Vizitiu [1], Vlad Răzniceanu [1] and Daniela Rodica Mitrea [1]

[1] Department of Physiology, University of Medicine and Pharmacy, Clinicilor 1, Cluj-Napoca, 400006, Romania

[2] Department of Pharmaceutical Physics-Biophysics, Faculty of Pharmacy, "Iuliu Hatieganu" University of Medicine and Pharmacy, 6 Pasteur St., 400349 Cluj-Napoca, Romania

* Correspondence: cristian.iacovita@umfcluj.ro

Abstract

Iron oxide nanoparticles (IONPs) have emerged as key materials in magnetic hyperthermia (MH), a minimally invasive cancer therapy capable of selectively inducing apoptosis, ferroptosis, and other cell death pathways while sparing surrounding healthy tissue. This review synthesizes advances in the design, functionalization, and biomedical application of magnetic nanoparticles (MNPs) for MH, highlighting strategies to optimize heating efficiency, biocompatibility, and tumor targeting. Key developments include tailoring particle size, shape, and composition; doping with metallic ions; engineering multicore nanostructures; and employing diverse surface coatings to improve colloidal stability, immune evasion, and multifunctionality. We discuss preclinical and clinical evidence for MH, its integration with chemotherapy, radiotherapy, and immunotherapy, and emerging theranostic applications enabling simultaneous imaging and therapy. Special attention is given to the role of MNPs in immunogenic cell death induction and metastasis prevention, as well as novel concepts for circulating tumor cell capture. Despite promising results in vitro and in vivo, clinical translation remains limited by insufficient tumor accumulation after systemic delivery, safety concerns, and a lack of standardized treatment protocols. Future progress will require interdisciplinary innovations in nanomaterial engineering, active targeting technologies, and real-time treatment monitoring to fully integrate MH into multimodal cancer therapy and improve patient outcomes.

Keywords: magnetic hyperthermia; iron oxide nanoparticles; cancer therapy; nanotheranostics; targeted drug delivery; ferroptosis; immunotherapy; biocompatibility; multifunctional nanoplatforms; clinical translation

1. Introduction

As one of the leading global health challenges, malignant diseases remain a major cause of mortality, primarily arising from the progressive accumulation of genetic mutations in normal cells that promote unchecked cell division and tumor development. Despite decades of research and therapeutic advances, the overall mortality rates for several cancer types have only modestly declined [1]. Conventional cancer treatment strategies typically include surgical resection, radiotherapy, and systemic therapies such as chemotherapy, hormonal therapy, and targeted biological agents [2]. While these modalities have demonstrated clinical efficacy, they are frequently associated with significant adverse effects. Surgical interventions, for instance, can result in postoperative complications, tissue damage, and the potential dissemination of malignant cells, thereby increasing the risk of metastasis [3]. Chemotherapy involves the administration of cytotoxic agents that often

 doi:10.20944/preprints202508.0830.v1

lack tumor specificity, leading to collateral damage to healthy tissues and systemic toxicity [4]. Similarly, radiotherapy employs ionizing radiation which, when applied over extended periods, may compromise the structural and functional integrity of surrounding normal tissues [5].

Hyperthermia treatment, or thermotherapy, has emerged as a promising adjunct or alternative to conventional treatments. This approach involves elevating the temperature of body tissues to induce cancer cell apoptosis while sparing normal cells [6]. The therapeutic application of heat dates back to ancient civilizations, including those of Greece, Egypt, Rome, and India [7]. In the 19th century, spontaneous tumor regression in febrile patients was documented, prompting early investigations into hyperthermia for oncological applications, such as in the treatment of cervical cancer [7,8]. Since the 1970s, hyperthermia has garnered renewed clinical interest, with controlled trials exploring its efficacy in cancer treatment. Studies have demonstrated that cancer cells are more susceptible to temperatures between 42–45 °C, undergoing apoptosis, whereas normal cells exhibit greater thermal resilience [9].

Depending on the tumor's location, depth, and stage of progression, three main hyperthermia strategies have been established for clinical application: local, regional, and whole-body hyperthermia. Whole-body hyperthermia is typically employed in cases involving deep-seated tumors or disseminated metastases, where the entire body is uniformly heated using methods such as hot water baths, thermal chambers, or infrared radiation [10–13]. For advanced-stage malignancies confined to specific areas, regional hyperthermia is applied through techniques like thermal perfusion, external applicators, or microwave antennas to deliver targeted heat [10–13]. Local hyperthermia, the least invasive approach, is primarily used for treating localized tumors situated either superficially or within accessible body cavities.

Over the past century, substantial technological progress has led to the development of magnetic nanoparticles (MNPs), which have attracted growing interest in biomedical research, particularly in oncology. These nanomaterials possess the unique ability to convert electromagnetic energy into heat when exposed to an external alternating magnetic field (AMF) [14,15]. Importantly, the penetration depth of AMF is not significantly attenuated by biological tissues, allowing effective activation of MNPs even within deep-seated tumors [15,16]. Once internalized by cancer cells, MNPs function as localized heat sources, raising the temperature of tumor tissue to levels sufficient to induce apoptosis. This approach, known as magnetic hyperthermia (MH), has emerged as a promising and innovative therapeutic strategy with the potential to enhance cancer treatment outcomes while minimizing damage to surrounding healthy tissues [16,17].

The first experimental evidence supporting the use of MH for cancer treatment was reported in 1957 by Gilchrist et al. [18], who conducted an *in vitro* study involving lymph nodes containing colon and rectal cancer metastases. In this pioneering work, maghemite (γ-Fe_2O_3) nanoparticles, ranging in size from 20 to 100 nm, were introduced into the lymph nodes and subjected to an AMF with an amplitude (H) of 16 - 19.2 kA/m at a frequency (f) of 1.2 MHz. The resulting temperature increases to 43 - 46 °C successfully eradicated carcinoma cells by destroying the metastatic tissue [18]. As a result of extensive research and due to their favorable biocompatibility and biodegradability, both maghemite (γ-Fe_2O_3) and its reduced form, magnetite (Fe_3O_4), were approved by the U.S. Food and Drug Administration (FDA) for clinical trials [19]. Consequently, iron oxide nanoparticles have become the most widely used agents in magnetic hyperthermia (MH) applications [20,21]. The therapeutic potential of MH reached a significant milestone with the advancement of the German company MagForce AG, which received regulatory approval from the European Union to clinically treat glioma patients [22–25].

The interaction between AMFs and biological tissues generates non-specific heating through the induction of eddy currents. This can activate the body's thermoregulatory responses and produce complex thermal gradients throughout the patient's body [26,27]. To ensure safety, a limit has been established for human exposure to AMFs by restricting the product of H and f to a maximum of 5×10^9 $A \cdot m^{-1} \cdot s^{-1}$ [28]. However, the heat dissipation capabilities of commercially available magnetic nanoparticles (MNPs), such as Nanotherm, Feridex, and Resovist, remain inadequate within

 doi:10.20944/preprints202508.0830.v1

physiologically safe AMF parameters. As a result, the therapeutic effect is often insufficient for complete tumor ablation, limiting the widespread adoption of MH as a standalone treatment option in clinical settings.

To advance the clinical application of MH in cancer therapy, two principal strategies have been identified in scientific literature. The first approach focuses on the design and synthesis of magnetic nanoparticles (MNPs) with enhanced intrinsic magnetic properties, such as increased saturation magnetization (M_s) and magnetic anisotropy (K), to improve heat generation efficiency even at low concentrations. This can be achieved by manipulating parameters such as particle size, shape, chemical composition, and surface morphology. As these aspects have been extensively covered in previous reviews [29–31], therefore we will briefly summarize the most significant developments in this area in the first part of our review. Notably, numerous studies have reported that only a small fraction of systemically administered MNPs effectively accumulate at the tumor site [32]. Consequently, clinical efficacy often relies on direct intratumoral injections, which restrict treatment to tumors that are accessible [33]. To address this limitation, recent research has increasingly focused on combining MH with other anticancer modalities within a single, multifunctional MNP-based nanoplatform [34]. The aim of this review is to highlight the advancements and the challenges that the magnetic hyperthermia faces from the design of magnetic nanoparticles to ensure biocompatibility, tumor specificity and clean biodegradation in the living organisms, while still preserving the hyperthermic and drug delivery properties, towards the biological testing on different in *vitro*, respectively *in vivo* models and eventually clinical patients. This integrative strategy represents the second major approach in the field and will be explored in detail in the second part of this review. Clinical advancements in the field, based on clinical studies of MH efficacy in oncologic patients, will be further discussed in the third part of this review. Finally, the challenges, outlook and conclusions regarding the advances of magnetic hyperthermia in oncological research and the prospects of MH to become an important adjuvant therapy in the oncologic patients are described.

2. Relevant Sections and Discussions

2.1. Toxicity Issues

Magnetite (Fe_3O_4) nanoparticles (MNPs) are among the most widely investigated nanomaterials in biomedicine due to their superparamagnetic (SP) properties, ease of functionalization, and intrinsic biocompatibility. They are extensively employed in applications such as magnetic resonance imaging (MRI) contrast enhancement, targeted drug delivery, and MH therapy. However, despite their promising biomedical potential, MNPs are not inherently risk-free. Concerns about both acute and chronic toxicity have emerged, particularly under conditions of MH, where deliberate nanoparticle heating can inadvertently damage surrounding healthy tissues [35–37].

In vitro cytotoxicity studies have revealed that Fe_3O_4 nanoparticle-induced toxicity is both dose- and time-dependent, typically associated with increased production of reactive oxygen species (ROS) and lipid peroxidation, evidenced by elevated malondialdehyde (MDA) levels. This oxidative stress can impair cellular enzymes, damage membranes, and compromise cell viability. For instance, Ahamed et al. [38] demonstrated significant ROS and MDA elevation in A431 and A549 cell lines exposed to 25–100 μg/mL MNPs, correlating with reduced cell viability. Similarly, recent findings on human umbilical vein endothelial cells (HUVECs) identified oxidative stress and genotoxic effects at an IC_{50} of approximately 79 μg/mL [39]. Iron overload from internalized nanoparticles may further exacerbate toxicity by triggering ferroptosis—a form of programmed cell death driven by lipid peroxidation—and catalyzing Fenton-type reactions that generate hydroxyl radicals. These highly reactive species induce DNA strand breaks, protein carbonylation, and membrane damage. Such mechanisms have been implicated in neuropathological contexts like intracerebral hemorrhage, and may similarly contribute to nanotoxicity in non-neuronal tissues [40,41]. The surface chemistry of Fe_3O_4 nanoparticles plays a pivotal role in modulating their biocompatibility. For example, in porcine aortic endothelial cells, dextran- or polyethylene glycol (PEG)-coated particles (5 nm and 30 nm)

 doi:10.20944/preprints202508.0830.v1

induced no significant loss of viability or increase in ROS generation even at 0.5 mg/mL after 24 h exposure. Notably, PEG reduced ROS production by 62.6%, and dextran by 35.2% compared to uncoated cores, with apoptosis levels remaining below 10% [42]. In contrast, polyethylenimine (PEI)-functionalized Fe_3O_4 particles (30 nm) displayed pronounced cytotoxicity in SH-SY5Y, MCF-7, and U937 cell lines, decreasing viability by up to 50% within 24 hours at 100 μg/mL, and even further after 168 hours. These effects, marked by increased ROS, lipid peroxidation, and lactate dehydrogenase (LDH) release, were largely mitigated upon PEGylation of the PEI coating [43].

In vivo, the toxicity profile of MNPs is influenced by parameters such as dose, administration route, biodistribution, and particle size. Following systemic administration, MNPs tend to accumulate in organs of the mononuclear phagocyte system, notably the liver and spleen, where they may trigger inflammation and tissue injury. For instance, high-dose administration of dextran-coated iron oxide particles in mice, followed by AMF exposure, resulted in severe hepatosplenic damage or mortality, whereas lower-dose groups survived but still exhibited signs of tissue stress, including elevated liver enzymes and splenic necrosis [44]. Particle size is equally critical: ultrasmall MNPs (2.3 and 4.2 nm) administered intravenously at 100 mg/kg induced fatal multiorgan oxidative stress, particularly affecting cardiac tissue, whereas 9.3 nm particles of identical composition showed no overt toxicity at the same dose [45]. Long-term studies suggest that MNPs are only partially cleared from the body. Residual iron, often sequestered in ferritin-like structures, can persist in the liver and spleen for several months post-administration. This has been associated with chronic low-grade hepatic inflammation and disruption of iron metabolism, although conclusive evidence linking this persistence to long-term health consequences remains limited [46,47].

2.2. Methods to Enhance the Hyperthermic Capability of Iron Oxide Nanoparticles

The thermal effect generated by MNPs under AMF stimulation is quantified by a physical parameter known as the specific absorption rate (SAR), also referred to as specific loss power (SLP). SAR represents the amount of heat released per unit time per unit mass of MNPs and is typically expressed in watts per gram ($W \cdot g^{-1}$) [48]. The SAR value is influenced by both the intrinsic properties of the MNPs—such as particle volume and saturation magnetization—and the extrinsic parameters of the applied AMF. To enhance the induction heating performance, efforts have been directed toward optimizing the intrinsic magnetic properties of MNPs. Simultaneously, thermal efficiency has been externally improved by increasing the frequency and amplitude of the AMF in different MH setups.

2.2.1. Formulation

For biomedical applications requiring "injectable" nanoprobes, superparamagnetic nanoparticles—commonly referred to as SPIONs (superparamagnetic iron oxide nanoparticles)—are generally preferred. Their lack of remanent magnetization in the absence of an external magnetic field facilitates colloidal stability, enhances dispersion in biological fluids, and minimizes the risk of particle aggregation. Among these, ultra-small SPIONs (typically <5 nm in core diameter) have emerged as promising candidates for magnetic resonance imaging (MRI) contrast enhancement due to their excellent magnetic relaxation properties [49,50]. However, in the context of magnetic hyperthermia (MH), such ultra-small SPIONs often exhibit low specific absorption rate (SAR) values, limiting their heating efficiency [51]. Furthermore, a significant reduction in heating performance is commonly observed when SPIONs are internalized into cells or embedded in tissues, likely due to restrictions in Brownian motion and changes in local viscosity [52]. As a result, considerable research efforts have been directed toward optimizing nanoparticle properties within the superparamagnetic regime to enhance the efficacy of magnetically induced hyperthermia under physiological conditions.

The magnetic properties of MNPs are strongly influenced by their size. An increase in the size or volume of MNPs typically results in a higher M_s, which reflects the net alignment of all magnetic spins within the particle. This increase continues up to a critical threshold, beyond which M_s stabilizes and approaches the bulk material value. Numerous studies have reported a significant increase in

 doi:10.20944/preprints202508.0830.v1

the SAR with the growth of spherical SPIONs, ranging from several tens to several hundreds of W/g [53–58]. As the diameter of MNPs increases, their magnetic anisotropy energy — the energy responsible for maintaining the magnetic moment in a preferred orientation — also increases. For each MNP composition, there exists a characteristic size at which the anisotropy energy surpasses the thermal energy, stabilizing the magnetic moment along a preferred axis known as the easy axis of magnetization. This transition drives MNPs from a superparamagnetic to a ferromagnetic regime, characterized by the appearance of hysteresis loops. These loops exhibit remanent magnetization (M_r), representing the residual magnetization at zero external field, and coercivity (H_c), the magnetic field required to bring the magnetization to zero. The magnetic MH efficiency of MNPs is governed by their dynamic hysteresis behavior [59], which is influenced not only by Neel and Brownian relaxation mechanisms but also by DC magnetic hysteresis. As a result, SAR values in ferromagnetic particles can be nearly an order of magnitude higher than in their superparamagnetic counterparts [60–63]. However, despite their high heating efficiency, ferromagnetic nanoparticles are generally less suitable for biomedical applications due to their colloidal instability and finite coercive field, which promote aggregation and reduce biocompatibility [64–66].

Individual SPIONs often exhibit limited magnetic moments, which restrict their efficiency in MH. However, when these SPIONs are organized into clusters through self-assembly or aggregation, magnetic interactions between the closely packed cores can induce collective magnetic behaviors, resulting in enhanced net magnetic moments [67]. This clustering significantly improves key magnetic properties, such as M_s and magnetic susceptibility, thereby increasing their responsiveness to external magnetic fields. Moreover, the clustered architecture provides improved colloidal stability and resistance to uncontrolled aggregation, preserving SP behavior while ensuring long-term performance under physiological conditions [68,69]. Cluster formation can occur via two primary strategies. In a two-step process, SPIONs are first synthesized as discrete particles, followed by their assembly into clusters mediated by ligand-induced colloidal interactions, such as hydrophobic or electrostatic forces [70]. Alternatively, clustering can occur in a single-step synthetic route, wherein the nanoparticles aggregate during formation [71,72]. The polyol method has been widely employed for this purpose in the past decade due to its adaptability, scalability, and ability to control particle morphology. This method enables the formation of various hierarchical structures, including nanoclusters, nanoflowers, and hollow spheres, by tuning reaction parameters such as temperature, solvent polarity, and precursor concentration [73–78]. Particularly, flower-like magnetic nanoparticles (nanoflowers) with coherent crystallographic orientation between cores have garnered attention for their superior magnetic heating performance [79–81]. The improved SAR values are thought to arise from collective spin dynamics and magnetic coupling effects within the multicore structure, which favor more efficient energy dissipation under AMF [82,83].

2.2.2. Shape

In the case of MNPs, surface atoms represent a significant proportion of the total atomic content, and their magnetic and chemical behavior often diverges from that of the bulk material. This is primarily due to the intrinsically high surface-to-volume ratio of MNPs, which causes surface effects to dominate their overall magnetic properties. Notably, the asymmetric coordination of surface atoms gives rise to spin disorder or spin canting, ultimately reducing the M_s of the nanoparticles [84]. This phenomenon is especially pronounced in spherical SPIONs, which expose multiple crystallographic facets with numerous edges and corners [85]. These structural features enhance surface anisotropy and require greater energy to reorient surface magnetic moments, negatively impacting their heat dissipation efficiency under AMF. Consequently, the synthesis of anisotropic SPIONs has gained considerable interest as a strategy to enhance MH performance [86]. Various non-spherical morphologies, including nanocubes [87–91], octopods [92], octahedrons [93,94], nanorods [95–97], nanodiscs [98], nanorings [99], and polyhedral structures [100], have demonstrated improved heating efficiency compared to their spherical counterparts (Figure 1).

 doi:10.20944/preprints202508.0830.v1

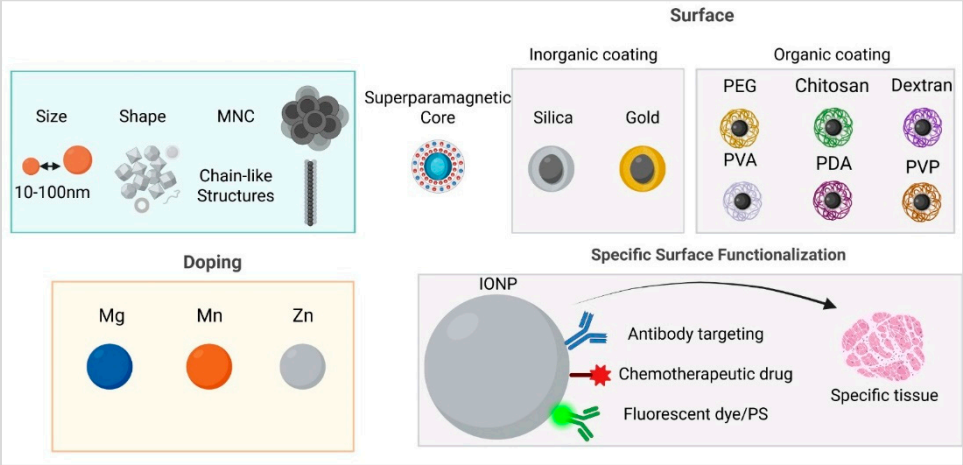

Figure 1. Various strategies have been developed to design efficient nanoplatforms with enhanced MH capabilities, as increasing size or tunning the shape. Metallic doping mangan, zinc, with magnesium improves magnetic properties as well as heating capabilities. Additionally, assembling nanoparticles into magnetic nanoclusters (MNCs) or chain-like structures can further amplify their hyperthermic effects. Another approach involves either inorganic or organic surface coatings, also applied to improve biocompatibility, facilitate cellular uptake, and provide functional binding sites, using silica, gold, organics such as synthetic polymers (such as polyethylene glycol (PEG), polyvinyl alcohol (PVA), polydopamine (PDA), or polyvinylpyrrolidone (PVP)) or natural polymers (like chitosan and dextran). These nanoplatforms can also be functionalized to achieve theranostic capabilities by modifying the shell or polymer coating. Ligands (e.g., folic acid or antibody fragments) can be added for specific targeting of tumor cells, while therapeutic agents (such as chemotherapeutic drugs) enable combined MH and chemotherapy. For imaging purposes, fluorescent dyes may be incorporated to enhance tumor visualization, together with MRI imaging. Moreover, photosensitizers can be included to facilitate combined photodynamic or photothermal therapy alongside MH.

2.2.3. Doping with Metallic Ions

Magnetite (Fe_3O_4) exhibits an inverse cubic spinel structure, in which O^{2-} anions form a face-centered cubic (FCC) lattice that accommodates two distinct cationic sublattices: tetrahedral (A) sites, exclusively occupied by trivalent iron ions (Fe^{3+}), and octahedral (B) sites, shared by both divalent (Fe^{2+}) and trivalent (Fe^{3+}) cations. Superexchange interactions mediated by O^{2-} anions govern the magnetic coupling between these cations, resulting in three main interaction types: A–O–A, B–O–B (intra-sublattice), and A–O–B (inter-sublattice). While intra-sublattice interactions tend to be ferromagnetic, the inter-sublattice (A–O–B) interactions are antiferromagnetic in nature, giving rise to the characteristic ferrimagnetism of magnetite. The net magnetic moment per formula unit is determined by the difference between the magnetic moments at B and A sites ($\mu_{oct} - \mu_{tet}$), primarily attributed to the presence of Fe^{2+} ions on B sites, resulting in a net moment of approximately 4 μ_B (Bohr magnetons) per formula unit.

Tailoring the magnetic properties of Fe_3O_4 nanoparticles (MNPs), can be effectively achieved through substitutional doping of Fe^{2+} ions with other divalent transition metal cations such as Mn^{2+}, Co^{2+}, Ni^{2+}, Cu^{2+}, and Zn^{2+} (Figure 1). For instance, replacing Fe^{2+} ($3d^6$) with Mn^{2+} ($3d^5$), which possesses a higher magnetic moment, enhances the overall magnetic moment to 5 μ_B per formula unit. This substitution has been shown to significantly increase the saturation magnetization (M_s), reaching values up to 110 emu/g_{metal}, and consequently, improve both heating efficiency in MH [101–106]. Interestingly, zinc doping—despite Zn^{2+} ($3d^{10}$) having zero magnetic moment—also leads to modulation of M_s due to site-specific cation rearrangement within the spinel lattice. At low doping concentrations ($x < 0.5$ in $Zn_xFe_{3-x}O_4$), Zn^{2+} preferentially occupies A sites, displacing Fe^{3+} cations to B sites. This redistribution increases the magnetic moment at B sites (μ_{oct}) and reduces that at A sites (μ_{tet}), resulting in a substantial increase in M_s (161 emu/g_{metal}), displaying approximately four times greater heating efficiency compared to conventional SPIONs [85,107–109]. Another example is the

 doi:10.20944/preprints202508.0830.v1

use of magnesium as a dopant. $Mg_xFe_2O_3$ nanoparticles (x = 0 – 0.15) with an average size of 7 nm demonstrated exceptional heating power — approximately 100 times higher than commercial Fe_3O_4 (Feridex) — attributed to enhanced magnetic susceptibility and ~50% octahedral Fe^{3+} vacancy occupation by Mg^{2+} ions, as supported by atomic structural modeling [110]. Although $M_xFe_{3-x}O_4$ nanoferrites are often doped to M_s and SAR, results vary significantly depending on synthesis parameters and dopant distribution across T_d and O_h sites. Thus, precise control of dopant incorporation within the Fe_3O_4 lattice is essential to optimize magnetic and thermal performance.

2.2.4. Controlled Nanoscale Assembly of MNPs

It has been demonstrated that during MH experiments, the application of an AMF promotes the organization of MNPs into elongated assemblies or chains. This field-induced structuring significantly influences the SAR and overall heat generation capabilities of the MNPs [111–113]. Chain formation behavior has also been observed intracellularly, where MNPs internalized by cells tend to align in response to the AMF [114]. Further studies have revealed that such alignment occurs within intracellular vesicles and does not compromise cellular morphology or nuclear integrity [115]. In a related context, magnetosomes—magnetic nanoparticles biosynthesized by magnetotactic bacteria—exhibit superior heating efficiency compared to their synthetic analogs, primarily due to their intrinsic chain-like organization [116–118]. Consequently, the controlled nanoscale assembly of MNPs to enhance SAR represents an important topic in MH research.

Several groups have investigated the effect of pre-aligning MNPs in a static magnetic field (H_{DC}) on their heating performance. They have demonstrated that MNPs pre-aligned under a H_{DC} before immobilization (e.g., via gelation in a solid matrix) produce significantly higher SAR values when aligned parallel to the AMF, compared to randomly oriented nanoparticles [119–123]. Furthermore, two in vitro studies have shown that either culturing cancer cells with MNPs under a H_{DC} or pre-aligning incubated MNPs significantly improves MH efficiency and enhances cancer cell destruction, compared to the non-aligned scenario [124,125].

Another promising strategy for boosting MNP heating efficacy involves the superposition of a s H_{DC} on the AMF during MH treatment. Experimental evidence indicates that for SPIONs, this approach can lead to SAR enhancements of up to 40% relative to AMF-only conditions [16]. Chain formation in this system was confirmed by atomic force microscopy [126]. In contrast, ferromagnetic MNPs, when aligned under an H_{DC} in low-viscosity agar matrices (0.10–2.00 wt%), exhibit even more pronounced SAR increases—up to threefold—especially at low agar concentrations (0.1 wt%), where particle mobility is less restricted [10]. Similarly, the application of static fields (H_{DC} = 10-20 kA/m) parallel to the AMF during MH measurements has been shown to significantly increase the SAR of zinc ferrite nanoparticles in a concentration-dependent manner, with greater effects observed at lower particle concentrations [127].

2.2.5. Controlled Nanoscale Assembly of MNPs

An effective strategy to enhance the specific absorption rate (SAR) of superparamagnetic iron oxide nanoparticles (SPIONs) lies in tailoring their surface coating properties. Surface coatings influence both magnetic behavior and colloidal stability, ultimately impacting heating efficiency under an alternating magnetic field (AMF) [128].

Liu et al. investigated the influence of coating thickness on the SAR of Fe_3O_4 magnetic nanoparticles (MNPs) coated with phosphorylated methoxy polyethylene glycol 2000 (PEG2000). Their findings revealed that for smaller-sized nanoparticles (e.g., 9 nm and 19 nm), SAR increased as coating thickness decreased, an effect attributed to enhanced Brownian relaxation losses. Notably, the PEGylated SPIONs retained high SAR values under various physiological conditions, indicating strong colloidal and functional stability [129].

In another study, Fe_3O_4 nanoparticles coated with PEG of different molecular weights demonstrated resistance to the formation of collective coatings. This prevented the agglomeration of nanoparticles into large clusters and preserved their high SAR across environments with varying

 doi:10.20944/preprints202508.0830.v1

ionic strengths and viscosities, including distilled water, physiological saline, agar, and cell culture media [130]. Further investigations into the impact of surface functionalization demonstrated that hydrophilic SPIONs synthesized via oleate capping and subsequently modified with diverse ligands (PEG, dimercaptosuccinic acid – DMSA, cetrimonium bromide – CTAB, stearic acid – SA, and poloxamer 188 – P188) exhibited different heating profiles [131]. Ligand exchange with PEG and DMSA promoted nanoparticle dispersion, whereas intercalation with CTAB and SA or encapsulation with P188 led to agglomeration into spherical clusters. Magnetic hyperthermia experiments showed significantly higher SAR for the PEG- and DMSA-modified samples, emphasizing the detrimental effect of aggregation on heating performance [131]. Additionally, dextran-coated SPIONs with a diameter of 7 nm have also demonstrated high SAR values [132], supporting the notion that both organic and inorganic surface coatings can substantially enhance magnetic heating efficiency.

Inorganic coatings, such as gold or silica shells, have also proven effective [133]. Mohammad et al. [134] reported a 4–5-fold enhancement in SAR when SPIONs were coated with a thin gold shell (0.5 nm). Moreover, a maximum SAR value of 1300 W/g_Fe was achieved for dumbbell-shaped hybrid nanostructures comprising a 24 nm Fe_3O_4 domain attached to a 9 nm gold seed [135]. These structures benefit from synergistic effects between magnetic and plasmonic components, improving thermal response. Silica coating represents another widely used approach for surface functionalization of SPIONs [136–138]. Individual SPIONs coated with a silica shell were shown to maintain colloidal stability and avoid magnetic dipolar interactions, particularly under AMF exposure [139]. This led to superior heating performance compared to uncoated SPIONs or clusters encapsulated within a common silica shell [140–143]. These findings collectively emphasize the critical role of surface chemistry and nanoparticle architecture in optimizing the magnetic hyperthermia potential of SPIONs.

2.2.6. AFM Characteristics

In general, MH experiments demonstrate that SAR tends to increase with both the frequency (f) and amplitude (H) of the applied alternating magnetic field (AMF). However, the heat released during MH cannot be indefinitely enhanced solely by tuning these two external AMF parameters, due to both biological safety limits and intrinsic magnetic nanoparticle (MNP) properties.

First, to prevent overheating of healthy tissues due to eddy currents, safety guidelines such as the well-known Brezovich limit ($H \cdot f \leq 5 \times 10^9$ $A \cdot m^{-1} \cdot s^{-1}$) have been established [28]. Although some recent studies suggest that higher limits could be acceptable under certain conditions [144,145], García-Alonso et al. propose a more permissive threshold of $H \cdot f \leq 9.6 \times 10^9$ $A \cdot m^{-1} \cdot s^{-1}$ [146].

Second, while SAR is often assumed to scale linearly with frequency across various MNP types and sizes, its dependence on field amplitude H is more complex. For SPIONs smaller than ~10 nm, SAR typically follows a quadratic relationship with H (i.e., $SAR \propto H^2$) [48,147,148]. In contrast, for larger nanoparticles, SAR exhibits more complex field dependencies, sometimes deviating from simple power-law behavior [63]. Importantly, the quadratic dependence is generally observed only at low H; beyond this range, SAR tends to saturate [149]. This saturation effect has been correlated with the nanoparticle saturation magnetization (M_s) and is supported by numerical simulations that incorporate the field dependence of both Néel and Brown relaxation times [149]. For ferromagnetic particles, SAR saturation follows a sigmoidal trend as a function of H, a behavior that has been reported in several experimental and theoretical studies [74,100,122,127,150,151].

The saturation of SAR with increasing field amplitude (H), together with the safety constraints imposed by the H·f product limit, highlights a fundamental limitation of MH: the amount of heat that can be safely and effectively delivered to deep-seated tumors is inherently restricted. Consequently, MH alone is unlikely to achieve full tumor eradication, particularly in aggressive or resistant cancer types. For this reason, MH is more appropriately used as an adjuvant strategy, enhancing the efficacy of conventional treatments such as chemotherapy, radiotherapy, or immunotherapy. When applied in combination, MH can sensitize tumor cells to these therapies by promoting localized hyperthermia, thereby offering a synergistic anticancer approach [152]

 doi:10.20944/preprints202508.0830.v1

2.3. Organic Coating

A great deal of research was conducted on biocompatibility and cellular uptake enhancement by using synthetic polymer coating, such as polyethylene glycol (PEG), polyvinylpyrrolidone (PVP), polydopamine (PDA) and PDA analogues or natural derived coatings like chitosan and dextran (Figure 1).

2.3.1. Synthetic Polymers

PEG is one of the most common nanoparticle formulations, having wide-ranging applications by decreasing clearance and increasing water solubility. PEG forms a "stealth" hydration layer, reducing opsonization and MPS capture along with preventing hydrophobic aggregation of hydrophobic particles, shielding the NP surface from enzymes and antibodies [153–156]. Polyvinylpyrrolidone (PVP) is a colorless, water-soluble, biocompatible polymer known for its exceptional pH stability and binding capabilities, which aid in drug solubility and dispersion. Its amphiphilic structure allows it to interact effectively with solvents of varying polarities, making it versatile for constructing complex macromolecules, often via conjugation with polyacids like polyvinyl alcohol PVA or PAA. PVA-PVP composites improve mechanical strength and thermal stability along with boosting ferrimagnetic performance [157,158].

Polymerizing catecholamines leads to polydopamine (PDA) and PDA analogue polymers on the surface of the nanoparticles, particularly nanoclusters, which allow many potential applications due to their multiple surface functions. Dopamine and L-DOPA from the catecholamine class can act as surfactants and therefore can be used for making core-shell structures, in a single step by using the solvothermal/hydrothermal method of synthesis. Magnetic nanoclusters containing a magnetite core and a polymeric shell synthesized by in situ solvothermal process, using, 3,4-dihydroxybenzhydrazide (DHBH) and poly[3,4-dihydroxybenzhydrazide] (PDHBH) as stabilizers showed biocompatibility, antitumor efficacy and tumor selectivity against colon cancer cells (CACO2), melanoma cells (A375) when used for MH *in vitro* [159]. Other MNC synthetized by solvothermal polyol reaction and using as a coating dopamine, 3,4-dihydroxybenzylamine, 2-aminomethyl-3-(3,4-dihydroxyphenyl) propionamide and 3,4-dihydroxybenzylidenehydrazine yielded PDA and PDA analogues coating onto the core-shell MNCs. These nanoparticles showed good biocompatibility in normal cells (fibroblasts and endothelial cells) and melanoma (A375), and emitted a fluorescent signal, which can be used for tumor imaging purposes [160].

2.3.2. Natural Polymers

Chitosan, derived from the deacetylation of chitin (found in insect exoskeletons), carries multiple hydroxyl (–OH) and amino ($–NH_2$) functional groups, which facilitate the binding of antitumor drugs such as paclitaxel (PTX). Chitosan is biocompatible, biodegradable, and antibacterial, making it a leading candidate for nanoscale drug delivery systems. Magnetite nanoparticles coated with a chitosan shell demonstrated an 18% increase in paclitaxel adherence compared to uncoated particles [161,162]. Chitosan also exhibits stimuli-responsive release patterns due to its pH-dependent solubility, and its mucoadhesive properties, while useful in mucosal delivery, can reduce specificity by increasing the risk of off-target accumulation in normal tissues [163].

Dextran-coated IONPs are widely used due to their exceptional biocompatibility, and enhanced magnetic performance, it provides a stabilizing effect inhibiting aggregation and preserving superparamagnetic behavior. Dextran-coated IONPs have been successfully employed in drug delivery applications, with notable effects due to controlled drug release [164,165].

2.4. Combination with Other Therapeutic Methods

Although MH is apt for the induction of cell death by itself, it is particularly effective by sensitizing tumors to other treatments, its results proving significant as an adjunct therapy. For

 doi:10.20944/preprints202508.0830.v1

instance, studies point to the ability of MH to increase the proportion of complete responders to radiation therapy by 20 percentage points or more in breast, cervical and head and neck cancers [166], while a 2010 phase III trial in high-risk soft-tissue sarcoma showed that adding regional hyperthermia to chemotherapy nearly doubled the response rate: 28.8% versus 12.7% with chemotherapy alone ($p = 0.002$) [167].

Combining MH with modalities such as chemotherapy, radiotherapy, immunotherapy, and advanced drug carriers or natural compounds has shown synergistic efficacy in preclinical studies and emerging clinical applications [168]. IONPs are a central focus due to their biocompatibility and strong heat induction, but similar combination approaches are being explored with other nanoparticle types as well (e.g. gold nanostructures for photothermal therapy or high-Z radiosensitizers) [169,170].

Although both combination therapies effectively induce the death of tumor cells and stromal components, there is a risk of selecting resistant tumor cell subpopulations [171], such as anastatic cells[172], blebbishield emergency program cells [173], phoenix rising [174,175], CASP3+ islands of cells [176], nuclear expulsion cells [177], or senescence reversal [178] capable of repopulating the tumor. However, due to their multi-targeted approach, combination therapies are potentially less likely to promote emergence of resistant cells. Therefore, the most promising advancement in oncotherapy is immunotherapy and the downstream awakening of the body's own immune defense to tumor antigens released by the MH, or other therapies which can detect and attack distant and dormant tumor cells, eventually leading to a stable antitumor immunity (Figure 2).

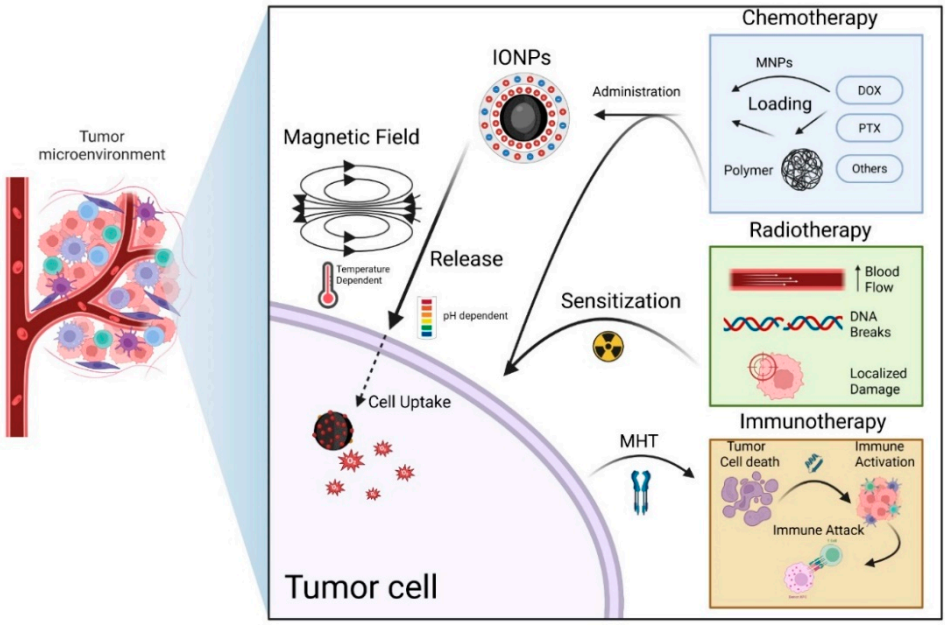

Figure 2. *Chemotherapy* **-** Nanoparticles can be loaded with chemotherapeutic agents such as doxorubicin (DOX), paclitaxel (PCT), gemcitabine, sorafenib, or platinum-based drugs (Pt), either by attaching them to surface polymers or directly incorporating them into the nanoparticles. Once internalized by tumor cells, the drug is more selectively released, a process facilitated by the hyperthermic effect or the acidic tumor microenvironment. This approach can help overcome multidrug resistance (MDR) by enhancing drug uptake and efficacy. *Radiotherapy*- Radiation therapy increases local blood flow, thereby improving nanoparticle delivery to the tumor and enhancing tumor specificity. Additionally, irradiation induces DNA damage in tumor cells, making them more susceptible to hyperthermia-induced cell death when combined with MH. *Immunotherapy* - MH combination with immune-based therapies, such as interferons, interleukins, or PD-L1 immune checkpoint inhibitors can produce a synergistic effect. Destruction of tumor cells by MH releases tumor antigens, which, in conjunction with immunotherapy, stimulates both local and systemic immune responses against the tumor, potentially improving therapeutic outcomes.

 doi:10.20944/preprints202508.0830.v1

2.4.1. Chemotherapy

Moderate hyperthermia increases tumor blood flow and cell membrane permeability, improving drug delivery to the tumor and potentiating drug uptake [179]. Furthermore, heating can interfere with DNA repair and induce apoptosis, making cancer cells more susceptible to chemotherapeutic agents. In practice, IONPs have been engineered as dual hyperthermia and drug-delivery agents: they can be loaded or coated with chemotherapeutics (like doxorubicin or paclitaxel) and then remotely heated to simultaneously release drugs and damage cancer cells. For example, in a murine model, intratumoral injection of doxorubicin-conjugated iron oxide nanoparticles in a breast cancer xenograft led to greater tumor regression under an AMF than either MHT alone or doxorubicin alone, indicating a potentiating effect of the combination [180]. Similarly, paclitaxel-loaded magnetic nanoparticles have shown synergistic efficacy with MHT: one study reported both *in vitro* and *in vivo* results that supported the conclusion that paclitaxel-bearing IONPs under AMF produced significantly higher cancer cell death and tumor growth inhibition compared to either paclitaxel or hyperthermia alone [181]. This combined approach can reduce the required drug dose (mitigating systemic side effects) while achieving enhanced tumor response (Figure 3).

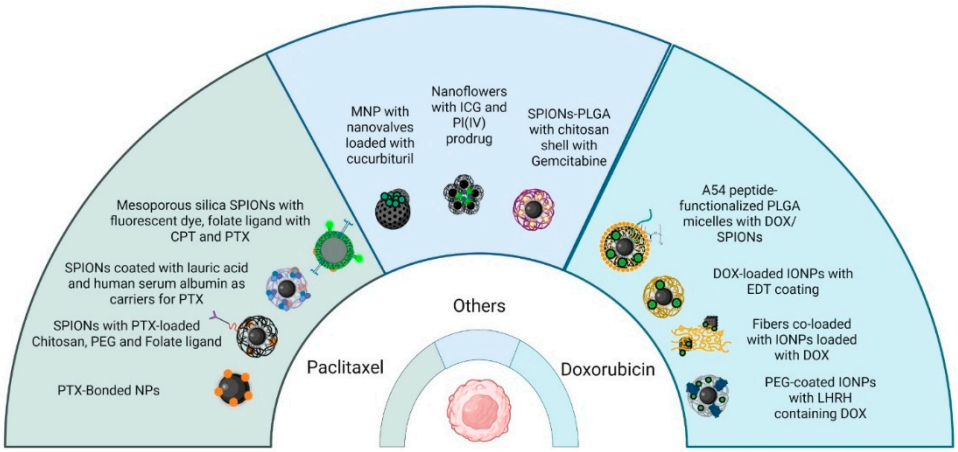

Figure 3. Schematic representation of several core-shell nanoplatforms, containing chemotherapeutic drugs. The nanoparticles with a IONPs core and various shells were loaded with paclitaxel (left), doxorubicin (right) or others (such as cucurbituril, platinum- prodrug, gemcitabine) used for tumor targeting, and combined magnetic hyperthermia with chemotherapy on in vitro/in vivo experimental models.

Thermosensitive carriers can further refine chemo-hyperthermia synergy. For instance, magneto-liposomes or polymer-encapsulated IONPs can be designed to release a payload when the local temperature rises during MHT. In one design, thermosensitive magnetic liposomes loaded with doxorubicin, and a cell-penetrating peptide achieved targeted drug release upon heating and significantly improved therapeutic outcomes both *in vitro* and in an MCF-7 xenograft murine model [182]. Thus, magnetic IONPs offer a promising prospect in the shape of thermo-chemotherapy, including noninvasive control and deep tissue penetration of the activating magnetic field, making them especially suitable for treating hard-to-reach tumors [30].

2.4.2. Radiotherapy

Heat can radiosensitize tumor cells through several mechanisms. Hyperthermia induces protein and DNA damage and can impede the repair of radiation-induced DNA breaks, thereby increasing radiation efficacy. It also improves tumor oxygenation by increasing blood flow at mild heating, countering hypoxia-driven radio resistance, until higher temperatures cause vascular collapse and direct cell killing [166]. Furthermore, while traditional hyperthermia techniques struggled to heat deep or irregularly shaped tumors uniformly [12], magnetic hyperthermia via IONPs offers a more targeted solution: IONPs can be delivered into the tumor (systemically or via direct injection) and

 doi:10.20944/preprints202508.0830.v1

then heated *in situ* by an external magnetic field, focusing thermal damage within the tumor and sparing surrounding tissue [166].

In human glioblastoma xenograft models, for instance, adjuvant magnetic hyperthermia elevated tumor cell DNA damage (γ-H2AX levels) and apoptosis when combined with radiation, translating into delayed tumor growth and longer survival in treated animals [179]. These benefits are being explored clinically. In a single-arm pilot clinical study, intratumoral MHT plus radiotherapy was tested in patients with recurrent glioblastoma multiforme. Iron oxide nanoparticles (aminosilane-coated magnetite) were injected into the tumor and an AMF applied to produce heating alongside fractionated RT. The combined treatment was found to be safe and led to prolonged survival in these patients compared to historical controls (median overall survival ~13–14 months after recurrence, which was notably longer than with radiotherapy alone) [183]. This approach has since received regulatory approval in Europe as an adjunct therapy for glioblastoma, validating the potential of clinically exploiting the properties of magnetite nanoparticles [184].

2.4.3. Immunotherapy

MH can trigger immunogenic cell death (ICD), through the release of DAMPs such as ATP, HMGB1, and calreticulin that activate dendritic and T cells, turning dying tumor cells into immunostimulants. Intracellular heating from IONPs induced broader ICD marker expression than external heating, highlighting MH's unique immunological effect [185]. Thus, MH subsumes mechanisms which, beside local tumor control, offer a pathway to systemic immune activation. Recent reviews highlight that nanoparticle-mediated hyperthermia boosts tumor immunogenicity and permeability, thereby enhancing immune cell infiltration and increases responsiveness to checkpoint inhibitors [185,186]. In one model, MH combined with anti-CTLA-4 therapy suppressed both primary and metastatic tumors, inducing long-term immune memory [187]. Other studies showed that iron in superparamagnetic iron-oxide nanoparticle can shift macrophages to a tumor-suppressive phenotype [188]. Combining MH with immunotherapy may also reduce immune escape by increasing antigen presentation and induce inflammation into the tumor microenvironment [189,190]. Although still preclinical, these findings suggest MH may help turn immunologically "cold" tumors into "hot," responsive ones.

2.4.4. Role of Natural Compounds and Polymer-Based Carriers in MH

Polymer and natural-compound–based carriers enhance IONPs function through stability, targeted delivery, and stimuli-responsive payload release. For example, quercetin-loaded chitosan-coated magnetic nanoparticles improved stability and tumor targeting in colon cancer models [191]. Similarly, polysaccharide-based magnetic hydrogels – such as chitosan-alginate combined with PNIPAM – exhibited efficient on-demand drug delivery and controlled release under AMF heating [192]. These systems improved both therapeutic specificity and systemic toxicity, making them promising platforms for combining hyperthermia and pharmacotherapy.

Polymer coatings like chitosan and PEG improve IONP stability, circulation, and drug loading. Chitosan-coated IONPs, for example, loaded ~3.2 mg doxorubicin/mg nanoparticle – six times more than uncoated versions – yielded higher *in vitro* cancer cell death [193]. PEGylated magnetite with folate or peptide ligands improved tumor uptake and PEG-stability [194]. These systems can also reduce premature clearance and minimize systemic toxicity.

Natural compounds may also synergize with MH. One PLA–PEG–curcumin–Fe_3O_4 formulation allowed AMF-triggered curcumin release and tumor shrinkage *in vivo*, outperforming curcumin or hyperthermia alone [195]. Other natural agents (e.g. resveratrol) and biodegradable hydrogels further expand MHT's versatility by enabling controlled release and retention at specific sites [192,196–198]. These strategies added multifunctionality while maintaining biocompatibility.

Another strategy for designing specific nanoparticles revolves around targeting specific receptors on the cellular membrane, leading to highly specific therapeutic benefits. Using an engineered antibody fragment, Christian Ndong and his team managed to target folate receptor

 doi:10.20944/preprints202508.0830.v1

alpha overexpressing cancer cells, which leading to high accumulation intracellularly [199]. A similar formulation was used by Monty Liong, achieving drug delivery, magnetic resonance, fluorescence imaging and cell targeting with the same formulation [200]. Formulations targeting the transferrin receptor have also been used [201,202].

2.5. Experimental Studies of Biocompatibility and Oncologic Efficiency of IONPs In Vitro

2.5.1. In Vitro Cancer Models Used for Testing of IONPs

Modern in vitro models are being used more frequently to explore novel approaches for cancer detection and treatment, including the use of iron oxide nanoparticles. These models range from 2D cell cultures, where cancer cells are grown in flat monolayers to more advanced 3D systems like tumor spheroids and organoids, which better mimic the tumor microenvironment. In addition, more complex simulated models are also employed (Table 1).

Certain 2D models have been widely adopted and have produced promising outcomes while remaining reproducible and accurate. Therefore, cancer cell lines, whether human: glioblastoma [203], lung cancer [204], breast cancer [205], cervical cancer [206], pancreatic cancer [200], hepatic cancer [207]; or murine: breast cancer/colon carcinoma [208], fibrosarcoma [209], were used to test nanoparticle cytotoxicity, cellular uptake, and drug delivery efficacy. Fibroblast-like cell lines from humans [203] and mice [209,210]) were also employed, primarily as controls. Bacteria such as Staphylococcus aureus, Proteus vulgaris, and Pseudomonas aeruginosa were used as models for the testing of the antibacterial activity of MNPs [204].

3D tumor models are generally considered more accurate than monolayer-based systems in replicating tumor physiology and predicting the response to chemotherapeutic agents. A study conducted on breast cancer spheroids revealed that MCF-7 spheroids exhibited considerable heterogeneity, with notable differences in spheroid morphology. This variability suggests that these spheroids may not be ideal for evaluating the cytotoxicity or resistance of anticancer drugs [205]. Porcine aortic endothelial cells (PAEC) were exposed to superparamagnetic iron oxide nanoparticles to assess reactive oxygen species (ROS) levels, cytoskeletal structure, and cell stiffness, yielding significant and consistent results [211].

Norouzi et al. developed an MDCK-MDR1-GBM co-culture model to replicate the human blood-brain barrier (BBB) and GBM tumor interface. As a result, the MDCK-MDR1 layer, which consisted of kidney epithelial cells genetically engineered to overexpress the human MDR1 gene, mimicked the BBB, whereas the GBM layer, which comprised human glioblastoma U251 cells, was used to assess nanoparticle uptake and cytotoxicity [212].

Table 1. Biocompatibility and anti-cancer efficacy of iron nanoparticles w/wt MH *in vitro.*

Nanoparticles	Model	Main results
IONPs with PEG coating/IONPs with PEI coating	SKOV-3 human ovarian cancer/ RAW 264.7 murine macrophages	Cytotoxic effects by ROS production and apoptosis induction [156]
SPIONs loaded with curcumin, coated with poly (lactic-co-glycolic acid)-poly (ethylene glycol) di-block copolymer (PLGA-b-PEG)conjugated with	T98G-glioblastoma multiforme, fibroblast -like cell line	Induced cytotoxic effects increased by exposure to radiofrequency hyperthermia application [203]

 doi:10.20944/preprints202508.0830.v1

glycine-arginine-glycine-aspartic acid-serine (GRGDS)		
IONPs	A549 human lung cancer cell line Staphylococcus aureus, Proteus vulgaris, Pseudomonas aeruginosa	Cytotoxic effect Antibacterial effect through ROS generation [204]
SPIONS- functionalized with SDS and loaded with curcumin and coated with chitosan SPIONs-SDS-CU-CHIT	HeLAa human cervical cancer	Decreased viability in a dose and time related manner related to drug release in the medium [206]
green iron nanoparticles (Rosemary-FeNPs)	4T1 murine breast cancer C26 cancer cell lines	Cytotoxic effect against cancer cells, efficient intracellular delivery of the rosemary flavonoid components [208]
Bare superparamagnetic iron oxide nanoparticles (SPIONs)	Porcine aortic endothelial cells (PAEC)	ROS formation leads to morphological changes and forms actin stress fibers; blocking ROS formation by functionalization could increase medical applications [211]
IONPs coated with chitosan IONPs coated with polyvinyl alcohol (PVA)	Human fibroblasts	IONPs coated with chitosan induced mild toxicity, IONPs coated with PVA were well tolerated [222]
ferumoxytol carboxymethyldextran coating	mammary adeno carcinoma cells incubated with macrophages	Macrophages showed pro-inflammatory M1 phenotype upon ferumoxytol exposure Increased caspase -3 in mammary tumor cells [305]
IONPs load with LLY-507 (inhibitor of SMYD2), coated with PVA	A549 human non-small cell lung cancer cell line RBC- human	Efficient delivery of the SMYD2 inhibitor by the IONPs , dose dependent decrease in viability, hemolysis below 5%[306]
poly(ethylene glycol)-*block*-poly(lactic-*co*-glycolic acid) copolymer-encapsulated Fe_3O_4 superparticles (SPs), loaded with imiquimod	4T1 triple negative human breast cancer cells	Efficient photothermal ablation of 4T1 cells by apoptosis/necrosis upon PTT irradiation, efficient delivery of R837 in vivo against primary tumors to enhance immune response [307]

 doi:10.20944/preprints202508.0830.v1

(R837 a Toll-like receptor 7 agonist)		
Fe_3O_4@PDA SPs	HeLa human cervical cancer cell line, mice bearing tumor (HeLa)	Biocompatible, increased efficacy of photothermal therapy against tumors in vivo [308]
IONPs - loaded with curcumin and coated with dextran CUR/DEX/Fe3O4-NPs	MCF-7 human breast cancer	Decreased cell viability in a dose and time related manner [309]
SPIONS- functionalized with SDS and loaded with curcumin and coated with chitosan SPIONs-SDS-CU-CHIT	HeLAa human cervical cancer	Decreased viability in a dose and time related manner related to drug release in the medium [310]

2.5.2. MNP Formulation

The primary type of iron-based nanoparticles used in cancer therapy are iron oxide nanoparticles (IONPs), known for their magnetic properties and biocompatibility. Among these, superparamagnetic iron oxide nanoparticles (SPIONs) are particularly significant, as they facilitate magnetic drug targeting, MH, and function as contrast agents in MRI [200]. There are two main approaches in the study of iron nanoparticles used in cancer therapy research, (1) functionalized bare nanoparticles, evaluated for their biocompatibility, tumor-targeting ability, and cytotoxic effects w/wt MH and (2) drug-loaded nanoparticles, designed for delivering chemotherapeutic agents, photosensitizers, or for use in combined MH and chemotherapy [217].

Natural compounds rich in antioxidants serve a dual purpose in nanoparticle synthesis: they act as reducing agents that promote nanoparticle formation and prevent aggregation, and they function as coatings that enhance the biocompatibility of magnetic nanoparticles (MNPs) by forming a natural antioxidant shell. Additionally, these compounds facilitate the targeted delivery of bioactive agents into tumor cells. Many cancer cells are particularly sensitive to polyphenols, resveratrol, flavonoids or anthocyanins [213] present in natural extracts, which can trigger apoptosis or increase the cells' responsiveness to other treatments, such as chemotherapy, photodynamic therapy (PDT), or hyperthermia. Natural compounds, such as polyphenols, synergize with anticancer drugs like cisplatin, doxorubicin, and 5-fluorouracil [214]. Rosemary terpenes also showed antitumoral activity on colon cancer cells in vitro inducing necrosis by an acute ROS increase and on in vivo colon cancer models, they inhibit proliferation and increased animal survival [215]. Green iron nanoparticles (Rosemary-FeNPs) phyto synthesized by using the natural antioxidants from the rosemary extract showed an average diameter range of 50-100 nm and excellent homogenization [208]. Turmeric extracts and their key compounds, carnosic acid and curcumin also showed antiproliferative effects of cancer cells [216]. SPIONs loaded with curcumin and coated with organic polymers, poly (lactic-co-glycolic acid)-poly (ethyleneglycol) di-block copolymer (PLGA-b-PEG) conjugated with glycine-arginine-glycine-aspartic acid-serine (GRGDS). GRGDS peptide has been found to allow targeting of integrins, typically overexpressed in cancer cells, moreover the combined delivery of curcumin enhanced therapy efficiency and can serve as a drug delivery platform for a chemotherapeutic in view of a synergistic effect [203]. Multiple chemotherapeutic drugs, such as paclitaxel (PTX) [200,217], doxorubicin (DOX) [207,212,218], camptothecin (CPT) [200], gemcitabine [219], sorafenib [220], temozolomide [179] were loaded on magnetic nanoparticles. Despite its efficiency as an antitumor drug, Paclitaxel (PTX) administration is difficult due to its hydrophobic nature. To address this issue,

 doi:10.20944/preprints202508.0830.v1

MNPs loaded with PTX were synthesized using chitosan as coating: Fe_3O_4@LaF_3: Ce^{3+}/Tb^{3+}/chi NPs associated with Paclitaxel (PTX). This formulation increased the water-solubility, of PTX while preserving the superparamagnetic behavior of the MNPs, and provided a biocompatible method for Paclitaxel administration with reduced side-effects and possibility for a synergic therapy using MH and chemotherapy (Table 2) [217].

Folic acid receptors are overexpressed in many cancers; therefore folic acid can be used for selective targeting of the malignant cells cancers including ovary, kidney, uterus, testis, brain, colon, lung, myelocytic blood cells [221]. This strategy was used for the synthesis of PTX-loaded nanoparticles, such as SPIONs with PTX-loaded chitosan (Cs), polyethylene glycol (PEG), and folic acid (FA), and yielded improved tumor targeting and PTX uptake in the malignant cells [209]. A study on SPIONs- PLGA core / poly(N-isopropylacrylamide)-carboxymethyl chitosan shell with NU7441/Gemcitabine found that targeting folate receptors increased specific uptake, while the pH-sensitive shell ensured gemcitabine was preferentially released in the tumor environment. The nanoplatform retained magnetic properties, which make it suitable for combined MH and chemotherapy combined therapy [219]. Another coating, such as lauric acid (LA) and human serum albumin (HSA) was used for the synthesis of SPIONs (SPION-LA-HSA-Ptx) for the delivery of PTX. The presence of lauric acid improved the PTX hydrophobic drug loading and nanoparticle stability, while LA and HSA increased MNPs biocompatibility and colloidal stability [205]. Magnetic nanoparticles coated with an amphiphilic polymer containing disulphide linkages (hyaluronic acid-disulfide bond-polylactic acid) loaded with PTX showed efficient drug delivery by combining magnetic tumor targeting and redox-triggered specific release of paclitaxel, leading to improved therapeutic efficacy and minimizing side effects [206]. Mesoporous silica-coated SPIONs with fluorescent dyes, hydrophilic groups, cancer-specific targeting ligands, and co-loaded with camptothecin (CPT) and paclitaxel (PTX) showed advantages in magnetic manipulation, targeted drug delivery, and efficient drug loading and release [200].

A54-Dex-PLGA micelles with DOX exhibited strong encapsulation efficiency (approximately 80%) and prolonged release (up to 72 hours). MNPs demonstrated tumor targeting and enhanced efficacy compared to free medication [207]. Doxorubicin-loaded IONPs with surface coatings such as trimethoxysilylpropyl-ethylenediamine triacetic acid (EDT) were also effective, as EDT coating had a significant impact on blood-brain barrier penetration. Furthermore, this formulation achieved sustained DOX release, with quicker release in acidic conditions (tumor microenvironment), allowing for more tailored therapeutic action [212]. The DOX-loaded Fe_3O_4@MnO_2@PPy nanocomposite improved hypoxia tolerance and PDT efficiency by integrating photothermal, photodynamic, and chemotherapeutic treatments [218].

SPIONs synthesized by using a double coating of polyvinyl alcohol (PVA) or polyethylene glycol (PEG) and magnesium–aluminum-layered double hydroxide (MLDH) were loaded with Sorafenib. The resulting nanoparticles were spherical, with an average diameter of 17nm and released sorafenib over a period of 72 hours, more effectively when exposed to an acidic pH (4.8), simulating tumor microenvironment. This system showed increased toxicity towards HepG2 hepatoma cells and decreased towards fibroblast 3T3 cells, which served as controls, compared to sorafenib [220].

Table 2. Biocompatibility and anti-cancer efficacy of iron nanoparticles w/wt MH *in vitro.*

PACLITAXEL		
Nanoparticles	**Model**	**Main results**
Multifunctional mesoporous silica nanoparticles SPIONs Surface modifications: Fluorescent dye molecules/ Hydrophilic groups / Cancer-specific targeting ligands –	Human pancreatic cancer cell lines: PANC-1, BxPC3, human foreskin	Selective cytotoxicity; dual imaging capability; targeted drug delivery through ligands (FA) [200]

 doi:10.20944/preprints202508.0830.v1

folate (FA), Drugs: Camptothecin (CPT) /Paclitaxel (PTX)	fibroblasts (HFF) as control	
SPIONs coated with lauric acid and human serum albumin as carriers for paclitaxel (SPION-LA-HSA-Ptx)	human breast cancer cell lines (T-47D, BT-474, MCF-7, and MDA-MB-231 cells)	High potential for magnetically targeted drug delivery in breast cancer Similar effects on human breast cancer as PTX alone [205]
SPION@Cs-PTX-PEG-FA SPIONs with paclitaxel (PTX)-loaded chitosan (Cs), polyethylene glycol (PEG) and receptors that target folate (FA)	WEHI-164: Mouse fibrosarcoma; MEF: Mouse embryonic fibroblast (normal) cell line	High nanoparticle stability, selective uptake, reduced systemic toxicity due to the FA receptors, apoptosis of cancer cells [209]
Fe_3O_4@LaF_3:Ce^{3+},Tb^{3+}/chi NPs bonded with Paclitaxel (PTX)	A549 human lung cancer cell line	Increased cell toxicity compared to free paclitaxel; efficient imaging (MRI and fluorescence imaging); reduced side effects [217]
MNPs coated with an amphiphilic polymer containing disulfide linkages (Hyaluronic Acid–disulfide bond–Polylactic Acid, HA-SS-PLA), loaded with PTX	HeLa cells human cervical cancer cell line)	Targeted delivery, through magnetism and redox response; improved cytotoxicity, and biocompatibility [311]
DOXORUBICIN		
A54 peptide-functionalized poly(lactic-co-glycolic acid)-grafted dextran (A54-Dex-PLGA) micelles with DOX/ SPIO	BEL-7402, HepG2 hepatic cancer	MNPs easy synthesis of SPIO, low off-target distribution and toxicity; controlled drug release; dual imaging/ therapy function [207]
Electro-spun fibers co-loaded with magnetic IONPs, cubic shaped loaded with doxorubicin	Mouse embryonic fibroblast cell line (NIH 3 T3 cells), DOX-sensitive HeLa-WT cervical cancer cells and the DOX-resistant MCF7 breast cancer cells	Hyperthermia combined with enhanced diffusion of doxorubicin - effective oncotherapy [210]
Doxorubicin-loaded IONPs with surface coatings like trimethoxysilylpropyl-	MDCK-MDR1-GBM co-culture model	High DOX penetration through BBB; effective magnetic targeting and reduced systemic toxicity; possibly overcoming MDR cancer cells [212]

 doi:10.20944/preprints202508.0830.v1

ethylenediamine triacetic acid (EDT)		
Fe_3O_4@MnO_2@PPy nanocomposite loaded with DOX; Fe_3O_4 (Iron oxide) core; MnO_2 (Manganese dioxide) shell; PPy (Polypyrrole) outer layer	human hepatoma (HepG2)	Good magnetic targeting delivery and enhanced cancer toxicity improved photodynamic (PDT) /photothermal therapy (PTT) reduced side effects and better tolerance to hypoxia induced by PDT/PTT [218]
IONP DOX: PEG-coated, doxorubicin-loaded nanoparticles	HeLa cells (human cervical cancer cell line)	Delivery of DOX directly into the cytoplasm trough macro pinocytosis and endocytosis; high biocompatibility [223]
PEG-coated Fe_3O_4 luteininzing hormone-releasing hormone (LHRH) ligand containing doxorubicin	A549 and MCF-7 cancer cells	Theranostic nanoparticle formulation using LHRH ligand with individual chemotherapy and thermotherapy, effective on both cell lines [312]
OTHERS		
Magnetic IONPs/ temozolomide	SD3, G-16, G-302, GL-261 cell lines	Combined hyperthermia using magnetic IONPs with temozolomide and radiation showed synergistic anti-glioblastoma effects [179]
SPIONs- PLGA core / poly(N-isopropylacrylamide)-carboxymethyl chitosan shell with NU7441/Gemcitabine	A549 and H460 lung cancer cells	Approach for simultaneous radiotherapy and chemotherapy, Folate receptor targeting increased specific uptake [219]
SPIONs- (PVA/LDH-coated and PEG/LDH-coated) with Sorafenib	HepG2 human hepatoma/ 3T3 mouse fibroblast cell line	Strong superparamagnetic behavior; enhanced anticancer activity and selectivity; minimal side effects [220]
Magnetic-core silica nanoparticles with nano valves and loaded with cucurbituril	MDA-MB-231 breast cancer cells	Targeted delivery using a nano valve system and hyperthermia [313]
Fe-NP2 coated with PEI conjugated with cisplatin (IV) prodrug	Human ovarian carcinoma A2780 cells / cisplatin-resistant A2780DDP cells	Efficient drug delivery overcoming cisplatin resistance through unique internalization pathway of nanoparticles/ increased production of ROS [314]
Phospholipid-modified Pt(IV) prodrug-loaded IONP-filled micelles	B16-F10 melanoma cells	Redox-triggered release of cisplatin, ferroptosis of melanoma cells, lower concentration threshold, lymphatic delivery [315]

 doi:10.20944/preprints202508.0830.v1

Nanoflowers MoS_2@Fe_3O_4-loaded with ICG/Pt(IV) indocyanine green (ICG) and platinum (IV) prodrugs {c,c,t-$Pt(NH_3)_2Cl_2(OOCCH_2CH_2COOH)_2$}	I.929 fibroblasts, HeLa, H22 tumor-bearing Balb/c mice	Biocompatible, theranostics bioimaging capabilities and laser-induced cytotoxicity [316]
Fe(Salen) nanoparticles with μ-oxo N,N′-bis (salicylidene) ethylene diamine	tongue cancer VX2 (rabbit), HSC-3 (human), and OSC-19 (human)	Hyperthermia-guided, temperature stable cytotoxic effects, even at low concentrations [317]

2.5.3. Eficiency, Side Effects

Iron nanoparticles have been widely studied and applied in cancer therapy due to their effectiveness in targeted treatment, imaging, and hyperthermia, along with their generally favorable biocompatibility.

MNPs cytotoxic effects may arise either through hyperthermia-induced mechanisms [203] or from the intrinsic properties of the nanoparticles themselves [204]. Functionalization has been shown to enhance both cytotoxicity against cancer cells and intracellular targeting. MNPs incorporating rosemary flavonoid compounds demonstrated improved efficacy [208]. Tran et al showed that chitosan or PVA coating of iron oxide nanoparticles reduced the cell toxicity towards normal mouse fibroblasts, with PVA coating having a better result and also reduced nanoparticle aggregation, underscoring the role of surface coating for biocompatibility [222].

The generation of reactive oxygen species (ROS) has been identified as a key mechanism driving the biological activity and toxicity of nanoparticles, contributing not only to their antibacterial effects [204] but also to cellular morphological changes and the formation of actin stress fibers [211]. Overall, the use of iron nanoparticles loaded with various anticancer agents has proven beneficial, improving therapeutic effectiveness and targeting specificity while minimizing adverse side effects. MNPs loaded with PTX demonstrated enhanced tumor cell toxicity compared to free paclitaxel, with less side effects and increased imaging properties, by both MRI and fluorescence imaging [217], induced apoptosis in cancer cells [209], demonstrated a high potential of PTX-loaded SPIONs for magnetically based targeted drug delivery in breast cancer, but the effects were similar to those of PTX alone [205]. PTX-loaded MNPs were used for targeted administration, which combined magnetic drug delivery with redox dependent release to increase cytotoxicity [206].

DOX-loaded nanoparticles also demonstrated significant potential for cancer treatment. Doxorubicin-loaded IONPs with surface coatings such as trimethoxysilylpropyl-ethylenediamine triacetic acid (EDT) were able to overcome MDR cancer cells in a GBM model, combined with magnetic targeting and low systemic toxicity [212]. Popescu et al. presented direct delivery of DOX loaded nanoparticles into the cytoplasm via macropinocytosis and endocytosis, with promising future possibilities [223]. Fe_3O_4@MnO_2@PPy nanocomposites used DOX-loaded nanoparticles to deliver the chemotherapeutic and enhance two types of phototherapy (PDT and PTT) at the tumor site, resulting in more effective cancer treatment [218].

2.5.4. Type of Cell Death

- Apoptosis

Nanoparticles, depending on their dose and physicochemical properties, can influence various cell fates (Figure 4), including necrosis and apoptosis [224]. Apoptosis is a distinct type of cell death characterized by particular morphological changes, such as membrane blebbing, cell shrinkage,

 doi:10.20944/preprints202508.0830.v1

chromatin condensation, and tiny vesicles (apoptotic bodies) [225]. The most important apoptosis mechanisms occur via three different pathways involving death receptors, mitochondria, or the endoplasmic reticulum, with caspases mediating all morphological and biochemical changes [226,227]. As a result, multiple studies indicate the necessity of linking nanoparticle dosage and exposure time with apoptotic intensity, such as the one published by Naqvi et al., who examined SPIONs coated with Tween 80 on murine macrophage (J774) cells. Cell viability was higher at lower concentrations (25-200 μg/mL) and up to three hours of exposure but decreased to 55-65% at higher concentrations (300-500 μg/mL) and longer exposure (six hours). According to the same study, apoptosis was the main registered cause of cell death, with oxidative stress serving as the primary toxicity mechanism. [228] Functionalized iron oxide nanoparticles, particularly those conjugated with therapeutic agents (such as, IONs conjugated with lysine and methotrexate tested on breast cancer), can effectively induce apoptosis in cancer cells *in vitro* [229]. Tousi et al. found that mPEG-b-PLGA coated IONs loaded with the flavonoid eupatorin increased apoptosis and decreased necrosis in prostate cancer cells compared to free eupatorin or uncoated nanoparticles, suggesting that they could be an effective drug delivery system for cancer therapy [230].

- Necrosis

Necrosis has long been thought to be the outcome of general cell injury caused by trauma. As a result, it is seen as an uncontrolled form of cell death that is not caused by specific signaling processes. Various clinical circumstances, including toxin exposure, ischemia, viral or bacterial infection can cause necrotic cell death [224]. Also in this case, the key mechanism appears to be reactive oxygen species (ROS), as supported by Khan et al. The study reveals that ROS generated by iron oxide nanoparticles lead to necrosis and cell death in lung cancer cells (Figure 4). The type of cell death (necrosis vs. apoptosis) is determined by the level of oxidative stress and the cellular antioxidant capability [231]. Another study found that certain coatings and greater doses of IONPs can cause necrosis, notably PEI-coating, which is known to be cytotoxic and damage the cell membrane [156]. There are just a few in vitro studies that particularly address necrosis caused by iron nanoparticles (figure 4). Most of the studies focus on apoptosis, with necrosis as a secondary consequence at higher doses, frequently related to increased oxidative stress or membrane damage [228,232].

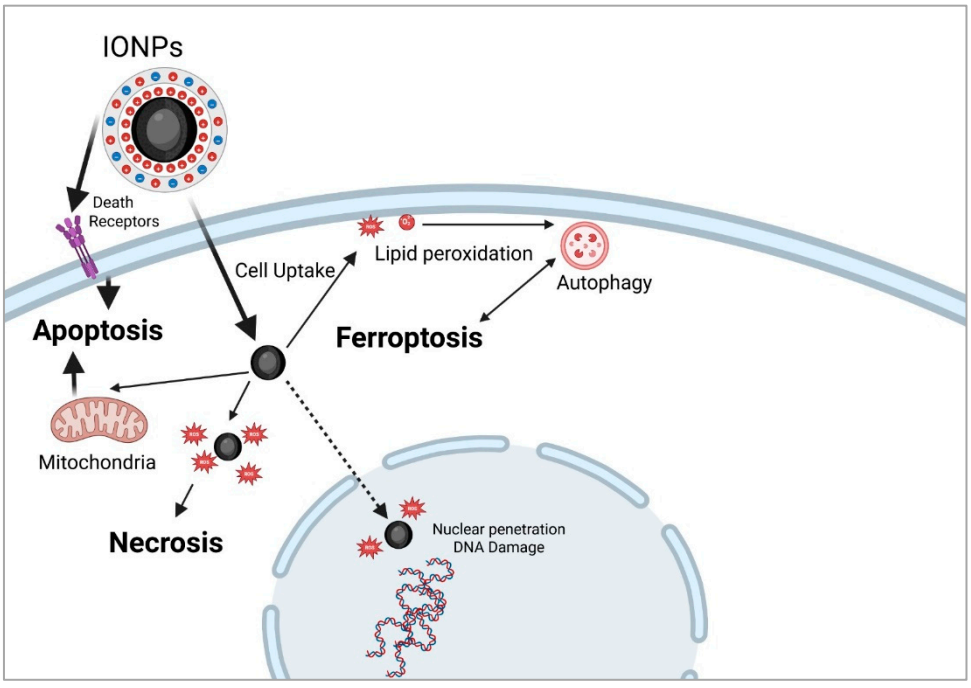

Figure 4. Mechanisms of cell death induced by magnetic hyperthermia. Following cellular uptake, and exposure to an alternating magnetic field (AMF), MHT triggers apoptosis via either the membrane pathway, through death receptor activation, or the mitochondrial pathway, both leading to caspase cascade activation. Higher

 doi:10.20944/preprints202508.0830.v1

temperatures, nutrient deprivation, or combined therapies favor necrosis, typically caused by rapid ROS accumulation that overwhelms antioxidant defenses, leading to terminal oxidation of cellular components. ROS can also damage nuclear DNA, leading to necroptosis or activating DNA repair. Ferroptosis results from intracellular iron buildup, which generates ROS through Fenton reactions, and causes lipid peroxidation. This process can culminate in cell death or trigger autophagy, particularly described on *in vivo* models, with lysosomal activation. Autophagy may enable cell survival by recycling damaged organelles to provide energy and restore cellular functions acting as a tumor escape mechanism. However, when damage is extensive, autophagy serves as a programmed cell death pathway.

- Ferroptosis

Ferroptosis represents a type of cellular death due to lethal accumulation of iron intracellularly. Ferroptosis is mainly caused by accumulation of reactive oxygen species, that lead to lipid peroxidation, cellular membrane instability and eventually, cellular death. One of the main pathways in which IONPs act to induce ferroptosis is by intracellular accumulation, internalization in lysosomes which act to dissolve the formulations, leading to release of iron ions intracellularly (figure 4). Ferroptosis is driven by ferrous iron through Fenton reactions, generating reactive oxygen species (ROS, among these, radical hydroxyl, HO•, responsible for lipid peroxidation intensifying) [233], disruption of mitochondria functions [234,235], cellular membrane rupture [236], and other alteration processes at ultrastructural levels (endoplasmic reticulum, peroxisomes, etc.) [237,238]. Antioxidant defenses, through the cysteine/glutamate antiporter and FSP1/ubiquinol systems are overloaded. Ferroptosis represents an attractive target for current and future anticancer therapies as tumor cells are surprisingly susceptible to its effects. [239–241]. *In vivo*, ferroptosis (iron-dependent cell death) was considered a helpful mechanism that may destroy the tumors but the accumulation of IONPs in healthy tissues limited the usage of this therapeutic method. Medication associated with ferroptosis such as Lanperisone, Sorafenib, Trigonelline, Cisplatin, Ferumoxytol etc. is used in cancer [233], as a therapeutic method only affecting tumors. IONPs are especially suitable for inducing ferroptosis through several mechanisms and may act as theranostic, providing multiple capabilities at the same time. Another strategy concentrates on creating synergistic therapies, for example, Qi Nie and her research team used IONPs loaded with paclitaxel (PTX) to increase intracellular concentration of iron ions, with higher ROS formation and confirmed ferroptosis by evaluating cellular upregulation as a response to ferroptosis [242], results that were echoed by a similar article focusing on inhibiting non-small cell lung cancer cells. Ferroptosis appears to be associated with autophagy, as several studies presented this possible correlation [243,244]. Autophagy, the physiological cellular removal and replacement of degraded organelles represents a mechanism that protects against tumor development or destroys healthy cells. When the stressors, like IONPs, accumulate in healthy tissues, intracellular environment is modified toward the production of reactive oxygen species in high concentration that induce damage inside the cells and transforms autophagy into a cancer promoter [245].

2.6. Biocompatibility and Oncologic Efficiency of IONPs In Vivo

In vivo studies were realized for theranostic purposes of magnetic iron oxide nanoparticles (IONPs), superparamagnetic iron oxide nanoparticles (SPIONs), surface-coated IONPs, charged polyvinyl alcohol-coated SPIONs (PVA-coated SPIONs), protein-coated IONPs, SPIONs coated with anti-biofouling polymers etc. Technological advances permit the drug delivery at nanoscale inside the tumor, the small dimensions and coating giving the possibility of their transport even through tumor stromal components.

2.6.1. Biodistribution

IONPs biodistribution depends on several factors such as the nanoparticle's dimension and shape the type, chemical composition, or electric charges of their coating, properties that make them able to also migrate in healthy tissues. In living organisms, iron oxide nanoparticles may follow

 doi:10.20944/preprints202508.0830.v1

different pathways, especially depending on their dimension (Figure 5). Nanoparticles with diameters higher than 100 nm are rapidly captured in spleen and liver, and their penetration inside the tumor is limited by the tumor pathological characteristics of the vessels' wall, that differ with the cancer type and stage [246]. Wang et al. showed that after oral administration of IONPs with dimensions lower than 100 nm in mice, the liver was exposed to two picks of nanoparticles concentration, in the first day and in the seventh day. These particles also accumulated in other organs, with maximum levels: at 6 hours after gavage (lungs, kidneys), in the first day (stomach, small intestine, bone marrow) and during the first 3 days (heart, spleen, brain) [247].

IONPs with dimensions between 20 nm and 100 nm are preferred for cancer treatments, to avoid IONPs urinary excretion (< 20 nm) and spleen/liver capture (> 100 nm) [248]. Several studies presented their role on vascular permeability. In tumors with reduced vascularization, administration of IONPs coupled with external magnetic field exposure leads to endothelial layer alterations, increasing the accumulation of drugs inside the cancer area [249]. Endothelium permeability may also be increased by IONPs through the oxidative stress that they generate, reorganizing the microtubules position in the cellular cytoskeleton [250].

Small IONPs, with dimensions lower than 20 nm, may pass easily the endothelium toward different organs and may be filtered by the kidneys, processes that occur when they are administered intravenously, orally or when they migrate from the tumor back into the blood flow [251]. Since the endothelial glycocalyx presents 20 nm gaps between proteoglycan chains, the small nanoparticles can pass freely the healthy endothelium layer [252]. At tumor level, endothelial layer develops pores of 100 nm till 1 μm (pores dimensions depend on cancer type and stage) that are passed easily by the small IONPs (<20 nm) [253].

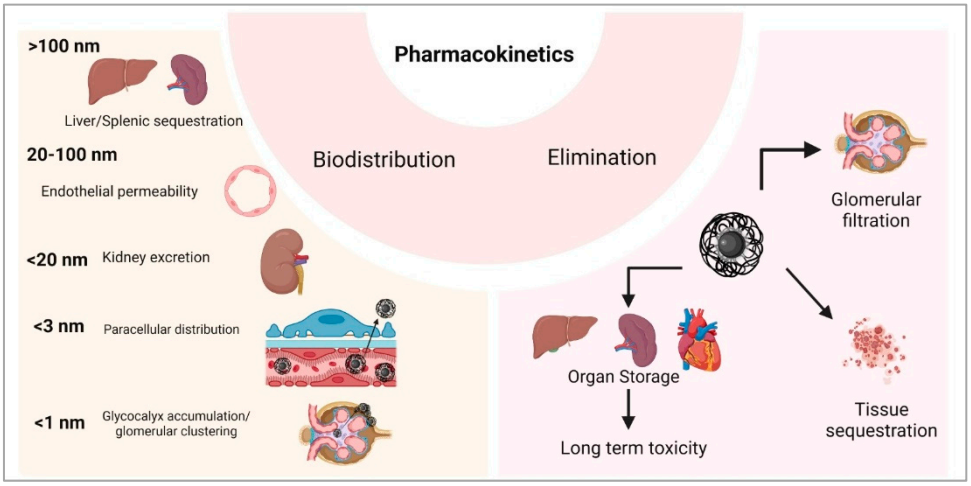

Figure 5. Pharmacokinetics of IONPs in vivo after systemic administration or vascular leakage post-intratumoral injection. Biodistribution of the MNPs strongly depends on their size, with nanoparticles between 20-100 nm diameter being the most suitable for MHT, due to their ability to pass through the endothelial layer into the tissue leading to selective tumor accumulation (EPR effect), that can be enhanced by application of an external magnetic field. Smaller particles (<1 nm) are fast eliminated by the kidney or can cluster into the glomerular cells glycocalyx leading to impaired nephron function, while bigger MNPs (>100nm) can be stored in the internal organs, leading to medium/long term toxicity.

Injected IONPs with sizes lower than 10 nm are excreted in large amounts through urine. Studies showed that more than 40% of administered IONPs were eliminated within 24 hours after administration. PEGylated IONPs with dimensions around 10 nm are transported easily inside the cells, accumulate in high concentrations inside the tumors, but also in spleen and liver where their degradation is realized very slowly (Figure 5). The PEGylated IONPs are toxic at high concentrations and may trigger the autophagy [156].

 doi:10.20944/preprints202508.0830.v1

IONPs with sizes lower than 3 nm can pass through the vessel wall also paracellular [254], while those of around 1 nm are blocked in the glycocalyx of the glomerular filtration membrane, forming nanoclusters that remain for a long time at kidney level [255].

2.6.2. Coating

For drug delivery, IONPs are coated with different materials: natural polymers (dextran, chitosan, starch, etc.) [256], synthetic polymers (polyethylene glycol -PEG; polyvinyl alcohol -PVA; polyvinyl pyrrolidone -PVP; etc.) [256,257], proteins (albumin) [258], lipids [259], silane [260], silica [261] or combination of synergistic materials [262]. To avoid the IONPs agglomeration that can produce embolism inside the capillaries [263] and to prevent the nanoparticles rapid systemic dispersion, amines, aldehydes, thiols or the carboxylic acids are used for IONPs synthesis [264]. Iron nanoparticles can be synthesized with specific coating that may increase the cytotoxicity of the transported drug, like gold-coated IONPs [265], or with coverings that may present a prolonged drug release, even over 4 days after their administration, like hyaluronic acid-coated IONPs [266]. Intraperitoneal administration of gold-coated IONPs in mice with melanoma tumor leaded to nanoparticles accumulation in high amounts in tumor area but also in spleen, liver, kidney, lungs and brain, with ultrastructural modification at tissue levels [267].

2.6.3. Shape

Iron nanoparticles were developed in different shapes: cubes, concave cubes, spheres, tetrahedrons, hexagons, octahedrons, octapods, polypods [268], ellipsoids, discs, cylinders, cones, hemispheres, etc. [248]. The shape of IONPs is very important for their transport through the circulatory system and for the drug delivery to the target tissue. The elongated drug carriers travel through the blood stream closer to the vessel wall, compared to the spherical nanosystems, margination property that permits the easier transport of these nanoparticles into the adjacent tissues [269]. The spike-shaped IONPs adhere easily to the endothelium while the lengthen-shaped IONPs interact with the vessel wall through the long axis, mechanisms that keep these drug delivery systems attached to areas that may not be of treatment interest, blocking their transport toward the tumor zone, when they are administered through intravenous or intraarterial injections [270]. The spherical nanoparticles are transported easier along the circulatory system because of their small area of contact [248].

2.6.4. Electrical Charge

Zeta potential of iron nanoparticles affects their cellular uptake. Several studies present a higher internalization when IONPs zeta potential is positive [271]. IONPs penetration inside the cells is affected by their size, chemical composition of coating, hydrophobicity, or by the proteins that can attach to them. Administration of IONPs with positive zeta potential (30 nm, 10 mg/kg, for 8 days) in pregnant mice produced fetal death and accumulation of nanoparticles in fetal liver and placenta [272]. PEGylated IONPs, through its hydrophilic properties, has prolonged systemic circulation, while PVP-coated IONPs has anti-opsonization properties [248]. The cell type exposed to IONPs is also important, affecting the nanoparticles internalization [273]. Cancer tissue is more acidic than the healthy zones of the body, a tumor feature that stimulated the development of IONPs that can attach and release the drug in a pH-controlled manner [274].

2.6.5. IONPs Internalization

Inside the cell, IONPs can bind different molecules or ions, leading to reactions that may affect the desired result [275]. Nanoparticles are captured by lysosomes (spherical IONPs) or are transported in endosomes (spherical, elongated, or spiked IONPs along the microtubules till the storage and processing area. Inside the cell, the ultrasmall spherical IONPs are rapidly transported to the nucleus, inhibit DNA synthesis and activate apoptosis [276]. Similar effects on DNA were in a

 doi:10.20944/preprints202508.0830.v1

study performed in mice with intravenous administration of ultrasmall IONPs (4 - 6 nm) [277]. The hexagonal-shaped nanoparticles remain in the cytoplasm [248] where they initiate oxidative stress.

2.6.6. Immune Response Following IONPs Administration

Systemic administration of IONPs triggers complex responses of the organism. The administration of iron nanoparticles through inhalations, injections (intraperitoneal, intravenous, intraarterial) or through oral gavage decreases the immune responses, suppressing the activity of helper T lymphocytes [278,279]. Macrophages easily phagocytize iron nanoparticles of large dimensions [280], with positive zeta potential [281] or spherical-shaped. The elliptical nanoparticles are phagocytized by macrophages in less than 6 minutes if the first contact with the cell is realized with the major axis perpendicular on the phagocyte membrane [282], while other approaches delay the phagocytosis for hours [283]. The worm-shaped IONPs avoid the macrophages phagocytosis [284] and present a higher accumulation inside the tumor compared to spherical nanoparticles [285].

2.6.7. Routes of Administration and Toxicity

Intratumoral injection of IONPs could be considered the most efficient because it avoids the systemic complex responses, but the possibility of migration from the cancer area into the circulatory system or into the surrounding areas cannot be neglected and must be explored. The iron nanoparticles can be synthesized in shapes, dimensions and chemical compositions for the transport and release of the drug in a controlled manner and can be used for magnetic hyperthermia to induce the apoptosis of tumoral cells. Wojtera et al. investigated the importance of iron content in nanostructures exposed to radio electromagnetic fields and demonstrated that a higher iron concentration produced a higher heat [286].

Applying an electromagnetic field for the transport of iron nanoparticles toward the tumor area can interfere with other electromagnetic fields (wi-fi, static magnetic fields, etc.) [287,288] and the response of IONPs depends not only on their dimension but also on their composition, local structure of IONPs assemble organized under magnetic field effects, etc. [289]. The number and the arrangement of blood vessels inside the tumor can also affect the drug delivery [290]. The IONPs transport through tissues toward the tumor area using an external electromagnetic field may disrupt healthy organs and vessels functions, processes that can be avoided by choosing the intratumorally administration route. Johannsen et al. injected intratumorally 13 nm IONPs in rats with prostate cancer for magnetic hyperthermia (45 °C or 50°C, for 30 minutes) that led to homogenously distributed nanoparticles inside the tumor, but not all the animals survived [291].

Toxicity of IONPs depends on different factors related to the nanoparticle's properties, healthy tissues characteristics, tumor specificity, electromagnetic fields, etc. [292]. Wu et al. presented the important role of nanoparticles dimensions in IONPs toxicity. The intravenous administration of 2.3 nm or of 4.2 nm IONPs, 100 mg/kg, produced the mice death, probably of cardiac cause, the results showing increased oxidative stress in heart, lung, liver, spleen and serum. The death of mice was not recorded when the same dose was administered of 9.3 nm IONPs size [45]. Oral administration of 30 nm IONPs, through gavage for 5 days, in Wistar rats, showed that 500 mg IONPs/kg leaded to anorexia and lethargy while 5000 mg IONPs/kg had severe effects like ataxia, respiratory arrhythmia with hemorrhages in the lungs and in the heart, and liver degeneration [293]. A previous study noticed the noxious effects on liver of Wistar rats when a lower doze of IONPs (150 μg/kg) but of the same size (30 nm) was orally administered for longer period (15 days) [294].

2.6.8. Elimination

IONPs can be excreted from the body if several conditions are accomplished: the size, shape, zeta potential and other characteristics inhibit the nanoparticles dispersion, agglomeration and storage but permit their glomerular filtration. The systemic administration of IONPs permits the storage of nanoparticles in organs, according to their properties and tissues characteristics [295].

 doi:10.20944/preprints202508.0830.v1

IONPs can interfere with iron metabolism, participate in electron transfer reactions or can combine with proteins, they are immunogenic and promoters of oxidative stress that initiates ferroptosis. *In vivo* or in clinical trials, IONPs were investigated for the treatment of several cancer types, with hyperthermia (induced by radiofrequencies, microwaves, magnetic field excitation or ultrasounds) or followed by radiotherapy.

2.6.9. Combined Radiotherapy and MH

Magnetic hyperthermia may be used combined with radiotherapy; the effects of latter being enhanced by heating of administered IONPs [166]. Several iron nanoparticles were developed and studied for radio sensitization: dextran-coated IONPs (in prostate carcinoma, glioblastoma), gold coating (in melanoma), sodium citrate coating IONPs (in breast adenocarcinoma) [279]. Li et al. studied, in their experiment performed in mice with non-small cell lung cancer, the effects of superparamagnetic iron oxide nanoclusters (60 nm), able to respond to different pH by self-assembling, administered intratracheally, followed by radiotherapy, and noticed that all the animals survived and presented reduced tumor areas [296]. Zhu et al. investigated the distribution of intratracheally administrated IONPs (22 nm) in Sprague-Dawley rats and found these nanoparticles in systemic circulatory system at 10 minutes after instillation, and stored inside the liver, kidney, and spleen even after 50 days [297]. Hyaluronic acid-based IONPs (40 mg/kg, peritumoral injections) were administered for radiosensitization in mice with subcutaneous tumors, combined with X-rays irradiation, in an experiment performed by Bae et al. that showed significant decreases of tumor dimensions with 100% survival rate [298]. The literature data provides conflicting results related to the effects of iron nanoparticles on cancer tumors.

2.7. Clinical Studies

The importance and relevance of the topic of this study are supported by the large number and variety of clinical studies conducted in recent years, and especially by the fact that some iron oxide nanoparticles have already been approved for clinical use. Therefore, Nanotherm (MagForce Ag, Berlin, Germany), Superparamagnetic iron oxide nanoparticle, Fe_3O_4 or γ-Fe_2O_3 with aminosilane coating), approved by both EMA and FDA, is used for magnetic hyperthermia therapy in recurrent Glioblastoma and prostate cancer. [19,24] Other FDA approved nanoparticles, with no use in cancer therapy are Ferumoxytol (Feraheme, Superparamagnetic iron oxide (magnetite) coated with Polyglucose sorbitol carboxymethylether produced by AMAG Pharmaceuticals, Inc. (Cambridge, MA, UK), for the treatment of iron deficiency anemia in patients with chronic kidney disease; Fermoxtran-10 (Sinerem, produced by Guerbet, Saint-Ouen, France, or named as Combidex produced by Advanced Magnetics, USA), Superparamagnetic iron oxide (magnetite) coated with Dextran, as an MRI contrast agent; and Ferumoxsil (Lumirem- Guerbet), Superparamagnetic iron oxide (magnetite) with Siloxane coating as an oral gastrointestinal tract imaging agent [19].

The clinical trials aimed to investigate the diagnostic and therapeutic properties of iron nanoparticles in various malignancies. In a phase 1 clinical trial, Carbon Nanoparticle-Loaded Iron CNSI-Fe(II) in doses of 30 mg, 60 mg, 90 mg, and 150 mg was tested on breast cancer and other advanced solid tumors, with a partial response of 25% for the 60mg dose and serious adverse events of 33.33% for 30mg, 25% for 60mg, 83.33% for 90mg, and 0% for 150 mg [299]. When it comes to the diagnostic role of Superparamagnetic Iron Oxide Nanoparticles (SPION), two clinical trials highlight the advantages of using them for sentinel lymph node detection: the procedure using MagTrace (SPIONs coated with carboxydextran) (Sysmex Europe SE, Norderstedt, Germany) was successful in all patients (100%), and no adverse effects were reported [300]; and it detected even more sentinel lymph nodes (97.4% vs 91.2%) than radioisotope ($P = 0.057$) [301]. NanoTherm is also the first nanoparticle-based therapy approved for the treatment of Glioblastoma Multiforme. An ongoing clinical trial, ANCHIALE, is recruiting in Poland to examine the efficacy and tolerability of this medication in the treatment of glioblastomas [302].

 doi:10.20944/preprints202508.0830.v1

Intra-venous injection of SPION- contrast agent Ferumoxytol proved effective in the identification of liver neoplasms as it improved liver heterogeneity in MRI scans, allowing for more accurate characterization of liver function and tumours [303].

In rectal cancer, clinical trials are now investigating a NanoEcho Particle-1 (NEP-1, Ferumoxtran Lyophilisate 20 mg Fe/mL) based contrast agent to improve the diagnosis of lymph node metastases and staging in patients [304]. The combination therapy of MH and radiotherapy was also tested in a clinical study performed in 66 patients with glioblastoma. The pacients received intratumoral IONPs followed by magnetic hyperthermia and radiotherapy showed adverse effects during thermotherapy: the increase of body temperature at 38°C, headaches (probably because of the increase of intracranial pressure), convulsions, motor impairments, tachycardia, and blood pressure variations [183].

3. Conclusions

Although superparamagnetic iron oxide nanoparticles are widely regarded as biocompatible and clinically translatable, their safe application requires a nuanced understanding of the parameters influencing toxicity. Optimization of surface coatings, control of administered dose and core diameter, and careful design of external stimuli (e.g., magnetic fields) are essential to mitigate adverse effects. Further research, particularly on long-term biodistribution and chronic toxicity—is warranted to ensure their safe and effective use in clinical settings. In the synthesis of IONPs all the factors that interfere with the treatment, factors related to the MNPs, targeted tissue, to the systemic body responses, to the environmental electromagnetic field, etc. must be considered. Magnetic hyperthermia's integration with other therapies – particularly immunotherapy, chemotherapy, and smart carriers – marks a shift from single-modality treatment to multifunctional platforms. With growing preclinical validation and early clinical success, iron oxide-based MH is positioned as a powerful adjunct strategy in cancer therapy, offering both targeted thermal control and synergistic therapeutic potential.

4. Future Directions

Magnetic nanoparticles (MNPs) are emerging as promising agents for enhancing the efficacy of cancer treatment. Among the innovative approaches involving MNPs, magnetic hyperthermia (MH) stands out due to its minimally invasive nature, ability to penetrate deep tissues, and potential to selectively induce various cell death pathways—including apoptosis, ferroptosis, necrosis and pyroptosis. MH allows for localized thermal ablation of tumor tissues, minimizing damage to surrounding healthy tissues. Despite numerous preclinical studies demonstrating the therapeutic potential of MH, its clinical translation remains limited. While MH has been approved for the treatment of recurrent glioblastoma, its safety and effectiveness for other types of malignancies still require validation through comprehensive clinical trials. Consequently, the transition of MH from an experimental therapeutic platform to a widely accepted clinical modality—used in conjunction with surgery, radiotherapy, and chemotherapy—will depend on future advancements in interdisciplinary materials science and the development of intelligent, adaptive treatment systems.

Significant progress was made in tailoring the intrinsic properties of MNPs, such as magnetic responsiveness, biocompatibility, and surface functionality. However, further refinement is needed to optimize their performance under clinically relevant alternating magnetic field (AMF) conditions. Standardization of experimental parameters—such as MNP concentration, exposure duration, AMF strength, and route of administration—is essential to ensure reproducibility and facilitate clinical translation.

Many MH studies were conducted on *in vitro* 2D models, containing tumor cells w/wt co-cultured stromal and/or vascular cells. The 2D models present certain advantages such as easy maintenance, reliability of the results, they usually involve human cell lines, and are suitable for toxicity screening of MNPs, researching mechanisms of cell death induction or tumor escape but they lack the complex spatial tumor structure. There is a great need for better tumor models that match

 doi:10.20944/preprints202508.0830.v1

the clinical scenario, particularly the tumor -stroma- immune system interactions, which is the key to understanding the mechanisms of tumor destruction generated by MH as a single therapy or combined with other options, such as radiotherapy, immunotherapy and/or chemotherapy. In view of this, the most reliable models, so far, have been developed *in vivo*, on lab animals, particularly rodents. There are, however, many limitations related to animal physiology, the ability to generate a certain type of tumor or to the ethical and financial considerations.

Recent advancements in the development of *in vitro* 3D models, such as the spheroids, organoids, microfluidics and the possibility of bioprinting creates opportunities for the design of human tumor models, that can comprise multiple human cell types grown on organic 3D scaffolds like collagen, Matrigel or others. These models can develop ingrown tumor vascularization and by adding immune cells can generate a certain immune response. Therefore, the 3D models can represent a step forward in standardized testing of MH to generate more reliable data in the preclinical testing. However, the creation of these models requires time, knowledge and financial resources, also reproducibility can be an issue, depending on the donor, media and reactives used for the model creation.

Future research should prioritize the design of multifunctional MNPs capable of integrating diagnostic and therapeutic modalities (so-called "theranostics") into a single nanoplatform. Such platforms would allow for precise *in vivo* tumor localization, real-time imaging, and patient-specific treatment, contributing to the realization of personalized oncology. A key challenge remains the efficient targeting and accumulation of MNPs at tumor sites. Passive targeting via the enhanced permeability and retention (EPR) effect often results in significant off-target deposition, particularly in organs such as the liver, spleen, and kidneys. To overcome this, advanced targeting strategies—including ligand-mediated active targeting and magnetic field-assisted navigation—should be further explored. In parallel, the development of next-generation imaging and tracking technologies will be critical to monitor *in vivo* distribution and enhance tumor-specific accumulation of MNPs via systemic administration. Looking forward, MNPs may also play a pivotal role in preventing metastasis. One conceptual application involves engineering MNPs to circulate within the bloodstream and capture circulating tumor cells, directing them toward an implanted magnetic device for sequestration and removal—a novel approach for metastasis interception. Combination of MH and immunotherapy has the potential to inhibit the suppressive effect of the tumor cytokines, particularly towards stroma infiltrating macrophages and trigger a phenotype switch. Combined with enhanced tumor antigen release by MH induced cell killing it can lead to an effective immune response against tumor antigens, leading to local and distant tumor destruction. Additionally, MNPs could be engineered to facilitate non-invasive biopsies of tumors that are otherwise inaccessible through conventional methods, offering new possibilities for early diagnosis and molecular profiling. In cancer immunotherapy, MNPs may serve as potent carriers for vaccine delivery, improving antigen presentation and immune activation. The continued convergence of nanotechnology, immunology, and bioengineering will likely unlock new therapeutic paradigms that exploit the full potential of MNPs in precision oncology.

Author Contributions: Conceptualization, I.B., C.I. and D.R.M.; methodology, I.B., R.A.G., A.V., V.R.; software, R.A.G.; validation, I.B., and C.I.; formal analysis I.B, C.I., D.R.M., investigation, R.A.G, V.R, A.V.; data curation, I.B, C.I.; writing—original draft preparation, R.A.G, V.R, A.V., D.R.M, C.I, I.B; writing—review and editing, I.B, C.I.; visualization, I.B, R.A.G., C.I.; supervision, I.B.; project administration, I.B. All authors have read and agreed to the published version of the manuscript.

Institutional Review Board Statement: Not applicable.

Informed Consent Statement: Not applicable.

Data Availability Statement: Data is contained within the article.

Acknowledgments: The authors have reviewed and edited the output and take full responsibility for the content of this publication.

 doi:10.20944/preprints202508.0830.v1

Conflicts of Interest: The authors declare no conflicts of interest.

References

1. Sung, H.; Ferlay, J.; Siegel, R.L.; Laversanne, M.; Soerjomataram, I.; Jemal, A.; Bray, F. Global cancer statistics 2020: GLOBOCAN estimates of incidence and mortality worldwide for 36 cancers in 185 countries. *CA Cancer J. Clin.* **2021**, *71*, 209–249. https://doi.org/10.3322/caac.21660
2. Siegel, R.L.; Miller, K.D.; Jemal, A. Cancer statistics, 2020. *CA Cancer J. Clin.* **2020**, *70*, 7–30. https://doi.org/10.3322/caac.21590
3. Gupta, G.P.; Massagué, J. Cancer metastasis: building a framework. *Cell* **2006**, *127*, 679–695. https://doi.org/10.1016/j.cell.2006.11.001
4. Chabner, B.A.; Roberts, T.G. Jr. Timeline: chemotherapy and the war on cancer. *Nat. Rev. Cancer* **2005**, *5*, 65–72. https://doi.org/10.1038/nrc1529
5. Baskar, R.; Lee, K.A.; Yeo, R.; Yeoh, K.W. Cancer and radiation therapy: current advances and future directions. *Int. J. Med. Sci.* **2012**, *9*, 193–199. https://doi.org/10.7150/ijms.3635
6. Kerr, J.F.; Winterford, C.M.; Harmon, B.V. Apoptosis. Its significance in cancer and cancer therapy. *Cancer* **1994**, *73*, 2013–2026. https://doi.org/10.1002/1097-0142(19940415)73:8
7. Moyer, H.R.; Delman, K.A. The role of hyperthermia in optimizing tumor response to regional therapy. *Int. J. Hyperthermia* **2008**, *24*, 251–261. https://doi.org/10.1080/02656730701772480
8. Baronzio, G.F.; Hager, E.D. Hyperthermia in Cancer Treatment: A Primer; Springer: New York, NY, USA, 2006. https://doi.org/10.1007/978-0-387-33441-7
9. Cavaliere, R.; Ciocatto, E.C.; Giovanella, B.C.; Heidelberger, C.; Johnson, R.O.; Margottini, M.; Mondovi, B.; Moricca, G.; Rossi-Fanelli, A. Selective heat sensitivity of cancer cells. Biochemical and clinical studies. *Cancer* **1967**, *20*, 1351–1381. https://doi.org/10.1002/1097-0142(196709)20:9<1351::aid-cncr2820200902>3.0.co;2-#.
10. Falk, M.H.; Issels, R.D. Hyperthermia in oncology. *Int. J. Hyperthermia* **2001**, *17*, 1–18. https://doi.org/10.1080/02656730150201552
11. Wust, P.; Hildebrandt, B.; Sreenivasa, G.; Rau, B.; Gellermann, J.; Riess, H.; Felix, R.; Schlag, P.M. Hyperthermia in combined treatment of cancer. *Lancet Oncol.* **2002**, *3*, 487–497. https://doi.org/10.1016/s1470-2045(02)00818-5
12. Chichel, A.; Skowronek, J.; Kubaszewska, M.; Kanikowski, M. Hyperthermia – description of a method and a review of clinical applications. *Rep. Pract. Oncol. Radiother.* **2007**, *12*, 267–275. https://doi.org/10.1016/S1507-1367(10)60065-X
13. Kampinga, H.H. Cell biological effects of hyperthermia alone or combined with radiation or drugs: a short introduction to newcomers in the field. *Int. J. Hyperthermia* **2006**, *22*, 191–196. https://doi.org/10.1080/02656730500532028
14. Pankhurst, Q.A.; Connolly, J.; Jones, S.K.; Dobson, J. Applications of magnetic nanoparticles in biomedicine. *J. Phys. D Appl. Phys.* **2003**, *36*, R167–R181. https://doi.org/10.1088/0022-3727/36/13/201
15. Dutz, S.; Hergt, R. Magnetic nanoparticle heating and heat transfer on a microscale: basic principles, realities and physical limitations of hyperthermia for tumour therapy. *Int. J. Hyperthermia* **2013**, *29*, 790–800. https://doi.org/10.3109/02656736.2013.822993
16. Jordan, A.; Scholz, R.; Wust, P.; Fähling, F.; Felix, R. Magnetic fluid hyperthermia (MFH): Cancer treatment with AC magnetic field-induced excitation of biocompatible superparamagnetic nanoparticles. *J. Magn. Magn. Mater.* **1999**, *201*, 413–419. https://doi.org/10.1016/S0304-8853(99)00088-8
17. Thiesen, B.; Jordan, A. Clinical applications of magnetic nanoparticles for hyperthermia. *Int. J. Hyperthermia* **2008**, *24*, 467–474. https://doi.org/10.1080/02656730802104757
18. Gilchrist, R.K.; Medal, R.; Shorey, W.D.; Hanselman, R.C.; Parrott, J.C.; Taylor, C.B. Selective inductive heating of lymph nodes. *Ann. Surg.* **1957**, *146*, 596–606. https://doi.org/10.1097/00000658-195710000-00007
19. Huang, Y.; Hsu, J.C.; Koo, H.; Cormode, D.P. Repurposing ferumoxytol: diagnostic and therapeutic applications of an FDA-approved nanoparticle. *Theranostics* **2022**, *12*, 796–816. https://doi.org/10.7150/thno.67375

 doi:10.20944/preprints202508.0830.v1

20. Revia, R.A.; Zhang, M. Magnetite nanoparticles for cancer diagnosis, treatment, and treatment monitoring: recent advances. *Mater. Today* **2016**, *19*, 157–168. https://doi.org/10.1016/j.mattod.2015.08.022
21. Pineiro, Y.; Vargas, Z.; Rivas, J.; López-Quintela, M.A. Iron oxide based nanoparticles for magnetic hyperthermia strategies in biological applications. *Eur. J. Inorg. Chem.* **2015**, 4495–4509. https://doi.org/10.1002/ejic.201500598
22. Gneveckow, U.; Jordan, A.; Scholz, R.; Brüss, V.; Waldöfner, N.; Ricke, J.; Feussner, A.; Hildebrandt, B.; Rau, B.; Wust, P. Description and characterization of the novel hyperthermia- and thermoablation-system MFH 300F for clinical magnetic fluid hyperthermia. *Med. Phys.* **2004**, *31*, 1444–1451. https://doi.org/10.1118/1.1748629
23. van Landeghem, F.K.; Maier-Hauff, K.; Jordan, A.; Hoffmann, K.T.; Gneveckow, U.; Scholz, R.; Thiesen, B.; Brück, W.; von Deimling, A. Post-mortem studies in glioblastoma patients treated with thermotherapy using magnetic nanoparticles. *Biomaterials* **2009**, *30*, 52–57. https://doi.org/10.1016/j.biomaterials.2008.09.044
24. Mahmoudi, K.; Bouras, A.; Bozec, D.; Ivkov, R.; Hadjipanayis, C. Magnetic hyperthermia therapy for the treatment of glioblastoma: a review of the therapy's history, efficacy and application in humans. *Int. J. Hyperthermia* **2018**, *34*, 1316–1328. https://doi.org/10.1080/02656736.2018.1430867
25. Egea-Benavente, D.; Ovejero, J.G.; Morales, M.D.P.; Barber, D.F. Understanding MNPs behaviour in response to AMF in biological milieus and the effects at the cellular level: implications for a rational design that drives magnetic hyperthermia therapy toward clinical implementation. *Cancers* **2021**, *13*, 4583. https://doi.org/10.3390/cancers13184583
26. Kwok, M.K.Y.; Maley, C.C.J.; Dworkin, A.; Hattersley, S.; Southern, P.; Pankhurst, Q.A. Nonspecific eddy current heating in magnetic field hyperthermia. *Appl. Phys. Lett.* **2023**, *122*, 240502. https://doi.org/10.1063/5.0153336
27. Pilpilidis, K.; Tsanidis, G.; Rouni, M.A.; Markakis, J.; Samaras, T. Revisiting the safety limit in magnetic nanoparticle hyperthermia: insights from eddy current induced heating. *Phys. Med. Biol.* **2025**, *70*, 035001. https://doi.org/10.1088/1361-6560/adaad0
28. Hergt, R.; Dutz, S. Magnetic particle hyperthermia-biophysical limitations of a visionary tumour therapy. *J. Magn. Magn. Mater.* **2007**, *311*, 187–192. https://doi.org/10.1016/j.jmmm.2006.10.1156
29. Xu, C.; Sun, S. New forms of superparamagnetic nanoparticles for biomedical applications. *Adv. Drug Deliv. Rev.* **2013**, *65*, 732–743. https://doi.org/10.1016/j.addr.2012.10.008
30. Liu, X.; Zhang, Y.; Wang, Y.; Zhu, W.; Li, G.; Ma, X.; Zhang, Y.; Chen, S.; Tiwari, S.; Shi, K.; Zhang, S.; Fan, H.M.; Zhao, Y.X.; Liang, X.J. Comprehensive understanding of magnetic hyperthermia for improving antitumor therapeutic efficacy. *Theranostics* **2020**, *10*, 3793–3815. https://doi.org/10.7150/thno.40805
31. Etemadi, H.; Plieger, P.G. Magnetic fluid hyperthermia based on magnetic nanoparticles: physical characteristics, historical perspective, clinical trials, technological challenges, and recent advances. *Adv. Therap.* **2020**, *2000061*, 1–49. https://doi.org/10.1002/adtp.202000061
32. Wilhelm, S.; Tavares, A.J.; Dai, Q.; Ohta, S.; Audet, J.; Dvorak, H.F.; Chan, W.C.W. Analysis of nanoparticle delivery to tumours. *Nat. Rev. Mater.* **2016**, *1*, 16014. https://doi.org/10.1038/natrevmats.2016.14
33. Albarqi, H.A.; Wong, L.H.; Schumann, C.; Sabei, F.Y.; Korzun, T.; Li, X.; Hansen, M.N.; Dhagat, P.; Moses, A.S.; Taratula, O.; Taratula, O. Biocompatible nanoclusters with high heating efficiency for systemically delivered magnetic hyperthermia. *ACS Nano* **2019**, *13*, 6383–6395. https://doi.org/10.1021/acsnano.8b06542
34. Hervault, A.; Thanh, N.T.K. Magnetic nanoparticle-based therapeutic agents for thermo-chemotherapy treatment of cancer. *Nanoscale* **2014**, *6*, 11553–11573. https://doi.org/10.1039/C4NR03482A
35. Häfeli, U.O.; Riffle, J.S.; Harris-Shekhawat, L.; Carmichael-Baranauskas, A.; Mark, F.; Dailey, J.P.; Bardenstein, D. Cell uptake and *in vitro* toxicity of magnetic nanoparticles suitable for drug delivery. *Mol. Pharmaceutics* **2009**, *6*, 1417–1428. https://doi.org/10.1021/mp900083m.
36. Weissleder, R.; Stark, D.D.; Engelstad, B.L.; Bacon, B.R.; Compton, C.C.; White, D.L.; Jacobs, P.; Lewis J. Superparamagnetic iron oxide: pharmacokinetics and toxicity. *AJR Am. J. Roentgenol.* **1989**, *152*, 167–173. https://doi.org/10.2214/ajr.152.1.167.
37. Mejías, R.; Delgado, A.; Herrero, V.; García, M.L.; Martín, C.; Rico, P.; Morales, M.D.P.; Barber, D.F. Long term biotransformation and toxicity of dimercaptosuccinic acid-coated magnetic nanoparticles support

 doi:10.20944/preprints202508.0830.v1

their use in biomedical applications. *J. Control Release* **2013**, *171*, 225–233. https://doi.org/10.1016/j.jconrel.2013.07.019.

38. Ahamed, M.; Alhadlaq, H.A.; Alam, J.; Khan, M.A.M.; Ali, D.; Alarafi, S. Iron oxide nanoparticle-induced oxidative stress and genotoxicity in human skin epithelial and lung epithelial cell lines. *Curr. Pharm. Des.* **2013**, *19*, 6681–6690. https://doi.org/10.2174/1381612811319370011.
39. Siddiqui, M. A.; Wahab, R.; Saquib, Q.; Ahmad, J.; Farshori, N. N.; Al-Sheddi, E. S.; Al-Oqail, M. M.; Al-Massarani, S. M.; Al-Khedhairy, A. A. Iron Oxide Nanoparticles Induced Cytotoxicity, Oxidative Stress, Cell Cycle Arrest, and DNA Damage in Human Umbilical Vein Endothelial Cells. *J. Trace Elem. Med. Biol.* **2023**, *80*, 127302 https://doi.org/10.1016/j.jtemb.2023.127302
40. Wan, J.; Ren, H.; Wang, J. Iron toxicity, lipid peroxidation and ferroptosis after intracerebral haemorrhage. *Stroke Vasc. Neurol.* **2019**, *4*, 93–95. https://doi.org/10.1136/svn-2018-000205.
41. Kruszewski, M. Labile iron pool: the main determinant of cellular response to oxidative stress. *Mutat. Res.* **2003**, *531*, 81–92. https://doi.org/10.1016/j.mrfmmm.2003.08.004.
42. Yu, M.; Huang, S.; Yu, K.J.; Clyne, A.M. Dextran and polymer polyethylene glycol (PEG) coating reduce both 5 and 30 nm iron oxide nanoparticle cytotoxicity in 2D and 3D cell culture. *Int. J. Mol. Sci.* **2012**, *13*, 5554–5570. https://doi.org/10.3390/ijms13055554.
43. Hoskins, C.; Cuschieri, A.; Wang, L. The cytotoxicity of polycationic iron oxide nanoparticles: Common endpoint assays and alternative approaches for improved understanding of cellular response mechanism. *J. Nanobiotechnol.* **2012**, *10*, 15. https://doi.org/10.1186/1477-3155-10-15.
44. Kut, C.; Zhang, Y.; Hedayati, M.; Zhou, H.; Cornejo, C.; Bordelon, D.; Mihalic, J.; Wabler, M.; Burghardt, E.; Gruettner, C.; Geyh, A.; Brayton, C.; Deweese, T. L.; Ivkov, R. Preliminary Study of Injury From Heating Systemically Delivered, Nontargeted Dextran–Superparamagnetic Iron Oxide Nanoparticles in Mice. *Nanomedicine 2012*, 7, 1697–1711, https://doi.org/10.2217/nnm.12.65
45. Wu, L.; Wen, W.; Wang, X.; Huang, D.; Cao, J.; Qi, X.; Shen, S. Ultrasmall Iron Oxide Nanoparticles Cause Significant Toxicity by Specifically Inducing Acute Oxidative Stress to Multiple Organs. Part. *Fibre Toxicol.* **2022**, *19*, 24, https://doi.org/10.1186/s12989-022-00465-y
46. Levy, M.; Luciani, N.; Alloyeau, D.; Elgrabli, D.; Deveaux, V.; Pechoux, C.; Chat, S.; Wang, G.; Vats, N.; Gendron, F.; Factor, C.; Lotersztajn, S.; Luciani, A.; Wilhelm, C.; Gazeau, F. Long term in vivo biotransformation of iron oxide nanoparticles. *Biomaterials* **2011**; 32(16):3988-3999. https://doi.org/10.1016/j.biomaterials.2011.02.031
47. Curcio, A.; Van de Walle, A.; Péchoux, C.; Abou-Hassan, A.; Wilhelm, C. In vivo assimilation of CuS, iron oxide and iron oxide@CuS nanoparticles in mice: A 6-month follow-up study. *Pharmaceutics* **2022**, *14*, 179. https://doi.org/10.3390/pharmaceutics14010179.
48. Rosensweig, R.E. Heating magnetic fluid with alternating magnetic field. *J. Magn. Magn. Mater.* **2002**, *252*, 370–374. https://doi.org/10.1016/S0304-8853(02)00706-0.
49. Tromsdorf, U.I.; Bruns, O.T.; Salmen, S.C.; Beisiegel, U.; Weller, H. A highly effective, nontoxic T1 MR contrast agent based on ultrasmall PEGylated iron oxide nanoparticles. *Nano Lett.* **2009**, *9*, 4434–4440. https://doi.org/10.1021/nl902715v.
50. Rui, Y.-P.; Liang, B.; Hu, F.; Xu, J.; Peng, Y.-F.; Yin, P.-H.; Duan, Y.; Zhang, C.; Gu, H. Ultra-large-scale production of ultrasmall superparamagnetic iron oxide nanoparticles for T1-weighted MRI. *RSC Adv.* **2016**, *6*, 22575–22585. https://doi.org/10.1039/C6RA00347H
51. Figuerola, A.; Di Corato, R.; Manna, L.; Pellegrino, T. From iron oxide nanoparticles towards advanced iron-based inorganic materials designed for biomedical applications. *Pharmacol. Res.* **2010**, *62*, 126–143. https://doi.org/10.1016/j.phrs.2009.12.012.
52. Fortin, J.P.; Gazeau, F.; Wilhelm, C. Intracellular heating of living cells through Néel relaxation of magnetic nanoparticles. *Eur. Biophys. J.* **2008**, *37*, 223–228. https://doi.org/10.1007/s00249-007-0197-4.
53. Jeun, M.; Lee, S.; Kang, J.K.; Tomitaka, A.; Kang, K.W.; Kim, Y.I.; Takemura, Y.; Chung, K.-W.; Kwak, J.; Bae, S. Physical limits of pure superparamagnetic Fe3O4 nanoparticles for a local hyperthermia agent in nanomedicine. *Appl. Phys. Lett.* **2012**, *100*, 092406:1–092406:4. https://doi.org/10.1063/1.3689751

 doi:10.20944/preprints202508.0830.v1

54. Gonzales-Weimuller, M.; Zeisberger, M.; Krishnan, K.M. Size-dependent heating rates of iron oxide nanoparticles for magnetic fluid hyperthermia. *J. Magn. Magn. Mater.* **2009**, *321*, 1947–1950. https://doi.org/10.1016/j.jmmm.2008.12.017.
55. Müller, R.; Dutz, S.; Neeb, A.; Cato, A.C.B.; Zeisberger, M. Magnetic heating effect of nanoparticles with different sizes and size distributions. *J. Magn. Magn. Mater.* **2013**, *328*, 80–85. https://doi.org/10.1016/j.jmmm.2012.09.064
56. Lévy, M.; Wilhelm, C.; Siaugue, J.-M.; Horner, O.; Bacri, J.-C.; Gazeau, F. Magnetically induced hyperthermia: size-dependent heating power of γ-Fe2O3 nanoparticles. *J. Phys.: Condens. Matter* **2008**, *20*, 204133:1–204133:5. https://doi.org/10.1088/0953-8984/20/20/204133
57. Fortin, J.-P.; Wilhelm, C.; Servais, J.; Ménager, C.; Bacri, J.-C.; Gazeau, F. Size-sorted anionic iron oxide nanomagnets as colloidal mediators for magnetic hyperthermia. *J. Am. Chem. Soc.* **2007**, *129*, 2628–2635. https://doi.org/10.1021/ja067457e.
58. Gazeau, F.; Lévy, M.; Wilhelm, C. Optimizing magnetic nanoparticle design for nanothermotherapy. *Nanomedicine* **2008**, *3*, 831–844. https://doi.org/10.2217/17435889.3.6.831.
59. Carrey, J.; Mehdaoui, B.; Respaud, M. Simple models for dynamic hysteresis loop calculations of magnetic single-domain nanoparticles: Application to magnetic hyperthermia optimization. *J. Appl. Phys.* **2011**, *109*, 083921. https://doi.org/10.1063/1.3551582.
60. Nemati, Z.; Alonso, J.; Martinez, L.M.; Khurshid, H.; Garaio, E.; Garcia, J.A.; Phan, M.H.; Srikanth, H. Improving the heating efficiency of iron oxide nanoparticles by tuning their shape and size. *J. Phys. Chem. C* **2018**, *122*, 2367–2381. https://doi.org/10.1021/acs.jpcc.7b10528.
61. Chen, R.; Christiansen, M.G.; Anikeeva, P. Maximizing hysteretic losses in magnetic ferrite nanoparticles via model-driven synthesis and materials optimization. *ACS Nano* **2013**, 7, 8990–9000. https://doi.org/10.1021/nn4035266
62. Mohapatra, J.; Zeng, F.; Elkins, K.; Xing, M.; Ghimire, M.; Yoon, S.; Mishra, S.R.; Liu, J.P. Size-dependent magnetic and inductive heating properties of Fe_3O_4 nanoparticles: Scaling laws across the superparamagnetic size. *Phys. Chem. Chem. Phys.* **2018**, 20, 12879–12887. https://doi.org/10.1039/C7CP08631H
63. Tong, S.; Xiang, J.; Zheng, C.; Gao, J.; Bao, G. Size-dependent heating of magnetic iron oxide nanoparticles. *ACS Nano* **2017**, *11*, 6808–6816. https://doi.org/10.1021/acsnano.7b01762.
64. Serantes, D.; Baldomir, D.; Martinez-Boubeta, C.; Simeonidis, K.; Angelakeris, M.; Natividad, E.; Castro, M.; Mediano, A.; Chen, D.-X.; Sanchez, A.; Balcells, L.I.; Martínez, B. Influence of dipolar interactions on hyperthermia properties of ferromagnetic particles. *J. Appl. Phys.* **2010**, *108*, 073918. https://doi.org/10.1063/1.3488881
65. Salas, G.; Camarero, J.; Cabrera, D.; Takacs, H.; Varela, M.; Ludwig, R.; Dähring, H.; Hilger, I.; Miranda, R.; Morales, M.P.; Teran, F.J. Modulation of magnetic heating via dipolar magnetic interactions in monodisperse and crystalline iron oxide nanoparticles. *J. Phys. Chem. C* **2014**, *118*, 19985–19994. https://doi.org/10.1021/jp5041234
66. Coral, D.F.; Mendoza Zélis, P.; Marciello, M.; Morales, M.P.; Craievich, A.; Sánchez, F.H.; Fernández van Raap, M.B. Effect of nanoclustering and dipolar interactions in heat generation for magnetic hyperthermia. *Langmuir* **2016**, *32*, 1201–1213. https://doi.org/10.1021/acs.langmuir.5b03559
67. Schaller, V.; Wahnstrom, G.; Sanz-Velasco, A.; Gustafsson, S.; Olsson, E.; Enoksson, P.; Johansson, C. Effective magnetic moment of magnetic multicore nanoparticles. *Phys. Rev. B* **2009**, *80*, 092406. https://doi.org/10.1103/PhysRevB.80.092406.
68. Tadica, M.; Kralj, S.; Jagodic, M.; Hanzel, D.; Makovec, D. Magnetic properties of novel superparamagnetic iron oxide nanoclusters and their peculiarity under annealing treatment. *Appl. Surf. Sci.* **2014**, *322*, 255–264. https://doi.org/10.1016/j.apsusc.2014.09.181.
69. Ganesan, V.; Lahiri, B.B.; Louis, C.; Philip, J.; Damodaran, S.P. Size-controlled synthesis of superparamagnetic magnetite nanoclusters for heat generation in an alternating magnetic field. *J. Mol. Liq.* **2019**, *281*, 315–323. https://doi.org/10.1016/j.molliq.2019.02.095

 doi:10.20944/preprints202508.0830.v1

70. Stolarczyk, J.K.; Deak, A.; Brougham, D.F. Nanoparticle clusters: Assembly and control over internal order, current capabilities, and future potential. *Adv. Mater.* **2016**, *28*, 5400–5424. https://doi.org/10.1002/adma.201505350.
71. Xiao, Z.; Zhang, L.; Colvin, V.L.; Zhang, Q.; Bao, G. Synthesis and application of magnetic nanocrystal clusters. *Ind. Eng. Chem. Res.* **2022**, *61*, 7613–7625. https://doi.org/10.1021/acs.iecr.1c04879.
72. Antone, A.J.; Sun, Z.; Bao, Y. Preparation and application of iron oxide nanoclusters. *Magnetochemistry* **2019**, *5*, 45. https://doi.org/10.3390/magnetochemistry5030045.
73. Deng, H.; Li, X.; Peng, Q.; Wang, X.; Chen, J.; Li, Y. Monodisperse magnetic single-crystal ferrite microspheres. *Angew. Chem. Int. Ed.* **2005**, *44*, 2782–2785. https://doi.org/10.1002/anie.200462551.
74. Iacovita, C.; Florea, A.; Dudric, R.; Pall, E.; Moldovan, A.; Tetean, R.; Stiufiuc, R.; Lucaciu, C. Small versus large iron oxide magnetic nanoparticles: Hyperthermia and cell uptake properties. *Molecules* **2016**, *21*, 1357. https://doi.org/10.3390/molecules21101357.
75. Sakellari, D.; Brintakis, K.; Kostopoulou, A.; Myrovali, E.; Simeonidis, K.; Lappas, A.; Angelakeris, M. Ferrimagnetic nanocrystal assemblies as versatile magnetic particle hyperthermia mediators. *Mater. Sci. Eng., C* **2016**, *58*, 187–193. https://doi.org/10.1016/j.msec.2015.08.023.
76. Hemery, G.; Keyes, A.C.; Garaio, E.; Rodrigo, I.; Garcia, J.A.; Plazaola, F.; Garanger, E.; Sandre, O. Tuning sizes, morphologies, and magnetic properties of monocore versus multicore iron oxide nanoparticles through the controlled addition of water in the polyol synthesis. *Inorg. Chem.* **2017**, *56*, 8232–8243. https://doi.org/10.1021/acs.inorgchem.7b00956.
77. Iacovita, C.; Dudric, R.; Vomir, M.; Ersen, O.; Donnio, B.; Gallani, J.L.; Rastei, M.V. Imaging large iron-oxide nanoparticle clusters by field-dependent magnetic force microscopy. *J. Phys. Chem. C* **2021**, *125*, 24001–24010. https://doi.org/10.1021/acs.jpcc.1c05426.
78. Bertuit, E.; Neveu, S.; Abou-Hassan, A. High temperature continuous flow syntheses of iron oxide nanoflowers using the polyol route in a multi-parametric millifluidic device. *Nanomaterials* **2022**, *12*, 119. https://doi.org/10.3390/nano12010119.
79. Hugounenq, P.; Levy, M.; Alloyeau, D.; Lartigue, L.; Dubois, E.; Cabuil, V.; Ricolleau, C.; Roux, S.; Wilhelm, C.; Gazeau, F.; Bazzi, R. Iron oxide monocrystalline nanoflowers for highly efficient magnetic hyperthermia. *J. Phys. Chem. C* **2012**, *116*, 15702–15712. https://doi.org/10.1021/jp3025478.
80. Gavilán, H.; Sánchez, E.H.; Brollo, M.E.F.; Asín, L.; Moerner, K.K.; Frandsen, C.; Lázaro, F.J.; Serna, C.J.; Veintemillas-Verdaguer, S.; Morales, M.P.; Gutiérrez, L. Formation mechanism of maghemite nanoflowers synthesized by a polyol-mediated process. *ACS Omega* **2017**, *2*, 7172–7184. https://doi.org/10.1021/acsomega.7b00975.
81. Storozhuk, L.; Besenhard, M. O.; Mourdikoudis, S.; LaGrow, A. P.; Lees, M. R.; Tung, L. D.; Gavriilidis, A.; Thanh, N. T. K. Stable Iron Oxide Nanoflowers with Exceptional Magnetic Heating Efficiency: Simple and Fast Polyol Synthesis. *ACS Appl. Mater. Interfaces* **2021**, *13*, 45870–45880, https://doi.org/10.1021/acsami.1c12323
82. Lartigue, L.; Hugounenq, P.; Alloyeau, D.; Clarke, S. P.; Lévy, M.; Bacri, J. C.; Bazzi, R.; Brougham, D. F.; Wilhelm, C.; Gazeau, F. Cooperative Organization in Iron Oxide Multi-Core Nanoparticles Potentiates Their Efficiency as Heating Mediators and MRI Contrast Agents. *ACS Nano* **2012**, *6*, 10935–10949 https://doi.org/10.1021/nn304477s
83. Jeong, M.; Lee, S.; Song, D. Y.; Kang, S.; Shin, T. H.; Choi, J. S. Hyperthermia Effect of Nanoclusters Governed by Interparticle Crystalline Structures. *ACS Omega* **2021**, 6, 31161–31167 https://doi.org/10.1021/acsomega.1c04632
84. Amorim, C.O. A compendium of magnetic nanoparticle essentials: A comprehensive guide for beginners and experts. *Pharmaceutics* **2025**, *17*, 137. https://doi.org/10.3390/pharmaceutics17010137.
85. Noh, S.-H.; Na, W.; Jang, J.-T.; Lee, J.-H.; Lee, E.J.; Moon, S.H.; Lim, Y.; Shin, J.-S.; Cheon, J. Nanoscale magnetism control via surface and exchange anisotropy for optimized ferrimagnetic hysteresis. *Nano Lett.* **2012**, *12*, 3716–3721. https://doi.org/10.1021/nl301499u.
86. Chang, F.; Davies, G.-L. From 0D to 2D: Synthesis and bio-application of anisotropic magnetic iron oxide nanomaterials. *Prog. Mater. Sci.* **2024**, *144*, 101267. https://doi.org/10.1016/j.pmatsci.2024.101267.

 doi:10.20944/preprints202508.0830.v1

87. Elsayed, W. E. M.; Al-Hazmi, F. S.; Memesh, L. S.; Bronstein, L. M. A Novel Approach for Rapid Green Synthesis of Nearly Mono-Disperse Iron Oxide Magnetic Nanocubes with Remarkable Surface Magnetic Anisotropy Density for Enhancing Hyperthermia Performance. *Colloids Surf. A Physicochem. Eng. Asp.* **2017**, *529*, 239–245, https://doi.org/10.1016/j.colsurfa.2017.06.008
88. Guardia, P.; Di Corato, R.; Lartigue, L.; Wilhelm, C.; Espinosa, A.; Garcia-Hernandez, M.; Gazeau, F.; Manna, L.; Pellegrino, T. Water-Soluble Iron Oxide Nanocubes with High Values of Specific Absorption Rate for Cancer Cell Hyperthermia Treatment. *ACS Nano* **2012**, *6*, 3080–3091, https://doi.org/10.1021/nn2048137
89. Guardia, P.; Riedinger, A.; Nitti, S.; Pugliese, G.; Marras, S.; Genovese, A.; Materia, M. E.; Lefevre, C.; Manna, L.; Pellegrino, T. One Pot Synthesis of Monodispersed Water Soluble Iron Oxide Nanocrystals with High Values of the Specific Absorption Rate. *J. Mater. Chem. B* **2014**, *2*, 4426–4434, https://doi.org/10.1039/C4TB00061G
90. Iacovita, C.; Stiufiuc, R.; Radu, T.; Florea, A.; Stiufiuc, G.; Dutu, A.; Mican, S.; Tetean, R.; Lucaciu, C.M. Polyethylene glycol-mediated synthesis of cubic iron oxide nanoparticles with high heating power. *Nanoscale Res. Lett.* **2015**, *10*, 1–16. https://doi.org/10.1186/s11671-015-1091-0.
91. Freis, B.; Ramirez, M.D.L.A.; Kiefer, C.; Harlepp, S.; Iacovita, C.; Henoumont, C.; Affolter-Zbaraszczuk, C.; Meyer, F.; Mertz, D.; Boos, A.; et al. Effect of the size and shape of dendronized iron oxide nanoparticles bearing a targeting ligand on MRI, magnetic hyperthermia, and photothermia properties—from suspension to in vitro studies. *Pharmaceutics* **2023**, *15*, 1104. https://doi.org/10.3390/pharmaceutics15041104.
92. Nemati, Z.; Alonso, J.; Martinez, L.M.; Khurshid, H.; Garaio, E.; Garcia, J.A.; Phan, M.H.; Srikanth, H. Enhanced magnetic hyperthermia in iron oxide nano-octopods: Size and anisotropy effects. *J. Phys. Chem. C* **2016**, *120*, 8370–8379. https://doi.org/10.1021/acs.jpcc.6b01426.
93. Lv, Y.; Yang, Y.; Fang, J.; Zhang, H.; Peng, E.; Liu, X.; Xiao, W.; Ding, J. Size dependent magnetic hyperthermia of octahedral Fe3O4 nanoparticles. *RSC Adv.* **2015**, *5*, 76764–76771. https://doi.org/10.1039/C5RA12558H.
94. Singh, P.; Duraisamy, K.; Raitmayr, C.; Sharma, K. S.; Korzun, T.; Singh, K.; Moses, A. S.; Yamada, K.; Grigoriev, V.; Demessie, A. A.; Park, Y.; Goo, Y. T.; Mamnoon, B.; Mesquita Souza, A. P.; Michimoto, K.; Farsad, K.; Jaiswal, A.; Taratula, O. R.; Taratula, O. Precision-Engineered Cobalt-Doped Iron Oxide Nanoparticles: From Octahedron Seeds to Cubical Bipyramids for Enhanced Magnetic Hyperthermia. *Adv. Funct. Mater.* **2025**, 2414719 https://doi.org/10.1002/adfm.202414719
95. Das, R.; Alonso, J.; Porshokouh, Z.N.; Kalappatti, V.; Torres, D.; Phan, M.-H.; Garaio, E.; Garcia, J.A.; Llamazares Sanchez, J.L.; Srikanth, H. Tunable high aspect ratio iron oxide nanorods for enhanced hyperthermia. *J. Phys. Chem. C* **2016**, *120*, 10086–10093. https://doi.org/10.1021/acs.jpcc.6b02006.
96. Geng, S.; Yang, H.; Ren, X.; Liu, Y.; He, S.; Zhou, J.; Su, N.; Li, Y.; Xu, C.; Zhang, X.; Cheng, Z. Anisotropic Magnetite Nanorods for Enhanced Magnetic Hyperthermia. *Chem. Asian J.* **2016**, *11*, 2996–3000 https://doi.org/10.1002/asia.201601042
97. Sugumaran, P.J.; Yang, Y.; Wang, Y.; Liu, X.; Ding, J. Influence of the aspect ratio of iron oxide nanorods on hysteresis-loss-mediated magnetic hyperthermia. *ACS Appl. Bio Mater.* **2021**, *4*, 4809–4820. https://doi.org/10.1021/acsabm.1c00040.
98. Nemati, Z.; Salili, S.M.; Alonso, J.; Ataie, A.; Das, A.; Phan, M.H.; Srikanth, H. Superparamagnetic iron oxide nanodiscs for hyperthermia therapy. Does size matter? *J. Alloys Compd.* **2017**, *714*, 709–714. https://doi.org/10.1016/j.jallcom.2017.04.211.
99. Dias, C.S.B.; Hanchuk, T.D.M.; Wender, H.; Shigeyosi, W.T.; Kobarg, J.; Rossi, A.L.; Tanaka, M.N.; Cardoso, M.B.; Garcia, F. Shape tailored magnetic nanorings for intracellular hyperthermia cancer therapy. *Sci. Rep.* **2017**, *7*, 14633. https://doi.org/10.1038/s41598-017-14633-0.
100. Iacovita, C.; Fizeșan, I.; Pop, A.; Scorus, L.; Dudric, R.; Stiufiuc, G.; Vedeanu, N.; Tetean, R.; Loghin, F.; Stiufiuc, R.; et al. In vitro intracellular hyperthermia of iron oxide magnetic nanoparticles, synthesized at high temperature by a polyol process. *Pharmaceutics* **2020**, *12*, 424. https://doi.org/10.3390/pharmaceutics12050424.
101. Cotin, G.; Perton, F.; Blanco-Andujar, C.; Pichon, B.; Mertz, D.; Begin-Colin, S. Design of anisotropic iron-oxide-based nanoparticles for magnetic hyperthermia. In *Nanomaterials for Magnetic and Optical*

 doi:10.20944/preprints202508.0830.v1

Hyperthermia Applications; Fratila, R.M., de la Fuente, J.M., Eds.; Elsevier Inc.: Amsterdam, The Netherlands, 2019; pp. 41–60.

102. Lee, J.-H.; Huh, Y.-M.; Jun, Y.-W.; Seo, J.-W.; Jang, J.-T.; Song, H.-T.; Kim, S.; Cho, E.-J.; Yoon, H.-G.; Suh, J.-S.; Cheon J. Artificially engineered magnetic nanoparticles for ultra-sensitive molecular imaging. *Nat. Med.* **2007**, *13*, 95–99. https://doi.org/10.1038/nm1467.
103. Jang, J.-T.; Nah, H.; Lee, J.-H.; Moon, S.H.; Kim, M.G.; Cheon, J. Critical enhancements of MRI contrast and hyperthermic effects by dopant-controlled magnetic nanoparticles. *Angew. Chem. Int. Ed.* **2009**, *48*, 1234–1238. https://doi.org/10.1002/anie.200805149.
104. Vamvakidis, K.; Sakellari, D.; Angelakeris, M.; Dendrinou-Samara, C. Size and compositionally controlled manganese ferrite nanoparticles with enhanced magnetization. *J. Nanopart. Res.* **2015**, *15*, 1743. https://doi.org/10.1007/s11051-013-1743-x.
105. Sabale, S.; Jadhav, V.; Khot, V.; Zhu, X.; Xin, M.; Chen, H. Superparamagnetic MFe2O4 (M = Ni, Co, Zn, Mn) nanoparticles: Synthesis, characterization, induction heating and cell viability studies for cancer hyperthermia applications. *J. Mater. Sci. Mater. Med.* **2015**, *26*, 127. https://doi.org/10.1007/s10856-015-5466-7.
106. Casula, M.F.; Conca, E.; Bakaimi, I.; Sathya, A.; Materia, M.E.; Casu, A.; Falqui, A.; Sogne, E.; Pellegrino, T.; Kanaras, A.G. Manganese doped-iron oxide nanoparticle clusters and their potential as agents for magnetic resonance imaging and hyperthermia. *Phys. Chem. Chem. Phys.* **2016**, *18*, 16848–16855. https://doi.org/10.1039/C6CP02094A.
107. Yang, Y.; Liu, X.; Yang, Y.; Xiao, W.; Li, Z.; Xue, D.; Li, F.; Ding, J. Synthesis of nonstoichiometric zinc ferrite nanoparticles with extraordinary room temperature magnetism and their diverse applications. *J. Mater. Chem. C* **2013**, *1*, 2875–2885. https://doi.org/10.1039/C3TC00790A.
108. Srivastava, M.; Alla, S.K.; Meena, S.S.; Gupta, N.; Mandala, R.K.; Prasad, N.K. ZnxFe3−xO4 ($0.01 \leq x \leq 0.8$) nanoparticles for controlled magnetic hyperthermia application. *New J. Chem.* **2018**, *42*, 7144–7153. https://doi.org/10.1039/C8NJ00547H.
109. He, S.; Zhang, H.; Liu, Y.; Su, F.; Yu, X.; Li, X.; Zhang, L.; Wang, L.; Mao, K.; Wang, G.; et al. Maximizing specific loss power for magnetic hyperthermia by hard-soft mixed ferrites. *Small* **2018**, *14*, 1800135. https://doi.org/10.1002/smll.201800135.
110. Jang, J.-t.; Lee, J.; Seon, J.; Ju, E.; Kim, M.; Kim, Y.I.; Kim, M.G.; Takemura, Y.; Arbab, A.S.; Kang, K.W.; Park, K.H.; Paek, S.H.; Bae, S. Giant magnetic heat induction of magnesium-doped γ-Fe2O3 superparamagnetic nanoparticles for completely killing tumors. *Adv. Mater.* **2018**, 30, 1704362 https://doi.org/10.1002/adma.201704362
111. Saville, S.L.; Qi, B.; Baker, J.; Stone, R.; Camley, R.E.; Livesey, K.L.; Ye, L.; Crawford, T.M.; Mefford, O.T. The Formation of Linear Aggregates in Magnetic Hyperthermia: Implications on Specific Absorption Rate and Magnetic Anisotropy. *J. Colloid Interface Sci.* **2014**, *424*, 141–151. https://doi.org/10.1016/j.jcis.2014.03.007
112. Morales, I.; Costo, R.; Mille, N.; Carrey, J.; Hernando, A.; de la Presa, P. Time-Dependent AC Magnetometry and Chain Formation in Magnetite: The Influence of Particle Size, Initial Temperature and the Shortening of the Relaxation Time by the Applied Field. *Nanoscale Adv.* **2021**, *3*, 5801–5812. https://doi.org/10.1039/d1na00463h
113. Mille, N.; De Massi, D.; Faure, S.; Asensio, J.M.; Chaudret, B.; Carrey, J. Probing dynamics of nanoparticle chains formation during magnetic hyperthermia using time-dependent high-frequency hysteresis loops. *Appl. Phys. Lett.* **2021**, *119*, 022407. https://doi.org/10.1063/5.0056449
114. Balakrishnan, P. B.; Silvestri, N.; Fernandez-Cabada, T.; Marinaro, F.; Fernandes, S.; Fiorito, S.; Miscuglio, M.; Serantes, D.; Ruta, S.; Livesey, K.; Hovorka, O.; Chantrell, R.; Pellegrino, T. Exploiting Unique Alignment of Cobalt Ferrite Nanoparticles, Mild Hyperthermia, and Controlled Intrinsic Cobalt Toxicity for Cancer Therapy. *Adv. Mater.* **2020**, *32*, e2003712, https://doi.org/10.1002/adma.202003712
115. Fernández-Afonso, Y.; Ruta, S.; Páez-Rodríguez, A.; van Zanten, T. S.; Gleadhall, S.; Fratila, R. M.; Moros, M.; Morales, M. del P.; Satoh, A.; Chantrell, R. W.; Serantes, D.; Gutiérrez, L. Reversible Alignment of Nanoparticles and Intracellular Vesicles during Magnetic Hyperthermia Experiments. *Adv. Funct. Mater.* **2024**, 2405334. https://doi.org/10.1002/adfm.202405334

 doi:10.20944/preprints202508.0830.v1

116. Hergt, R.; Hiergeist, R.; Zeisberger, M.; Schüler, D.; Heyen, U.; Hilger, I.; Kaiser, W. A. Magnetic Properties of Bacterial Magnetosomes as Potential Diagnostic and Therapeutic Tools. *J. Magn. Magn. Mater.* **2005**, *293*, 80–86, https://doi.org/10.1016/j.jmmm.2005.01.047
117. Alphandery, E.; Faure, S.; Raison, L.; Duguet, E.; Howse, P. A.; Bazylinski, D. A. Heat Production by Bacterial Magnetosomes Exposed to an Oscillating Magnetic Field. *J. Phys. Chem. C* **2011**, *115*, 18–22, https://doi.org/10.1021/jp104580t
118. Gandia, D.; Gandarias, L.; Rodrigo, I.; Robles-García, J.; Das, R.; Garaio, E.; García, J. Á.; Phan, M.-H.; Srikanth, H.; Orue, I.; Alonso, J.; Muela, A.; Fdez-Gubieda, M. L. Unlocking the Potential of Magnetotactic Bacteria as Magnetic Hyperthermia Agents. *Small* **2019**, *15*, 1902626. https://doi.org/10.1002/smll.201902626
119. Zhao, Z.; Rinaldi, C. Magnetization dynamics and energy dissipation of interacting magnetic nanoparticles in alternating magnetic fields with and without a static bias field. *J. Phys. Chem. C* **2018**, *122*, 21018–21030. https://doi.org/10.1021/acs.jpcc.8b04071.
120. Serantes, D.; Simeonidis, K.; Angelakeris, M.; Chubykalo-Fesenko, O.; Marciello, M.; del Puerto Morales, M.; Baldomir, D.; Martinez-Boubeta, C. Multiplying magnetic hyperthermia response by nanoparticle assembling. *J. Phys. Chem. C* **2014**, *118*, 5927–5934. https://doi.org/10.1021/jp410717m.
121. Myrovali, E.; Maniotis, N.; Makridis, A.; Terzopoulou, A.; Ntomprougkidis, V.; Simeonidis, K.; Sakellari, D.; Kalogirou, O.; Samaras, T.; Salikhov, R.; et al. Arrangement at the nanoscale: Effect on magnetic particle hyperthermia. *Sci. Rep.* **2016**, *6*, 37934. https://doi.org/10.1038/srep37934.
122. Iacovita, C.; Florea, A.; Scorus, L.; Pall, E.; Dudric, R.; Moldovan, A.I.; Stiufiuc, R.; Tetean, R.; Lucaciu, C.M. Hyperthermia, cytotoxicity and cellular uptake properties of manganese and zinc ferrite magnetic nanoparticles synthesized by a polyol-mediated process. *Nanomaterials* **2019**, *9*, 1489. https://doi.org/10.3390/nano9101489.
123. Freis, B.; Kiefer, C.; Ramirez, M. de los A.; Harlepp, S.; Mertz, D.; Pichon, B.; Iacovita, C.; Laurent, S.; Begin, S. Defects or No Defects? Or How to Design 20–25 nm Spherical Iron Oxide Nanoparticles to Harness Both Magnetic Hyperthermia and Photothermia. *Nanoscale* **2024**, *16*, 20542. https://doi.org/10.1039/d4nr01397b
124. Sanz, B.; Cabreira-Gomes, R.; Torres, T.E.; Valdés, D.P.; Lima, E., Jr.; De Biasi, E.; Zysler, R.D.; Ibarra, M.R.; Goya, G.F. Low-dimensional assemblies of magnetic MnFe2O4 nanoparticles and direct in vitro measurements of enhanced heating driven by dipolar interactions: Implications for magnetic hyperthermia. *ACS Appl. Nano Mater.* **2020**, *3*, 8719–8731. https://doi.org/10.1021/acsanm.0c01545.
125. Petru, A.-E.; Iacovita, C.; Fizeșan, I.; Dudric, R.; Crestin, I.-V.; Lucaciu, C.M.; Loghin, F.; Kiss, B. Evaluating manganese-doped magnetic nanoflowers for biocompatibility and in vitro magnetic hyperthermia efficacy. *Pharmaceutics* **2025**, *17*, 384. https://doi.org/10.3390/pharmaceutics17030384.
126. Ranoo, S.; Lahiri, B.B.; Philip, J. Enhancement in field-induced heating efficiency of TMAOH coated superparamagnetic Fe3O4 nanoparticles by texturing under a static bias field. *J. Magn. Magn. Mater.* **2019**, *498*, 166138. https://doi.org/10.1016/j.jmmm.2019.166138.
127. Lucaciu, C.M.; Nitica, S.; Fizesan, I.; Filip, L.; Bilteanu, L.; Iacovita, C. Enhanced magnetic hyperthermia performance of zinc ferrite nanoparticles under a parallel and a transverse bias DC magnetic field. *Nanomaterials* **2022**, *12*, 3578. https://doi.org/10.3390/nano12203578.
128. Zhu, N.; Ji, H.; Yu, P.; Niu, J.; Farooq, M.U.; Akram, M.W.; Udego, I.O.; Li, H.; Niu, X. Surface modification of magnetic iron oxide nanoparticles. *Nanomaterials* **2018**, *8*, 810. https://doi.org/10.3390/nano8100810.
129. Liu, X. L.; Fan, H. M.; Yi, J. B.; Yang, Y.; Choo, E. S. G.; Xue, J. M.; Fan, D. D.; Ding, J. Optimization of Surface Coating on Fe3O4 Nanoparticles for High Performance Magnetic Hyperthermia Agents. *J. Mater. Chem.* **2012**, *22*, 8235–8244, https://doi.org/10.1039/C2JM30472D
130. Castellanos-Rubio, I.; Rodrigo, I.; Olazagoitia-Garmendia, A.; Arriortua, O.; Gil de Muro, I.; Garitaonandia, J. S.; Bilbao, J. R.; Fdez-Gubieda, M. L.; Plazaola, F.; Orue, I.; Castellanos-Rubio, A.; Insausti, M. Highly Reproducible Hyperthermia Response in Water, Agar, and Cellular Environment by Discretely PEGylated Magnetite Nanoparticles. *ACS Appl. Mater. Interfaces* **2020**, *12*, 27917–27929, https://doi.org/10.1021/acsami.0c03222
131. Angotzi, M. S.; Mameli, V.; Khanal, S.; Veverka, M.; Vejpravova, J.; Cannas, C. Effect of Different Molecular Coatings on the Heating Properties of Maghemite Nanoparticles. *Nanoscale Adv.* **2022**, *4*, 408 https://doi.org/10.1039/d1na00478f

 doi:10.20944/preprints202508.0830.v1

132. Mornet, S.; Vasseur, S.; Grasset, F.; Duguet, E. Magnetic Nanoparticle Design for Medical Diagnosis and Therapy. *J. Mater. Chem.* **2004**, *14*, 2161–2175, https://doi.org/10.1039/B402025A
133. Ovejero, J.G.; Morales, I.; De La Presa, P.; Mille, N.; Carrey, J.; Garcia, M.A.; Hernando, A.; Herrasti, P. Hybrid nanoparticles for magnetic and plasmonic hyperthermia. *Phys. Chem. Chem. Phys.* **2018**, *20*, 24065–24073. https://doi.org/10.1039/C8CP02513D.
134. Mohammad, F.; Balaji, G.; Weber, A.; Uppu, R. M.; Kumar, C. S. Influence of Gold Nanoshell on Hyperthermia of Super Paramagnetic Iron Oxide Nanoparticles (SPIONs). *J. Phys. Chem. C Nanomater. Interfaces* **2010**, *114*, 19194–19201, https://doi.org/10.1021/jp105807r
135. Guardia, P.; Nitti, S.; Materia, M. E.; Pugliese, G.; Yaacoub, N.; Greneche, J.-M.; Lefevre, C.; Manna, L.; Pellegrino, T. Gold-Iron Oxide Dimers for Magnetic Hyperthermia: The Key Role of Chloride Ions in the Synthesis to Boost the Heating Efficiency. *J. Mater. Chem. B* **2017**, 5, 4587–4594. https://doi.org/10.1039/C7TB00968B
136. Guerrero-Martínez, A.; Pérez-Juste, J.; Liz-Marzán, L.M. Recent progress on silica coating of nanoparticles and related nanomaterials. *Adv. Mater.* **2010**, *22*, 1182–1195. https://doi.org/10.1002/adma.200901263.
137. Mamun, A.; Rumi, K.M.J.U.; Das, H.; Hoque, S.M. Synthesis, properties and applications of silica-coated magnetite nanoparticles: A review. *Nano* **2021**, *16*, 2130005. https://doi.org/10.1142/s179329202130005x.
138. Nitica, S.; Fizesan, I.; Dudric, R.; Barbu-Tudoran, L.; Pop, A.; Loghin, F.; Vedeanu, N.; Lucaciu, C.M.; Iacovita, C. A fast, reliable oil-in-water microemulsion procedure for silica coating of ferromagnetic Zn ferrite nanoparticles capable of inducing cancer cell death *in vitro*. *Biomedicines* **2022**, *10*, 1647. https://doi.org/10.3390/biomedicines10071647.
139. Gao, Z.; Ring, H.L.; Sharma, A.; Namsrai, B.; Tran, N.; Finger, E.B.; Garwood, M.; Haynes, C.; Bischof, J.C. Preparation of scalable silica-coated iron oxide nanoparticles for nanowarming. *Adv. Sci.* **2020**, *7*, 1901624. https://doi.org/10.1002/advs.201901624.
140. Wang, R.; Liu, J.; Liu, Y.; Zhong, R.; Yu, X.; Liu, Q.; Zhang, L.; Lv, C.; Mao, K.; Tang, P. The cell uptake properties and hyperthermia performance of Zn0.5Fe2.5O4/SiO2 nanoparticles as magnetic hyperthermia agents. *R. Soc. Open Sci.* **2020**, *7*, 191139. https://doi.org/10.1098/rsos.191139.
141. Horny, M.-C.; Gamby, J.; Dupuis, V.; Siaugue, J.-M. Magnetic hyperthermia on γ-Fe2O3@SiO2 core-shell nanoparticles for miRNA 122 detection. *Nanomaterials* **2021**, *11*, 149. https://doi.org/10.3390/nano11010149.
142. Villanueva, A.; de la Presa, P.; Alonso, J.M.; Rueda, T.; Martínez, A.; Crespo, P.; Morales, M.D.P.; Gonzalez-Fernandez, M.A.; Valdés, J.; Rivero, G. Hyperthermia HeLa cell treatment with silica-coated manganese oxide nanoparticles. *J. Phys. Chem. C* **2010**, *114*, 1976–1981. https://doi.org/10.1021/jp907046f.
143. Iacovita, C.; Fizesan, I.; Nitica, S.; Florea, A.; Barbu-Tudoran, L.; Dudric, R.; Pop, A.; Vedeanu, N.; Crisan, O.; Tetean, R.; et al. Silica coating of ferromagnetic iron oxide magnetic nanoparticles significantly enhances their hyperthermia performances for efficiently inducing cancer cell death *in vitro*. *Pharmaceutics* **2021**, *13*, 2026. https://doi.org/10.3390/pharmaceutics13122026.
144. Lei, S.; He, J.; Gao, P.; Wang, Y.; Hui, H.; An, Y.; Tian, J. Magnetic particle imaging-guided hyperthermia for precise treatment of cancer: Review, challenges, and prospects. *Mol. Imaging Biol.* **2023**, *25*, 1020–1033. https://doi.org/10.1007/s11307-023-01856-z.
145. Oskoui, P.R.; Rezvani, M. Revolution in cancer treatment methods: Perspective review of factors affecting the final results of nanoparticles used in magnetic fluid hyperthermia. *Health Sci. Rev.* **2025**, *14*, 100212. https://doi.org/10.1016/j.hsr.2025.100212.
146. Herrero de la Parte, B.; Rodrigo, I.; Gutierrez-Basoa, J.; Iturrizaga Correcher, S.; Mar Medina, C.; Echevarria-Uraga, J.J.; Garcia, J.A.; Plazaola, F.; Garcia-Alonso, I. Proposal of new safety limits for *in vivo* experiments of magnetic hyperthermia antitumor therapy. *Cancers* **2022**, *14*, 3084. https://doi.org/10.3390/cancers14133084.
147. Shah, R. R.; Davis, T. P.; Glover, A. L.; Nikles, D. E.; Brazel, C. S. Impact of Magnetic Field Parameters and Iron Oxide Nanoparticle Properties on Heat Generation for Use in Magnetic Hyperthermia. *J. Magn. Magn. Mater.* **2015**, *387*, 96–106, https://doi.org/10.1016/j.jmmm.2015.03.085
148. Lahiri, B.B.; Muthukumaran, T.; Philip, J. Magnetic hyperthermia in phosphate coated iron oxide nanofluids. *J. Magn. Magn. Mater.* **2016**, *407*, 101–113. https://doi.org/10.1016/j.jmmm.2016.01.044.

 doi:10.20944/preprints202508.0830.v1

149. Kerroum, M.A.A.; Iacovita, C.; Baaziz, W.; Ihiawakrim, D.; Rogez, G.; Benaissa, M.; Lucaciu, C.M.; Ersen, O. Quantitative analysis of the specific absorption rate dependence on the magnetic field strength in ZnxFe3−xO4 nanoparticles. *Int. J. Mol. Sci.* **2020**, *21*, 7775. https://doi.org/10.3390/ijms21207775.
150. Castellanos-Rubio, I.; Arriortua, O.; Iglesias-Rojas, D.; Barón, A.; Rodrigo, I.; Marcano, L.; Garitaonandia, J. S.; Orue, I.; Fdez-Gubieda, M. L.; Insausti, M. A milestone in the chemical synthesis of Fe3O4 nanoparticles: Unreported bulklike properties lead to a remarkable magnetic hyperthermia. *Chem. Mater.* **2021**, 33, 8693–8704. https://doi.org/10.1021/acs.chemmater.1c02654
151. Chen, R; Christiansen, MG; Sourakov, A; Mohr, A; Matsumoto, Y; Okada, S; Jasanoff, A; Anikeeva P. High-Performance Ferrite Nanoparticles through Nonaqueous Redox Phase Tuning. *Nano Lett.* **2016**, *16(2)*, 1345-51. https://doi.org/10.1021/acs.nanolett.5b04761
152. Dennis, C. L.; Krycka, K. L.; Borchers, J. A.; Desautels, R. D.; van Lierop, J.; Huls, N. F.; Jackson, A. J.; Gruettner, C.; Ivkov, R. Internal Magnetic Structure of Nanoparticles Dominates Time-Dependent Relaxation Processes in a Magnetic Field. *Adv. Funct. Mater.* **2015**, *25*, 4300–4311. https://doi.org/10.1002/adfm.201500405
153. Suk, J.S.; Xu, Q.; Kim, N.; Hanes, J.; Ensign, L.M. PEGylation as a strategy for improving nanoparticle-based drug and gene delivery. *Adv. Drug Deliv. Rev.* **2016**, *99*, 28–51. https://doi.org/10.1016/j.addr.2015.09.012
154. Padín-González, E.; Lancaster, P.; Bottini, M.; Gasco, P.; Tran, L.; Fadeel, B.; Wilkins, T.; Monopoli, M.P. Understanding the Role and Impact of Poly (Ethylene Glycol) (PEG) on Nanoparticle Formulation: Implications for COVID-19 Vaccines. *Front. Bioeng. Biotechnol.* **2022**, *10*, 882363. https://doi.org/10.3389/fbioe.2022.882363
155. Gaballa, S.; Naguib, Y.; Mady, F.; Khaled, K. Polyethylene glycol: Properties, applications, and challenges. *Journal of Advanced Biomedical and Pharmaceutical Sciences* **2024**, *7(1)*, 26-36. https://doi.org/10.21608/jabps.2023.241685.1205
156. Feng, Q.; Liu, Y.; Huang, J.; Chen, K.; Huang, J.; Xiao, K. Uptake, Distribution, Clearance, and Toxicity of Iron Oxide Nanoparticles with Different Sizes and Coatings. *Sci. Rep.* **2018**, *8*, 2082. https://doi.org/10.1038/s41598-018-19628-z
157. Franco, P.; De Marco, I. The Use of Poly(N-vinyl pyrrolidone) in the Delivery of Drugs: A Review. *Polymers* **2020**, *12*, 1114, https://doi.org/10.3390/polym12051114
158. Mahmood, H.S.; Habubi, N.F. Structural, mechanical and magnetic properties of PVA-PVP: iron oxide nanocomposite. *Appl. Phys. A* **2022**, *128*, 956. https://doi.org/10.1007/s00339-022-06107-6
159. Baldea, I.; Petran, A.; Florea, A.; Sevastre-Berghian, A.; Nenu, I.; Filip, G.A.; Cenariu, M.; Radu, M.T.; Iacovita, C. Magnetic Nanoclusters Stabilized with Poly[3,4-Dihydroxybenzhydrazide] as Efficient Therapeutic Agents for Cancer Cells Destruction. *Nanomaterials* **2023**, *13*, 933. https://doi.org/10.3390/nano13050933
160. Petran, A.; Suciu, M.; Baldea, I.; Boca, S.; Pana, O.; Leoștean, C.; Dan, M.; Bunge, A. One-pot synthesis and biological assessment of fluorescent magnetite clusters coated with polydopamine and -analogues. *Appl. Surf. Sci.* **2025**, *711*, 164028, https://doi.org/10.1016/j.apsusc.2025.164028
161. Escobar Zapata, E.V.; Martínez Pérez, C.A.; Rodríguez González, C.A.; Castro Carmona, J.S.; Quevedo Lopez, M.A.; García-Casillas, P.E. Adherence of paclitaxel drug in magnetite chitosan nanoparticles. *J. Alloys Compd.* **2012**, *536*, S441–S444, https://doi.org/10.1016/j.jallcom.2011.12.150
162. Hejjaji, E.M.A.; Smith, A.M.; Morris, G.A. Evaluation of the mucoadhesive properties of chitosan nanoparticles prepared using different chitosan to tripolyphosphate (CS:TPP) ratios. *Int. J. Biol. Macromol.* **2018**, *120*, 1610–1617. https://doi.org/10.1016/j.ijbiomac.2018.09.185
163. Ways, T.M.M.; Lau, W.M.; Khutoryanskiy, V.V. Chitosan and Its Derivatives for Application in Mucoadhesive Drug Delivery Systems. *Polymers* **2018**, *10*, 267. https://doi.org/10.3390/polym10030267
164. Shaterabadi, Z.; Nabiyouni, G.; Soleymani, M. High impact of in situ dextran coating on biocompatibility, stability and magnetic properties of iron oxide nanoparticles. *Mater. Sci. Eng. C* **2017**, *75*, 947–956. https://doi.org/10.1016/j.msec.2017.02.143
165. Predoi, D.; Balas, M.; Badea, M.A.; Ciobanu, S.C.; Buton, N.; Dinischiotu, A. Dextran-Coated Iron Oxide Nanoparticles Loaded with 5-Fluorouracil for Drug-Delivery Applications. *Nanomaterials* **2023**, *13*, 1811. https://doi.org/10.3390/nano13121811

 doi:10.20944/preprints202508.0830.v1

166. Spirou, S.V.; Basini, M.; Lascialfari, A.; Sangregorio, C.; Innocenti, C. Magnetic Hyperthermia and Radiation Therapy: Radiobiological Principles and Current Practice. *Nanomaterials* **2018**, *8*, 401. https://doi.org/10.3390/nano8060401
167. Issels, R.D.; Lindner, L.H.; Verweij, J.; Wust, P.; Reichardt, P.; Schem, B.-C.; et al. Neo-adjuvant chemotherapy alone or with regional hyperthermia for localised high-risk soft-tissue sarcoma: a randomised phase 3 multicentre study. *Lancet Oncol.* **2010**, *11*, 561–570. https://doi.org/10.1016/S1470-2045(10)70071-1
168. Yagawa, Y.; Tanigawa, K.; Kobayashi, Y.; Yamamoto, M. Cancer immunity and therapy using hyperthermia with immunotherapy, radiotherapy, chemotherapy, and surgery. *J. Cancer Metastasis Treat.* **2017**, *3*, 218–230. https://doi.org/10.20517/2394-4722.2017.35
169. Gautier, J.; Allard-Vannier, E.; Munnier, E.; Soucé, M.; Chourpa, I. Recent advances in theranostic nanocarriers of doxorubicin based on iron oxide and gold nanoparticles. *J. Control. Release* **2013**, *169*, 48–61. https://doi.org/10.1016/j.jconrel.2013.03.018
170. Zhao, X.; Li, J.; Wang, Q.; Zhang, Z.; Liu, J.; Zhang, C.; Shi, J. Recent Progress on High-Z Metal-Based Nanomaterials for Cancer Radiosensitization. *Chin. J. Org. Chem.* **2023**, *41(19)*, 2545-2556. https://doi.org/10.1002/cjoc.202300132
171. Mirzayans, R. Changing the Landscape of Solid Tumor Therapy from Apoptosis-Promoting to Apoptosis-Inhibiting Strategies. *Curr. Issues Mol. Biol.* **2024**, *46*, 5379–5396. https://doi.org/10.3390/cimb46060322
172. Mirzayans, R. Anastasis and Other Apoptosis-Related Prosurvival Pathways Call for a Paradigm Shift in Oncology: Significance of Deintensification in Treating Solid Tumors. *Int. J. Mol. Sci.* **2025**, *26*, 1881. https://doi.org/10.3390/ijms26051881
173. Ergün, S.; Aslan, S.; Demir, D.; Kayaoğlu, S.; Saydam, M.; Keleş, Y.; Kolcuoğlu, D.; Taşkurt Hekim, N.; Güneş, S. Beyond Death: Unmasking the Intricacies of Apoptosis Escape. *Mol. Diagn. Ther.* **2024**, *28*, 403–423. https://doi.org/10.1007/s40291-024-00718-w
174. Corsi, F.; Capradossi, F.; Pelliccia, A.; Briganti, S.; Bruni, E.; Traversa, E.; Torino, F.; Reichle, A.; Ghibelli, L. Apoptosis as Driver of Therapy-Induced Cancer Repopulation and Acquired Cell-Resistance (CRAC): A Simple In Vitro Model of Phoenix Rising in Prostate Cancer. *Int. J. Mol. Sci.* **2022**, *23*, 1152. https://doi.org/10.3390/ijms23031152
175. Eskandari, E.; Eaves, C.J. Paradoxical roles of caspase-3 in regulating cell survival, proliferation, and tumorigenesis. *J. Cell Biol.* **2022**, *221*, e202201159. https://doi.org/10.1083/jcb.202201159
176. Khatib, S.A.; Ma, L.; Dang, H.; Forgues, M.; Chung, J.-Y.; Ylaya, K.; Hewitt, S.M.; Chaisaingmongkol, J.; Rucchirawat, M.; Wang, X.W. Single-cell biology uncovers apoptotic cell death and its spatial organization as a potential modifier of tumor diversity in HCC. *Hepatology* **2022**, *76*, 599–611. https://doi.org/10.1002/hep.32345
177. Park, W.-Y.; Gray, J. M.; Holewinski, R. J.; Andresson, T.; So, J. Y.; Carmona-Rivera, C.; Hollander, M. C.; Yang, H. H.; Lee, M.; Kaplan, M. J.; Cappell, S. D.; Yang, L. Apoptosis-Induced Nuclear Expulsion in Tumor Cells Drives S100a4-Mediated Metastatic Outgrowth through the RAGE Pathway. *Nat. Cancer* **2023**, *4*, 419–435. https://doi.org/10.1038/s43018-023-00524-z
178. Yang, L.; Fang, J.; Chen, J. Tumor cell senescence response produces aggressive variants. *Cell Death Discov.* **2017**, *3*, 17049. https://doi.org/10.1038/cddiscovery.2017.49
179. Rivera, D.; Bouras, A.; Mattioli, M.; Anastasiadou, M.; Pacentra, A. C.; Pelcher, O.; Koziel, C.; Schupper, A. J.; Chanenchuk, T.; Carlton, H.; Ivkov, R.; Hadjipanayis, C. G. Magnetic Hyperthermia Therapy Enhances the Chemoradiosensitivity of Glioblastoma. *Sci. Rep.* **2025**, *15*, 10532. https://doi.org/10.1038/s41598-025-95544-3
180. Piehler, S.; Dähring, H.; Grandke, J.; Göring, J.; Couleaud, P.; Aires, A.; Cortajarena, A. L.; Courty, J.; Latorre, A.; Somoza, Á.; Teichgräber, U.; Hilger, I. Iron Oxide Nanoparticles as Carriers for DOX and Magnetic Hyperthermia after Intratumoral Application into Breast Cancer in Mice: Impact and Future Perspectives. *Nanomaterials* **2020**, *10*, 1016, https://doi.org/10.3390/nano10061016
181. Singh, A.; Jain, S.; Sahoo, S.K. Magnetic nanoparticles for amalgamation of magnetic hyperthermia and chemotherapy: An approach towards enhanced attenuation of tumor. *Mater. Sci. Eng. C Mater. Biol. Appl.* **2020**, *110*, 110695. https://doi.org/10.1016/j.msec.2020.110695

 doi:10.20944/preprints202508.0830.v1

182. Lin, W.; Xie, X.; Yang, Y.; Fu, X.; Liu, H.; Yang, Y.; Deng, J. Thermosensitive magnetic liposomes with doxorubicin cell-penetrating peptides conjugate for enhanced and targeted cancer therapy. *Drug Deliv.* **2016**, *23*, 3436–3443. https://doi.org/10.1080/10717544.2016.1189983
183. Maier-Hauff, K.; Ulrich, F.; Nestler, D.; Niehoff, H.; Wust, P.; Thiesen, B.; Orawa, H.; Budach, V.; Jordan, A. Efficacy and Safety of Intratumoral Thermotherapy Using Magnetic Iron-Oxide Nanoparticles Combined with External Beam Radiotherapy on Patients with Recurrent Glioblastoma Multiforme. *J. Neurooncol.* **2011**, *103*, 317–324. https://doi.org/10.1007/s11060-010-0389-0
184. Foo, C.Y.; Munir, N.; Kumaria, A.; Akhtar, Q.; Bullock, C.J.; Narayanan, A.; Fu, R.Z. Medical Device Advances in the Treatment of Glioblastoma. *Cancers* **2022**, *14*, 5341. https://doi.org/10.3390/cancers14215341
185. Yan, B.; Liu, C.; Wang, S.; Li, H.; Jiao, J.; Lee, W.S.V.; Zhang, S.; Hou, Y.; Hou, Y.; Ma, X.; Fan, H.; Lv, Y.; Liu, X. Magnetic hyperthermia induces effective and genuine immunogenic tumor cell death with respect to exogenous heating. *J. Mater. Chem. B* **2022**, *10*, 5364–5374. https://doi.org/10.1039/d2tb01004f
186. Song, Q.; Javid, A.; Zhang, G.; Li, Y. Applications of Magnetite Nanoparticles in Cancer Immunotherapies: Present Hallmarks and Future Perspectives. *Front. Immunol.* **2021**, *12*, 701485. https://doi.org/10.3389/fimmu.2021.701485
187. Chao, Y.; Chen, G.; Liang, C.; Xu, J.; Dong, Z.; Han, X.; Wang, C.; Liu, Z. Iron Nanoparticles for Low-Power Local Magnetic Hyperthermia in Combination with Immune Checkpoint Blockade for Systemic Antitumor Therapy. *Nano Lett.* **2019**, *19*, 4287–4296. https://doi.org/10.1021/acs.nanolett.9b00579
188. Laskar, A.; Eilertsen, J.; Li, W.; Yuan, X.M. SPION primes THP1 derived M2 macrophages towards M1-like macrophages. Biochem. Biophys. *Res. Commun.* **2013**, *441*, 737–742. https://doi.org/10.1016/j.bbrc.2013.10.115
189. Yan, B.; Wang, S.; Liu, C.; Wen, N.; Li, H.; Zhang, Y.; Wang, H.; Xi, Z.; Lv, Y.; Fan, H.; Liu, X. Engineering magnetic nano-manipulators for boosting cancer immunotherapy. *J. Nanobiotechnol.* **2022**, *20*, 547. https://doi.org/10.1186/s12951-022-01760-8
190. Carter, T.J.; Agliardi, G.; Lin, F.Y.; Ellis, M.; Jones, C.; Robson, M.; Richard-Londt, A.; Southern, P.; Lythgoe, M.; Zaw Thin, M.; Ryzhov, V.; de Rosales, R.T.M.; Gruettner, C.; Abdollah, M.R.A.; Pedley, R.B.; Pankhurst, Q.A.; Kalber, T.L.; Brandner, S.; Quezada, S.; Mulholland, P.; Shevtsov, M.; Chester, K. Potential of Magnetic Hyperthermia to Stimulate Localized Immune Activation. *Small* **2021**, *17*, e2005241. https://doi.org/10.1002/smll.202005241
191. Macedo, J.B.; Bueno, J.N.S.; Kanunfre, C.C.; Miranda, J.R.A.; Bakuzis, A.F.; Ferrari, P.C. Polymer-Functionalized Magnetic Nanoparticles for Targeted Quercetin Delivery: A Potential Strategy for Colon Cancer Treatment. *Pharmaceutics* **2025**, *17*, 467. https://doi.org/10.3390/pharmaceutics17040467
192. Hernández, R.; Sacristán, J.; Asín, L.; Torres, T. E.; Ibarra, M. R.; Goya, G. F.; Mijangos, C. Magnetic Hydrogels Derived from Polysaccharides with Improved Specific Power Absorption: Potential Devices for Remotely Triggered Drug Delivery. *J. Phys. Chem. B* **2010**, *114*, 12002–12007. https://doi.org/10.1021/jp105556e
193. Javid, A.; Ahmadian, S.; Saboury, A. A.; Kalantar, S. M.; Rezaei-Zarchi, S. Chitosan-Coated Superparamagnetic Iron Oxide Nanoparticles for Doxorubicin Delivery: Synthesis and Anticancer Effect Against Human Ovarian Cancer Cells. *Chem. Biol. Drug Des.* **2013**, *81*, 784–792. https://doi.org/10.1111/cbdd.12145
194. Javid, A.; Ahmadian, S.; Saboury, A. A.; Kalantar, S. M.; Rezaei-Zarchi, S.; Shahzad, S. Biocompatible APTES-PEG Modified Magnetite Nanoparticles: Effective Carriers of Antineoplastic Agents to Ovarian Cancer. Appl. Biochem. *Biotechnol.* **2014**, *173*, 36–54. https://doi.org/10.1007/s12010-014-0740-6
195. Thong, P.Q.; Thu Huong, L.T.; Tu, N.D.; My Nhung, H.T.; Khanh, L.; Manh, D.H.; Nam, P.H.; Phuc, N.X.; Alonso, J.; Qiao, J.; Sridhar, S.; Thu, H.P.; Phan, M.H.; Kim Thanh, N.T. Multifunctional Nanocarriers of Fe3O4@PLA-PEG/Curcumin for MRI, Magnetic Hyperthermia and Drug Delivery. Nanomedicine (Lond.) 2022, 17, 1677–1693. https://doi.org/10.2217/nnm-2022-0070
196. Sallem, F.; Haji, R.; Vervandier-Fasseur, D.; Nury, T.; Maurizi, L.; Boudon, J.; Lizard, G.; Millot, N. Elaboration of Trans-Resveratrol Derivative-Loaded Superparamagnetic Iron Oxide Nanoparticles for Glioma Treatment. *Nanomaterials* **2019**, *9*, 287. https://doi.org/10.3390/nano9020287

197. Abbas, H.; Refai, H.; El Sayed, N.; Rashed, L. A.; Mousa, M. R.; Zewail, M. Superparamagnetic Iron Oxide Loaded Chitosan Coated Bilosomes for Magnetic Nose to Brain Targeting of Resveratrol. *Int. J. Pharm.* **2021**, *610*, 121244, https://doi.org/10.1016/j.ijpharm.2021.121244
198. Boztepe, C.; Daskin, M.; Erdogan, A. Synthesis of Magnetic Responsive Poly(NIPAAm-co-VSA)/Fe3O4 IPN Ferrogels and Modeling Their Deswelling and Heating Behaviors under AMF by Using Artificial Neural Networks. *React. Funct. Polym.* **2022**, *173*, 105219. https://doi.org/10.1016/j.reactfunctpolym.2022.105219
199. Ndong, C.; Toraya-Brown, S.; Kekalo, K.; Baker, I.; Gerngross, T.; Fiering, S.; Griswold, K. Antibody-Mediated Targeting of Iron Oxide Nanoparticles to the Folate Receptor Alpha Increases Tumor Cell Association In Vitro and In Vivo. *Int. J. Nanomed.* **2015**, *10*, 2595–2617. https://doi.org/10.2147/IJN.S79367
200. Liong, M.; Lu, J.; Kovochich, M.; Xia, T.; Ruehm, S. G.; Nel, A. E.; Tamanoi, F.; Zink, J. I. Multifunctional Inorganic Nanoparticles for Imaging, Targeting, and Drug Delivery. *ACS Nano* **2008**, *2*, 889–896. https://doi.org/10.1021/nn800072t
201. Xu, Y.; Wu, H.; Huang, J.; Qian, W.; Martinson, D. E.; Ji, B.; Li, Y.; Wang, Y. A.; Yang, L.; Mao, H. Probing and Enhancing Ligand-Mediated Active Targeting of Tumors Using Sub-5 nm Ultrafine Iron Oxide Nanoparticles. *Theranostics* **2020**, *10*, 2479–2494. https://doi.org/10.7150/thno.39560
202. Jiang, W.; Xie, H.; Ghoorah, D.; Shang, Y.; Shi, H.; Liu, F.; Yang, X.; Xu, H. Conjugation of Functionalized SPIONs with Transferrin for Targeting and Imaging Brain Glial Tumors in Rat Model. *PLoS ONE* **2012**, *7*, e37376. https://doi.org/10.1371/journal.pone.0037376
203. Senturk, F.; Cakmak, S.; Kocum, I.C.; Gumusderelioglu, M.; Ozturk, G.G. GRGDS-Conjugated and Curcumin-Loaded Magnetic Polymeric Nanoparticles for the Hyperthermia Treatment of Glioblastoma Cells. *Colloids and Surfaces A: Physicochemical and Engineering Aspects* **2021**, *622*, 126648. https://doi.org/10.1016/j.colsurfa.2021.126648
204. Das, S.; Diyali, S.; Vinothini, G.; Perumalsamy, B.; Balakrishnan, G.; Ramasamy, T.; Dharumadurai, D.; Biswas, B. Synthesis, Morphological Analysis, Antibacterial Activity of Iron Oxide Nanoparticles and the Cytotoxic Effect on Lung Cancer Cell Line. *Heliyon* **2020**, *6*, e04953. https://doi.org/10.1016/j.heliyon.2020.e04953
205. Lugert, S.; Unterweger, H.; Mühlberger, M.; Janko, C.; Draack, S.; Ludwig, F.; Eberbeck, D.; Alexiou, C.; Friedrich, R.P. Cellular Effects of Paclitaxel-Loaded Iron Oxide Nanoparticles on Breast Cancer Using Different 2D and 3D Cell Culture Models. *IJN* **2018**, *14*, 161–180. https://doi.org/10.2147/ijn.s187886
206. Justin, C.; Samrot, A.V.; P., D.S.; Sahithya, C.S.; Bhavya, K.S.; Saipriya, C. Preparation, Characterization and Utilization of Coreshell Super Paramagnetic Iron Oxide Nanoparticles for Curcumin Delivery. *PLoS ONE* **2018**, *13*, e0200440. https://doi.org/10.1371/journal.pone.0200440
207. Situ, J.-Q.; Wang, X.-J.; Zhu, X.-L.; Xu, X.-L.; Kang, X.-Q.; Hu, J.-B.; Lu, C.-Y.; Ying, X.-Y.; Yu, R.-S.; You, J.; et al. Multifunctional SPIO/DOX-Loaded A54 Homing Peptide Functionalized Dextran-g-PLGA Micelles for Tumor Therapy and MR Imaging. *Sci Rep* **2016**, *6*, 35910. https://doi.org/10.1038/srep35910
208. Farshchi, H.K.; Azizi, M.; Jaafari, M.R.; Nemati, S.H.; Fotovat, A. Green Synthesis of Iron Nanoparticles by Rosemary Extract and Cytotoxicity Effect Evaluation on Cancer Cell Lines. *Biocatalysis and Agricultural Biotechnology* **2018**, *16*, 54–62, https://doi.org/10.1016/j.bcab.2018.07.017
209. Al-Obaidy, R.; Haider, A.J.; Al-Musawi, S.; Arsad, N. Targeted Delivery of Paclitaxel Drug Using Polymer-Coated Magnetic Nanoparticles for Fibrosarcoma Therapy: In Vitro and in Vivo Studies. *Sci Rep* **2023**, *13*, 3180, doi:10.1038/s41598-023-30221-x.
210. Serio, F.; Silvestri, N.; Kumar Avugadda, S.; Nucci, G.E.P.; Nitti, S.; Onesto, V.; Catalano, F.; D'Amone, E.; Gigli, G.; Del Mercato, L.L.; et al. Co-Loading of Doxorubicin and Iron Oxide Nanocubes in Polycaprolactone Fibers for Combining Magneto-Thermal and Chemotherapeutic Effects on Cancer Cells. *Journal of Colloid and Interface Science* **2022**, *607*, 34–44, doi:10.1016/j.jcis.2021.08.153.
211. Buyukhatipoglu, K.; Clyne, A.M. Superparamagnetic Iron Oxide Nanoparticles Change Endothelial Cell Morphology and Mechanics via Reactive Oxygen Species Formation. *J Biomedical Materials Res* **2011**, *96A*, 186–195, doi:10.1002/jbm.a.32972.
212. Norouzi, M.; Yathindranath, V.; Thliveris, J.A.; Kopec, B.M.; Siahaan, T.J.; Miller, D.W. Doxorubicin-Loaded Iron Oxide Nanoparticles for Glioblastoma Therapy: A Combinational Approach for Enhanced Delivery of Nanoparticles. *Sci Rep* **2020**, *10*, 11292, doi:10.1038/s41598-020-68017-y.

 doi:10.20944/preprints202508.0830.v1

213. Herranz-López, M.; Losada-Echeberría, M.; Barrajón-Catalán, E. The Multitarget Activity of Natural Extracts on Cancer: Synergy and Xenohormesis. *Medicines* **2018**, *6*, 6, doi:10.3390/medicines6010006.
214. Lewandowska, U.; Gorlach, S.; Owczarek, K.; Hrabec, E.; Szewczyk, K. Synergistic Interactions Between Anticancer Chemotherapeutics and Phenolic Compounds and Anticancer Synergy Between Polyphenols. *Postepy. Hig. Med. Dosw.* **2014**, *68*, 528–540. https://doi.org/10.5604/17322693.1102278
215. Pérez-Sánchez, A.; Barrajón-Catalán, E.; Ruiz-Torres, V.; Agulló-Chazarra, L.; Herranz-López, M.; Valdés, A.; Cifuentes, A.; Micol, V. Rosemary (Rosmarinus Officinalis) Extract Causes ROS-Induced Necrotic Cell Death and Inhibits Tumor Growth in Vivo. *Sci Rep* **2019**, *9*, 808, doi:10.1038/s41598-018-37173-7.
216. Einbond, L.S.; Wu, H.; Kashiwazaki, R.; He, K.; Roller, M.; Su, T.; Wang, X.; Goldsberry, S. Carnosic Acid Inhibits the Growth of ER-Negative Human Breast Cancer Cells and Synergizes with Curcumin. *Fitoterapia* **2012**, *83*, 1160–1168, doi:10.1016/j.fitote.2012.07.006.
217. Mangaiyarkarasi, R.; Chinnathambi, S.; Karthikeyan, S.; Aruna, P.; Ganesan, S. Paclitaxel Conjugated Fe3O4@LaF3:Ce3+,Tb3+ Nanoparticles as Bifunctional Targeting Carriers for Cancer Theranostics Application. *Journal of Magnetism and Magnetic Materials* **2016**, *399*, 207–215, doi:10.1016/j.jmmm.2015.09.084.
218. Yang, Y.; Wang, C.; Tian, C.; Guo, H.; Shen, Y.; Zhu, M. Fe_3O_4@MnO_2 @PPy Nanocomposites Overcome Hypoxia: Magnetic-Targeting-Assisted Controlled Chemotherapy and Enhanced Photodynamic/Photothermal Therapy. *J. Mater. Chem. B* **2018**, *6*, 6848–6857, doi:10.1039/C8TB02077A.
219. Menon, J.U.; Kuriakose, A.; Iyer, R.; Hernandez, E.; Gandee, L.; Zhang, S.; Takahashi, M.; Zhang, Z.; Saha, D.; Nguyen, K.T. Dual-Drug Containing Core-Shell Nanoparticles for Lung Cancer Therapy. *Sci Rep* **2017**, *7*, 13249, doi:10.1038/s41598-017-13320-4.
220. Ebadi, M.; Bullo, S.; Buskara, K.; Hussein, M.Z.; Fakurazi, S.; Pastorin, G. Release of a Liver Anticancer Drug, Sorafenib from Its PVA/LDH- and PEG/LDH-Coated Iron Oxide Nanoparticles for Drug Delivery Applications. *Sci Rep* **2020**, *10*, 21521, doi:10.1038/s41598-020-76504-5.
221. Wang, S.; Low, P.S. Folate-Mediated Targeting of Antineoplastic Drugs, Imaging Agents, and Nucleic Acids to Cancer Cells. *Journal of Controlled Release* **1998**, *53*, 39–48, doi:10.1016/S0168-3659(97)00236-8.
222. Tran, P.A.; Nguyen, H.T.; Fox, K.; Tran, N. In Vitro Cytotoxicity of Iron Oxide Nanoparticles: Effects of Chitosan and Polyvinyl Alcohol as Stabilizing Agents. *Materials Research Express* **2018**, *5*, 035051, doi:10.1088/2053-1591/aab5f3.
223. Popescu, R.C.; Savu, D.; Dorobantu, I.; Vasile, B.S.; Hosser, H.; Boldeiu, A.; Temelie, M.; Straticiuc, M.; Iancu, D.A.; Andronescu, E.; et al. Efficient Uptake and Retention of Iron Oxide-Based Nanoparticles in HeLa Cells Leads to an Effective Intracellular Delivery of Doxorubicin. *Sci Rep* **2020**, *10*, 10530, doi:10.1038/s41598-020-67207-y.
224. Mohammadinejad, R.; Moosavi, M.A.; Tavakol, S.; Vardar, D.Ö.; Hosseini, A.; Rahmati, M.; Dini, L.; Hussain, S.; Mandegary, A.; Klionsky, D.J. Necrotic, Apoptotic and Autophagic Cell Fates Triggered by Nanoparticles. *Autophagy* **2019**, *15*, 4–33, doi:10.1080/15548627.2018.1509171.
225. Elmore, S. Apoptosis: A Review of Programmed Cell Death. *Toxicol Pathol* **2007**, *35*, 495–516, doi:10.1080/01926230701320337.
226. Lockshin, R.A.; Zakeri, Z. Programmed Cell Death and Apoptosis: Origins of the Theory. *Nat Rev Mol Cell Biol* **2001**, *2*, 545–550, doi:10.1038/35080097.
227. Fink, S.L.; Cookson, B.T. Apoptosis, Pyroptosis, and Necrosis: Mechanistic Description of Dead and Dying Eukaryotic Cells. *Infect Immun* **2005**, *73*, 1907–1916, doi:10.1128/IAI.73.4.1907-1916.2005. 1
228. Naqvi, S.; Naqvi, S.; Samim, M.; Abdin, M.; Ahmad, F.J.; Maitra, A.; Dinda, A.K.; Prashant, C. Concentration-Dependent Toxicity of Iron Oxide Nanoparticles Mediated by Increased Oxidative Stress [Retraction]. *IJN* **2022**, *Volume 17*, 1459–1460, doi:10.2147/IJN.S367448.
229. Nosrati, H.; Salehiabar, M.; Davaran, S.; Danafar, H.; Manjili, H.K. Methotrexate-Conjugated L-Lysine Coated Iron Oxide Magnetic Nanoparticles for Inhibition of MCF-7 Breast Cancer Cells. *Drug Development and Industrial Pharmacy* **2018**, *44*, 886–894, doi:10.1080/03639045.2017.1417422.
230. Tousi, M.S.; Sepehri, H.; Khoee, S.; Farimani, M.M.; Delphi, L.; Mansourizadeh, F. Evaluation of Apoptotic Effects of mPEG-b-PLGA Coated Iron Oxide Nanoparticles as a Eupatorin Carrier on DU-145 and LNCaP

 doi:10.20944/preprints202508.0830.v1

Human Prostate Cancer Cell Lines. *Journal of Pharmaceutical Analysis* **2021**, *11*, 108–121, doi:10.1016/j.jpha.2020.04.002.

231. Moghimi, S.M.; Symonds, P.; Murray, J.C.; Hunter, A.C.; Debska, G.; Szewczyk, A. A Two-Stage Poly(Ethylenimine)-Mediated Cytotoxicity: Implications for Gene Transfer/Therapy. *Molecular Therapy* **2005**, *11*, 990–995, doi:10.1016/j.ymthe.2005.02.010.
232. Patil, U.; Adireddy, S.; Jaiswal, A.; Mandava, S.; Lee, B.; Chrisey, D. In Vitro/In Vivo Toxicity Evaluation and Quantification of Iron Oxide Nanoparticles. *IJMS* **2015**, *16*, 24417–24450, doi:10.3390/ijms161024417.
233. Su, Y.; Zhao, B.; Zhou, L.; Zhang, Z.; Shen, Y.; Lv, H.; AlQudsy, L.H.H.; Shang, P. Ferroptosis, a Novel Pharmacological Mechanism of Anti-Cancer Drugs. *Cancer Letters* **2020**, *483*, 127–136, doi:10.1016/j.canlet.2020.02.015.
234. Liu, Y.; Lu, S.; Wu, L.; Yang, L.; Yang, L.; Wang, J. The Diversified Role of Mitochondria in Ferroptosis in Cancer. *Cell Death Dis* **2023**, *14*, 519, doi:10.1038/s41419-023-06045-y.
235. Johnson, J.; Mercado-Ayon, E.; Mercado-Ayon, Y.; Dong, Y.N.; Halawani, S.; Ngaba, L.; Lynch, D.R. Mitochondrial Dysfunction in the Development and Progression of Neurodegenerative Diseases. *Archives of Biochemistry and Biophysics* **2021**, *702*, 108698, doi:10.1016/j.abb.2020.108698.
236. Liu, Y.; Xu, Z.; Jin, T.; Xu, K.; Liu, M.; Xu, H. Ferroptosis in Low-Grade Glioma: A New Marker for Diagnosis and Prognosis. *Med Sci Monit* **2020**, *26*, doi:10.12659/MSM.921947.
237. Dixon, S.J.; Olzmann, J.A. The Cell Biology of Ferroptosis. *Nat Rev Mol Cell Biol* **2024**, *25*, 424–442, doi:10.1038/s41580-024-00703-5.
238. Luo, C.; Li, X.; Yan, H.; Guo, Q.; Liu, J.; Li, Y. Iron Oxide Nanoparticles Induce Ferroptosis under Mild Oxidative Stress in Vitro. *Sci Rep* **2024**, *14*, 31383, doi:10.1038/s41598-024-82917-3.
239. Wang, S.; Guo, Q.; Zhou, L.; Xia, X. Ferroptosis: A Double-Edged Sword. *Cell Death Discov.* **2024**, *10*, 265, doi:10.1038/s41420-024-02037-9.
240. Rochette, L.; Dogon, G.; Rigal, E.; Zeller, M.; Cottin, Y.; Vergely, C. Lipid Peroxidation and Iron Metabolism: Two Corner Stones in the Homeostasis Control of Ferroptosis. *IJMS* **2022**, *24*, 449, doi:10.3390/ijms24010449.
241. Cui, K.; Wang, K.; Huang, Z. Ferroptosis and the Tumor Microenvironment. *J Exp Clin Cancer Res* **2024**, *43*, 315, doi:10.1186/s13046-024-03235-0.
242. Nie, Q.; Chen, W.; Zhang, T.; Ye, S.; Ren, Z.; Zhang, P.; Wen, J. Iron Oxide Nanoparticles Induce Ferroptosis via the Autophagic Pathway by Synergistic Bundling with Paclitaxel. *Mol Med Rep* **2023**, *28*, 198, doi:10.3892/mmr.2023.13085.
243. Dixon, S.J.; Lemberg, K.M.; Lamprecht, M.R.; Skouta, R.; Zaitsev, E.M.; Gleason, C.E.; Patel, D.N.; Bauer, A.J.; Cantley, A.M.; Yang, W.S.; et al. Ferroptosis: An Iron-Dependent Form of Nonapoptotic Cell Death. *Cell* **2012**, *149*, 1060–1072, doi:10.1016/j.cell.2012.03.042.
244. Liu, X.; Tuerxun, H.; Zhao, Y.; Li, Y.; Wen, S.; Li, X.; Zhao, Y. Crosstalk between Ferroptosis and Autophagy: Broaden Horizons of Cancer Therapy. *J Transl Med* **2025**, *23*, 18, doi:10.1186/s12967-024-06059-w.
245. Yun, C.W.; Lee, S.H. The Roles of Autophagy in Cancer. *IJMS* **2018**, *19*, 3466, doi:10.3390/ijms19113466.
246. Adiseshaiah, P.P.; Hall, J.B.; McNeil, S.E. Nanomaterial Standards for Efficacy and Toxicity Assessment. *Wiley Interdiscip Rev Nanomed Nanobiotechnol* **2010**, *2*, 99–112, doi:10.1002/wnan.66.
247. Chen, B. Pharmacokinetic Parameters and Tissue Distribution of Magnetic Fe3O4 Nanoparticles in Mice. *IJN* **2010**, 861, doi:10.2147/IJN.S13662.
248. Duan, X.; Li, Y. Physicochemical Characteristics of Nanoparticles Affect Circulation, Biodistribution, Cellular Internalization, and Trafficking. *Small* **2013**, *9*, 1521–1532, doi:10.1002/smll.201201390.
249. Israel, L.L.; Galstyan, A.; Holler, E.; Ljubimova, J.Y. Magnetic Iron Oxide Nanoparticles for Imaging, Targeting and Treatment of Primary and Metastatic Tumors of the Brain. *Journal of Controlled Release* **2020**, *320*, 45–62, doi:10.1016/j.jconrel.2020.01.009.
250. Apopa, P.L.; Qian, Y.; Shao, R.; Guo, N.L.; Schwegler-Berry, D.; Pacurari, M.; Porter, D.; Shi, X.; Vallyathan, V.; Castranova, V.; et al. Iron Oxide Nanoparticles Induce Human Microvascular Endothelial Cell Permeability through Reactive Oxygen Species Production and Microtubule Remodeling. *Part Fibre Toxicol* **2009**, *6*, 1, doi:10.1186/1743-8977-6-1.
251. Larsen, E.K.U.; Nielsen, T.; Wittenborn, T.; Birkedal, H.; Vorup-Jensen, T.; Jakobsen, M.H.; Østergaard, L.; Horsman, M.R.; Besenbacher, F.; Howard, K.A.; et al. Size-Dependent Accumulation of PEGylated Silane-

 doi:10.20944/preprints202508.0830.v1

Coated Magnetic Iron Oxide Nanoparticles in Murine Tumors. *ACS Nano* **2009**, *3*, 1947–1951, doi:10.1021/nn900330m.

252. Curry, F.E.; Adamson, R.H. Endothelial Glycocalyx: Permeability Barrier and Mechanosensor. *Ann Biomed Eng* **2012**, *40*, 828–839, doi:10.1007/s10439-011-0429-8.
253. Hobbs, S.K.; Monsky, W.L.; Yuan, F.; Roberts, W.G.; Griffith, L.; Torchilin, V.P.; Jain, R.K. Regulation of Transport Pathways in Tumor Vessels: Role of Tumor Type and Microenvironment. *Proc. Natl. Acad. Sci. U.S.A.* **1998**, *95*, 4607–4612, doi:10.1073/pnas.95.8.4607.
254. Mehta, D.; Malik, A.B. Signaling Mechanisms Regulating Endothelial Permeability. *Physiological Reviews* **2006**, *86*, 279–367, doi:10.1152/physrev.00012.2005.
255. Huang, Y.; Wang, J.; Jiang, K.; Chung, E.J. Improving Kidney Targeting: The Influence of Nanoparticle Physicochemical Properties on Kidney Interactions. *Journal of Controlled Release* **2021**, *334*, 127–137, doi:10.1016/j.jconrel.2021.04.016.
256. Aisida, S.O.; Akpa, P.A.; Ahmad, I.; Zhao, T.; Maaza, M.; Ezema, F.I. Bio-Inspired Encapsulation and Functionalization of Iron Oxide Nanoparticles for Biomedical Applications. *European Polymer Journal* **2020**, *122*, 109371, doi:10.1016/j.eurpolymj.2019.109371.
257. Sionkowska, A. Current Research on the Blends of Natural and Synthetic Polymers as New Biomaterials: Review. *Progress in Polymer Science* **2011**, *36*, 1254–1276, doi:10.1016/j.progpolymsci.2011.05.003.
258. Veronese, F.M. Peptide and Protein PEGylation. *Biomaterials* **2001**, *22*, 405–417, doi:10.1016/S0142-9612(00)00193-9.
259. Peñate Medina, T.; Gerle, M.; Humbert, J.; Chu, H.; Köpnick, A.-L.; Barkmann, R.; Garamus, V.M.; Sanz, B.; Purcz, N.; Will, O.; et al. Lipid-Iron Nanoparticle with a Cell Stress Release Mechanism Combined with a Local Alternating Magnetic Field Enables Site-Activated Drug Release. *Cancers* **2020**, *12*, 3767, doi:10.3390/cancers12123767.
260. Ogden, S.G.; Lewis, D.; Shapter, J.G. Silane Functionalisation of Iron Oxide Nanoparticles.; Voelcker, N.H., Thissen, H.W., Eds.; Melbourne, Australia, December 26 2008; p. 72670A.
261. Janjua, T.I.; Cao, Y.; Kleitz, F.; Linden, M.; Yu, C.; Popat, A. Silica Nanoparticles: A Review of Their Safety and Current Strategies to Overcome Biological Barriers. *Advanced Drug Delivery Reviews* **2023**, *203*, 115115, doi:10.1016/j.addr.2023.115115.
262. Jain, N.K.; R. S., P.; Bavya, M.C.; Prasad, R.; Bandyopadhyaya, R.; Naidu, V.G.M.; Srivastava, R. Niclosamide Encapsulated Polymeric Nanocarriers for Targeted Cancer Therapy. *RSC Adv.* **2019**, *9*, 26572–26581, doi:10.1039/C9RA03407B.
263. Kim, J.-E.; Shin, J.-Y.; Cho, M.-H. Magnetic Nanoparticles: An Update of Application for Drug Delivery and Possible Toxic Effects. *Arch Toxicol* **2012**, *86*, 685–700, doi:10.1007/s00204-011-0773-3. 1.
264. Turcheniuk, K.; Tarasevych, A.V.; Kukhar, V.P.; Boukherroub, R.; Szunerits, S. Recent Advances in Surface Chemistry Strategies for the Fabrication of Functional Iron Oxide Based Magnetic Nanoparticles. *Nanoscale* **2013**, *5*, 10729, doi:10.1039/c3nr04131j.
265. Wagstaff, A.J.; Brown, S.D.; Holden, M.R.; Craig, G.E.; Plumb, J.A.; Brown, R.E.; Schreiter, N.; Chrzanowski, W.; Wheate, N.J. Cisplatin Drug Delivery Using Gold-Coated Iron Oxide Nanoparticles for Enhanced Tumour Targeting with External Magnetic Fields. Inorganica Chimica Acta 2012, 393, 328–333, doi:10.1016/j.ica.2012.05.012.
266. Jeong, Y.; Kim, S.; Jin, S.; Ryu, H.; Jin, Y.; Jung, T.; Kim, I.; Jung, S. Cisplatin-incorporated Hyaluronic Acid Nanoparticles Based on Ion-complex Formation. *Journal of Pharmaceutical Sciences* **2008**, *97*, 1268–1276, doi:10.1002/jps.21103.
267. Mohamadkazem, M.; Neshastehriz, A.; Amini, S.M.; Moshiri, A.; Janzadeh, A. Radiosensitising Effect of Iron Oxide-gold Nanocomplex for Electron Beam Therapy of Melanoma in Vivo by Magnetic Targeting. *IET Nanobiotechnology* **2023**, *17*, 212–223, doi:10.1049/nbt2.12129.
268. Xie, W.; Guo, Z.; Gao, F.; Gao, Q.; Wang, D.; Liaw, B.; Cai, Q.; Sun, X.; Wang, X.; Zhao, L. Shape-, Size- and Structure-Controlled Synthesis and Biocompatibility of Iron Oxide Nanoparticles for Magnetic Theranostics. *Theranostics* **2018**, *8*, 3284–3307, doi:10.7150/thno.25220.

 doi:10.20944/preprints202508.0830.v1

269. Gentile, F.; Chiappini, C.; Fine, D.; Bhavane, R.C.; Peluccio, M.S.; Cheng, M.M.-C.; Liu, X.; Ferrari, M.; Decuzzi, P. The Effect of Shape on the Margination Dynamics of Non-Neutrally Buoyant Particles in Two-Dimensional Shear Flows. *Journal of Biomechanics* **2008**, *41*, 2312–2318, doi:10.1016/j.jbiomech.2008.03.021.
270. Doshi, N.; Prabhakarpandian, B.; Rea-Ramsey, A.; Pant, K.; Sundaram, S.; Mitragotri, S. Flow and Adhesion of Drug Carriers in Blood Vessels Depend on Their Shape: A Study Using Model Synthetic Microvascular Networks. *Journal of Controlled Release* **2010**, *146*, 196–200, doi:10.1016/j.jconrel.2010.04.007.
271. Öztürk, K.; Kaplan, M.; Çalış, S. Effects of Nanoparticle Size, Shape, and Zeta Potential on Drug Delivery. International Journal of Pharmaceutics 2024, 666, 124799, doi:10.1016/j.ijpharm.2024.124799.
272. Di Bona, K.R.; Xu, Y.; Ramirez, P.A.; DeLaine, J.; Parker, C.; Bao, Y.; Rasco, J.F. Surface Charge and Dosage Dependent Potential Developmental Toxicity and Biodistribution of Iron Oxide Nanoparticles in Pregnant CD-1 Mice. *Reproductive Toxicology* **2014**, *50*, 36–42, doi:10.1016/j.reprotox.2014.09.010.
273. Mahmoudi, M.; Shokrgozar, M.A.; Sardari, S.; Moghadam, M.K.; Vali, H.; Laurent, S.; Stroeve, P. Irreversible Changes in Protein Conformation Due to Interaction with Superparamagnetic Iron Oxide Nanoparticles. *Nanoscale* **2011**, 10.1039.c0nr00733a, doi:10.1039/c0nr00733a.
274. Xie, D.; Sun, L.; Wu, M.; Li, Q. From Detection to Elimination: Iron-Based Nanomaterials Driving Tumor Imaging and Advanced Therapies. *Front. Oncol.* **2025**, *15*, 1536779, doi:10.3389/fonc.2025.1536779.
275. Ju, H.; Liu, Y.; Wang, Y.; Lu, R.; Yang, B.; Wang, D.; Wang, J. The Cellular Response and Molecular Mechanism of Superoxide Dismutase Interacting with Superparamagnetic Iron Oxide Nanoparticles. *NanoImpact* **2024**, *35*, 100515, doi:10.1016/j.impact.2024.100515.
276. Ye, P.; Ye, Y.; Chen, X.; Zou, H.; Zhou, Y.; Zhao, X.; Chang, Z.; Han, B.; Kong, X. Ultrasmall Fe_3O_4 Nanoparticles Induce S-Phase Arrest and Inhibit Cancer Cells Proliferation. *Nanotechnology Reviews* **2020**, *9*, 61–69, doi:10.1515/ntrev-2020-0006.
277. Nemmar, A.; Beegam, S.; Yuvaraju, P.; Yasin, J.; Tariq, S.; Attoub, S.; Ali, B.H. Ultrasmall Superparamagnetic Iron Oxide Nanoparticles Acutely Promote Thrombosis and Cardiac Oxidative Stress and DNA Damage in Mice. *Part Fibre Toxicol* **2015**, *13*, 22, doi:10.1186/s12989-016-0132-x.
278. Hsiao, Y.-P.; Shen, C.-C.; Huang, C.-H.; Lin, Y.-C.; Jan, T.-R. Iron Oxide Nanoparticles Attenuate T Helper 17 Cell Responses in Vitro and in Vivo. International Immunopharmacology 2018, 58, 32–39, doi:10.1016/j.intimp.2018.03.007. 1.
279. Shestovskaya, M.V.; Luss, A.L.; Bezborodova, O.A.; Makarov, V.V.; Keskinov, A.A. Iron Oxide Nanoparticles in Cancer Treatment: Cell Responses and the Potency to Improve Radiosensitivity. *Pharmaceutics* **2023**, *15*, 2406, doi:10.3390/pharmaceutics15102406. 1.
280. Zhu, L.; Zhou, Z.; Mao, H.; Yang, L. Magnetic Nanoparticles for Precision Oncology: Theranostic Magnetic Iron Oxide Nanoparticles for Image-Guided and Targeted Cancer Therapy. *Nanomedicine (Lond.)* **2017**, *12*, 73–87, doi:10.2217/nnm-2016-0316.
281. Thiele, L.; Merkle, H.P.; Walter, E. Phagocytosis and Phagosomal Fate of Surface-Modified Microparticles in Dendritic Cells and Macrophages. *Pharm Res* **2003**, *20*, 221–228, doi:10.1023/A:1022271020390.
282. Champion, J.A.; Mitragotri, S. Role of Target Geometry in Phagocytosis. *Proc. Natl. Acad. Sci. U.S.A.* **2006**, *103*, 4930–4934, doi:10.1073/pnas.0600997103.
283. Doshi, N.; Mitragotri, S. Designer Biomaterials for Nanomedicine. *Adv Funct Materials* **2009**, *19*, 3843–3854, doi:10.1002/adfm.200901538.
284. Champion, J.A.; Mitragotri, S. Shape Induced Inhibition of Phagocytosis of Polymer Particles. *Pharm Res* **2009**, *26*, 244–249, doi:10.1007/s11095-008-9626-z.
285. Park, J.; Von Maltzahn, G.; Zhang, L.; Schwartz, M.P.; Ruoslahti, E.; Bhatia, S.N.; Sailor, M.J. Magnetic Iron Oxide Nanoworms for Tumor Targeting and Imaging. *Advanced Materials* **2008**, *20*, 1630–1635, doi:10.1002/adma.200800004.
286. Wojtera, K.; Pietrzak, L.; Szymanski, L.; Wiak, S. Investigation of Ferromagnetic Nanoparticles' Behavior in a Radio Frequency Electromagnetic Field for Medical Applications. *Electronics* **2024**, *13*, 2287, doi:10.3390/electronics13122287.
287. Baniasadi, F.; Hajiaghalou, S.; Shahverdi, A.; Ghalamboran, M.R.; Pirhajati, V.; Fathi, R. The Beneficial Effects of Static Magnetic Field and Iron Oxide Nanoparticles on the Vitrification of Mature Mice Oocytes. *Reprod. Sci.* **2023**, *30*, 2122–2136, doi:10.1007/s43032-022-01144-1.

 doi:10.20944/preprints202508.0830.v1

288. Semeano, A.T.; Tofoli, F.A.; Corrêa-Velloso, J.C.; De Jesus Santos, A.P.; Oliveira-Giacomelli, Á.; Cardoso, R.R.; Pessoa, M.A.; Da Rocha, E.L.; Ribeiro, G.; Ferrari, M.F.R.; et al. Effects of Magnetite Nanoparticles and Static Magnetic Field on Neural Differentiation of Pluripotent Stem Cells. *Stem Cell Rev and Rep* **2022**, *18*, 1337–1354, doi:10.1007/s12015-022-10332-0.
289. Nandakumaran, N.; Barnsley, L.; Feoktystov, A.; Ivanov, S.A.; Huber, D.L.; Fruhner, L.S.; Leffler, V.; Ehlert, S.; Kentzinger, E.; Qdemat, A.; et al. Unravelling Magnetic Nanochain Formation in Dispersion for In Vivo Applications. *Advanced Materials* **2021**, *33*, 2008683, doi:10.1002/adma.202008683. 1.
290. Wu, J. The Enhanced Permeability and Retention (EPR) Effect: The Significance of the Concept and Methods to Enhance Its Application. *JPM* **2021**, *11*, 771, doi:10.3390/jpm11080771.
291. Johannsen, M.; Jordan, A.; Scholz, R.; Koch, M.; Lein, M.; Deger, S.; Roigas, J.; Jung, K.; Loening, S. Evaluation of Magnetic Fluid Hyperthermia in a Standard Rat Model of Prostate Cancer. *Journal of Endourology* **2004**, *18*, 495–500, doi:10.1089/0892779041271715.
292. Ghazi, R.; Ibrahim, T.K.; Nasir, J.A.; Gai, S.; Ali, G.; Boukhris, I.; Rehman, Z. Iron Oxide Based Magnetic Nanoparticles for Hyperthermia, MRI and Drug Delivery Applications: A Review. *RSC Adv.* **2025**, *15*, 11587–11616, doi:10.1039/D5RA00728C.
293. Talesh, S.; Koohi, M.; Zayerzadeh, E.; Hasan, J.; Shabanian, M. Acute Toxicity Investigation Regarding Clinical and Pathological Aspects Following Repeated Oral Administration of Iron Oxide Nanoparticles in Rats. *Nanomed Res J* **2019**, *4*, doi:10.22034/nmrj.2019.04.004.
294. Parivar, K.; Malekvand Fard, F.; Bayat, M.; Alavian, S.M.; Motavaf, M. Evaluation of Iron Oxide Nanoparticles Toxicity on Liver Cells of BALB/c Rats. *Iran Red Crescent Med J* **2016**, *18*, doi:10.5812/ircmj.28939.
295. Manescu (Paltanea), V.; Paltanea, G.; Antoniac, I.; Vasilescu, M. Magnetic Nanoparticles Used in Oncology. *Materials* **2021**, *14*, 5948, doi:10.3390/ma14205948.
296. Li, Y.; Yang, J.; Gu, G.; Guo, X.; He, C.; Sun, J.; Zou, H.; Wang, H.; Liu, S.; Li, X.; et al. Pulmonary Delivery of Theranostic Nanoclusters for Lung Cancer Ferroptosis with Enhanced Chemodynamic/Radiation Synergistic Therapy. *Nano Lett.* **2022**, *22*, 963–972, doi:10.1021/acs.nanolett.1c03786.
297. Zhu, M.-T.; Feng, W.-Y.; Wang, Y.; Wang, B.; Wang, M.; Ouyang, H.; Zhao, Y.-L.; Chai, Z.-F. Particokinetics and Extrapulmonary Translocation of Intratracheally Instilled Ferric Oxide Nanoparticles in Rats and the Potential Health Risk Assessment. *Toxicological Sciences* **2009**, *107*, 342–351, doi:10.1093/toxsci/kfn245.
298. Bae, C.; Hernández Millares, R.; Ryu, S.; Moon, H.; Kim, D.; Lee, G.; Jiang, Z.; Park, M.H.; Kim, K.H.; Koom, W.S.; et al. Synergistic Effect of Ferroptosis-Inducing Nanoparticles and X-Ray Irradiation Combination Therapy. *Small* **2024**, *20*, 2310873, doi:10.1002/smll.202310873.
299. Carbon Nanoparticle-Loaded Iron [CNSI-Fe(II)] in the Treatment of Advanced Solid Tumor (CNSI-Fe(II)). https://clinicaltrials.gov/study/NCT06048367?term=NCT06048367%20&rank=1
300. Mirzaei, N.; Wärnberg, F.; Zaar, P.; Leonhardt, H.; Olofsson Bagge, R. Ultra-Low Dose of Superparamagnetic Iron Oxide Nanoparticles for Sentinel Lymph Node Detection in Patients with Breast Cancer. *Ann Surg Oncol* **2023**, *30*, 5685–5689, doi:10.1245/s10434-023-13722-x.
301. Pantiora, E.; Eriksson, S.; Wärnberg, F.; Karakatsanis, A. Magnetically Guided Surgery after Primary Systemic Therapy for Breast Cancer: Implications for Enhanced Axillary Mapping. *British Journal of Surgery* **2024**, *111*, znae008, doi:10.1093/bjs/znae008.
302. Michalak S. NanoTherm in Adjuvant Therapy of Glioblastoma Multiforme (ANCHIALE) [(accessed on 7 February 2025)]; https://clinicaltrials.gov/study/NCT06271421
303. Lee, D.; Sohn, J.; Kirichenko, A. Quantifying Liver Heterogeneity via R2*-MRI with Super-Paramagnetic Iron Oxide Nanoparticles (SPION) to Characterize Liver Function and Tumor. *Cancers* **2022**, *14*, 5269, doi:10.3390/cancers14215269.
304. To Evaluate Dose and Safety of NanoEcho Particle-1 Using NanoEcho Imaging Device Examinations of Rectal Lymph Nodes in Healthy Volunteers and Rectal Cancer Patients. https://clinicaltrials.gov/study/NCT06693375
305. Zanganeh, S.; Hutter, G.; Spitler, R.; Lenkov, O.; Mahmoudi, M.; Shaw, A.; Pajarinen, J.S.; Nejadnik, H.; Goodman, S.; Moseley, M.; et al. Iron Oxide Nanoparticles Inhibit Tumour Growth by Inducing Pro-

 doi:10.20944/preprints202508.0830.v1

Inflammatory Macrophage Polari-zation in Tumour Tissues. *Nature Nanotech* **2016**, *11*, 986–994. https://doi.org/10.1038/nnano.2016.168

306. Munawwar, A.; Sajjad, A.; Rasul, A.; Sattar, M.; Jabeen, F. Dissecting the Role of SMYD2 and Its Inhibitor (LLY-507) in the Treatment of Chemically Induced Non-Small Cell Lung Cancer (NSCLC) by Using Fe3O4 Nanoparticles Drug Delivery System. *Pharmaceuticals* **2023**, *16*, 986. https://doi.org/10.3390/ph16070986
307. Ge, R.; Liu, C.; Zhang, X.; Wang, W.; Li, B.; Liu, J.; Liu, Y.; Sun, H.; Zhang, D.; Hou, Y.; et al. Photothermal-Activatable Fe3 O4 Superparticle Nanodrug Carriers with PD-L1 Immune Checkpoint Blockade for Anti-Metastatic Cancer Immuno-therapy. *ACS Appl. Mater. Interfaces* **2018**, *10*, 20342–20355. https://doi.org/10.1021/acsami.8b05876
308. Ge, R.; Li, X.; Lin, M.; Wang, D.; Li, S.; Liu, S.; Tang, Q.; Liu, Y.; Jiang, J.; Liu, L.; et al. Fe3 O4 @polydopamine Composite Theranostic Superparticles Employing Preassembled Fe3 O4 Nanoparticles as the Core. *ACS Appl. Mater. Interfaces* **2016**, *8*, 22942–22952. https://doi.org/10.1021/acsami.6b07997
309. Khalkhali, M.; Sadighian, S.; Rostamizadeh, K.; Khoeini, F.; Naghibi, M.; Bayat, N.; Habibizadeh, M.; Hamidi, M. Synthesis and Characterization of Dextran Coated Magnetite Nanoparticles for Diagnostics and Therapy. *Bioimpacts* **2017**, *5*, 141–150. https://doi.org/10.15171/bi.2015.19
310. Jia, G.; Han, Y.; An, Y.; Ding, Y.; He, C.; Wang, X.; Tang, Q. NRP-1 Targeted and Cargo-Loaded Exosomes Facilitate Simultaneous Imaging and Therapy of Glioma in Vitro and in Vivo. *Biomaterials* **2018**, *178*, 302–316. https://doi.org/10.1016/j.biomaterials.2018.06.029
311. Ding, X.; Jiang, W.; Dong, L.; Hong, C.; Luo, Z.; Hu, Y.; Cai, K. Redox-Responsive Magnetic Nanovectors Self-Assembled from Amphiphilic Polymer and Iron Oxide Nanoparticles for a Remotely Targeted Delivery of Paclitaxel. *J. Mater. Chem. B* **2021**, *9*, 6037–6043. https://doi.org/10.1039/D1TB00991E
312. Srivastava, N.; Chudasama, B.; Baranwal, M. In Vitro Assessment of Polyethylene Glycol-Coated Iron Oxide Nano-particles Integrating Luteinizing Hormone Releasing-Hormone Targeted Magnetic Hyperthermia and Doxorubicin for Lung and Breast Cancer Cells. *Biointerphases* **2025**, *20*, 031001. https://doi.org/10.1116/6.0004228
313. Thomas, C.R.; Ferris, D.P.; Lee, J.-H.; Choi, E.; Cho, M.H.; Kim, E.S.; Stoddart, J.F.; Shin, J.-S.; Cheon, J.; Zink, J.I. Noninvasive Remote-Controlled Release of Drug Molecules in Vitro Using Magnetic Actuation of Mechanized Nanopar-ticles. *J. Am. Chem. Soc.* **2010**, *132*, 10623–10625. https://doi.org/10.1021/ja1022267
314. Ma, P.; Xiao, H.; Yu, C.; Liu, J.; Cheng, Z.; Song, H.; Zhang, X.; Li, C.; Wang, J.; Gu, Z.; et al. Enhanced Cisplatin Chemotherapy by Iron Oxide Nanocarrier-Mediated Generation of Highly Toxic Reactive Oxygen Species. *Nano Lett.* **2017**, *17*, 928–937. https://doi.org/10.1021/acs.nanolett.6b04269
315. Bilbao-Asensio, M.; Ruiz-de-Angulo, A.; Arguinzoniz, A.G.; Cronin, J.; Llop, J.; Zabaleta, A.; Michue-Seijas, S.; Sos-nowska, D.; Arnold, J.N.; Mareque-Rivas, J.C. Redox-Triggered Nanomedicine via Lymphatic Delivery: Inhibition of Melanoma Growth by Ferroptosis Enhancement and a Pt(IV)-Prodrug Chemoimmunotherapy Approach. *Advanced Therapeutics* **2023**, *6*, 2200179. https://doi.org/10.1002/adtp.202200179
316. Liu, B.; Li, C.; Chen, G.; Liu, B.; Deng, X.; Wei, Y.; Xia, J.; Xing, B.; Ma, P.; Lin, J. Synthesis and Optimization of MoS2 @Fe3 O4 -ICG/Pt(IV) Nanoflowers for MR/IR/PA Bioimaging and Combined PTT/PDT/Chemotherapy Triggered by 808 Nm Laser. *Advanced Science* **2017**, *4*, 1600540. https://doi.org/10.1002/advs.201600540
317. Sato, I.; Umemura, M.; Mitsudo, K.; Fukumura, H.; Kim, J.-H.; Hoshino, Y.; Nakashima, H.; Kioi, M.; Nakakaji, R.; Sato, M.; et al. Simultaneous Hyperthermia-Chemotherapy with Controlled Drug Delivery Using Single-Drug Nanoparticles. *Sci. Rep.* **2016**, *6*, 24629. https://doi.org/10.1038/srep24629